NIGROSTRIATAL DOPAMINE FUNCTION AND INSULIN RESISTANCE

BY

JILL KATHLEEN MORRIS, B.A.

Submitted to the graduate degree program in

Molecular and Integrative Physiology

and the Graduate Faculty of the University of Kansas

in partial fulfillment of the requirements for the degree of

Doctor of Philosophy

Dissertation Committee:

_____

Dr. John A. Stanford, Ph.D.
(Chairperson)

_____

Dr. Paige C. Geiger, Ph.D.
(Co-Chairperson)

_____

Dr. Jeffrey M. Burns, M.D.

_____

Dr. Russell H. Swerdlow, M.D.

_____

Dr. Lisa A. Stehno-Bittel, PT, Ph.D.

_____

Dr. Paul D. Cheney, Ph.D.

Date defended: June 17, 2011

The Dissertation Committee for Jill K. Morris

certifies that this is the approved version of the following dissertation:

NIGROSTRIATAL DOPAMINE FUNCTION AND INSULIN RESISTANCE

Dissertation Committee:

_____

Dr. John A. Stanford, Ph.D.
(Chairperson)

_____

Dr. Paige C. Geiger, Ph.D.
(Co-Chairperson)

Date Approved: June 17, 2011

ABSTRACT

Clinical studies have linked Type 2 Diabetes (T2D) with neurodegenerative diseases such as Alzheimer's disease and Parkinson's disease (PD). Although the link between T2D and AD is relatively well established, the potential link between T2D and PD is less understood. The mechanism by which such a link is mediated is unknown. It is also unclear whether the comorbidity between these diseases is bidirectional: whether T2D predisposes individuals to develop PD, or whether it is actually PD that increases T2D risk. The purpose of this work was to investigate this potential link using preclinical models. We used a high fat feeding regimen to model early stage T2D and analyzed the effects of this model on the basal ganglia, which is affected in Parkinson's disease. We used the 6-hydroxydopamine (6-OHDA) lesion model of PD to analyze glucose tolerance and peripheral insulin resistance following dopamine (DA) depletion. Finally, we combined a high fat diet and low dose 6-OHDA model to determine whether a high fat diet can exacerbate DA depletion. We found that high fat diet-induced insulin resistance elicits profound functional effects in the striatum. DA release was severely blunted in high fat-fed animals, and DA uptake was markedly slower. Interestingly, magnetic resonance imaging revealed increased iron content in the substantia nigra of these same animals, and expression of several proteins involved in iron transport was altered. The effects of 6-OHDA mediated dopamine depletion on peripheral glucose tolerance were less impressive. Although severe unilateral DA depletion induced insulin resistance in the striatum in both young and middle aged rats, glucose tolerance and peripheral insulin signaling were not affected. Finally, we observed that a high fat diet significantly increased DA depletion in response to the same dose of 6-OHDA, indicating that high fat feeding may increase the vulnerability of nigrostriatal neurons to toxins. While our studies do not support a role for DA depletion in mediating peripheral glucose tolerance, they do provide evidence that high fat diet-induced insulin resistance may contribute to impaired dopaminergic function and potentially neurodegeneration.

ACKNOWLEDGEMENTS

I would like to thank a number of individuals and entities who have made this dissertation possible. First, I need to thank my wonderful mentors, Dr. John Stanford and Dr. Paige Geiger. I am so fortunate to have experienced their leadership and guidance. Throughout my graduate career, I developed great respect for John and Paige both as scientists and as individuals. Most specifically, I truly admire their ability to balance family and career – an example that has become even more important after I became a parent for the first time. I am filled with gratitude to have had the opportunity to work with both of them and to have experienced such a successful collaboration.

I also need to acknowledge my dissertation committee: Dr. Paul Cheney, Dr. Russ Swerdlow, Dr. Jeff Burns, and Dr. Lisa Stehno-Bittel, who always provided great feedback and who were always willing to collaborate on projects or to offer ideas. Specifically, I would like to thank Dr. Swerdlow for his willingness to let us use his cybrid cell model. I am also appreciative for my predoctoral fellowship - a Ruth L. Kirschstein National Research Service Award awarded through the NINDS. This fellowship allowed me to purchase equipment needed for experiments and to travel to scientific conferences that enriched my experience as a graduate student. To this end, I appreciate the generosity of the Graduate School and Student Union Corporation, who also provided travel scholarships that helped fund travel to scientific meetings where I could present my research.

I am thankful for other collaborators – specifically, Dr. Greg Gerhardt, Verda Davis, Dr. Bill Brooks, and Dr. Jieun Kim, who provided invaluable expertise in various areas of research. Without their collaboration, many experiments simply would not have been possible. I would like to thank my colleagues in the lab: Greg Bomhoff, Dr. Anisha Gupte, Dr. Susan Smittkamp, Dr. Brittany Gorres, and Bob Rogers, who made research fun! And who provided an endless supply of sugary treats to make the days a little brighter. In addition, I would like to acknowledge my

good friends Dr. Tamara Jimenez and Brianne Guilford, for sharing the experience of graduate school. It would not have been the same without you.

I would like to thank my family. My parents, John and Donna, always encouraged me and helped me reach my highest potential, and provided support during the final months of my graduate work. My sister Joy gave me the gift of my first astronomy book, a hobby that I always love, my brother T.J. was always willing to watch science-related TV shows with me when we were kids and actually gave me a real rocket for Christmas one year. I love you all. However, most of all, I would like to thank my husband Corey. We were married the summer before I began graduate school classes, so we have truly experienced the highs and lows of this entire journey together. Words cannot express my gratefulness for his support. Finally, I would like to dedicate this dissertation to my beautiful daughter Ella. You always put life in perspective and make Corey and I appreciate every day. We thank God for you and are incredibly blessed.

TABLE OF CONTENTS

LIST OF FIGURES

LIST OF TABLES

Chapter 1

INTRODUCTION

I.I. Type 2 Diabetes

In the United States, the Center for Disease Control estimates that 23.6 million individuals have diabetes and an additional 57 million have pre-diabetes. Worldwide, the numbers are even more staggering: diabetes affects approximately 150 million individuals, and it is expected that this number will reach 300 million by 2025 (Adeghate et al., 2006). Clinically, diagnosis of diabetes is based upon blood glucose levels. These can be measured either after an overnight fast (fasting glucose) or after fasting and receiving a glucose bolus (glucose tolerance test). In humans, an oral glucose tolerance test is a widely used clinical assessment of glycemic status (Stumvoll et al., 2000) and consists of ingesting a glucose-rich beverage and monitoring blood glucose levels at predetermined time-points for 120 minutes following glucose administration. More sensitive techniques for determining glucose and insulin sensitivity include the hyperinsulinemic-euglycemic and hyperglycemic clamp techniques, but these are mainly used for research purposes and not for clinical diagnosis.

World Health Organization criteria for diabetes diagnosis are: fasting glucose greater than 126 mg/dL, or post-glucose tolerance test glucose levels of greater than 200 mg/dL. Individuals who exhibit fasting glucose of 100-126 mg/dL or post-glucose tolerance of 140-200 mg/dL are classified as pre-diabetic. Two main types of diabetes exist: Type 1 Diabetes (T1D), which makes up approximately 10% of diabetes cases, and Type 2 Diabetes (T2D), which constitutes the remaining 90% of diabetes cases. In T1D, individuals are sensitive to the hormone insulin but do not produce it, and must administer insulin daily to maintain proper blood glucose levels. Individuals with T2D produce insulin, but are resistant to its effects: a signaling deficit prohibits the signal from getting transduced. Because T2D has been linked to neurodegenerative disorders (Ristow, 2004), T2D and insulin resistance are the primary foci of this project. It is now widely accepted that insulin resistance is mediated

primarily through post-receptor effects on the insulin receptor substrate (IRS) protein, which will be discussed in the following section.

I.I.a. Insulin Signaling

The mechanisms involved in insulin signal transduction are similar for the periphery and the brain, (Reagan, 2005) and are detailed in Figure 1.1. Although four IRS isoforms exist, IRS3 and IRS4 play only minor roles in insulin signaling (Sykiotis and Papavassiliou, 2001), while IRS1 and IRS2 are widely expressed and modulate the majority of insulin signaling in the body (White, 2002). IRS1 is most important in skeletal muscle insulin signaling (Sykiotis and Papavassiliou, 2001), where it has been extensively characterized. Studies show that IRS2 plays a more prominent signaling role in tissues such as liver, pancreas, and brain (Dong et al., 2006, Lin et al., 2004, Taguchi et al., 2007), where its role has been most thoroughly characterized in the hypothalamus (Morton, 2007, Pardini et al., 2006, Porte et al., 2005).

Insulin signaling requires interactions between IRS proteins and the insulin receptor. These interactions are mediated by IRS tyrosine phosphorylation (Sykiotis and Papavassiliou, 2001), a process that allows for the binding of effector proteins. Specifically, tyrosine phosphorylation provides a docking site for proteins with Src Homology 2 (SH2) domains, such as phosphatidylinositol 3' kinase (PI3K) (Saltiel and Kahn, 2001). Thus, this pathway is often referred to as the "PI3K pathway." Activation of the catalytic subunit of PI3K catalyzes conversion of PI(4,5)-bisphosphate to PI(3,4,5)-triphosphate. This causes proteins that contain pleckstrin-homology domains, such as PDK-1 and AKT to be activated (Khan and Pessin, 2002). Many studies suggest that AKT is a crucial player in transmission of the insulin signal. It has been shown that a constitutively active form of AKT promotes glucose transport even in the absence of insulin, and that silencing of this protein decreases insulin-stimulated glucose uptake (reviewed in (Welsh et al., 2005)).

Unlike tyrosine phosphorylation, serine phosphorylation of IRS1 and IRS2 impairs IRS interaction with the insulin receptor and decreases propagation of the insulin signal via tyrosine phosphorylation (Aguirre et al., 2002, Paz et al., 1997). This is thought to be the primary mechanism behind insulin resistance. Serine phosphorylation of IRS1 (Pederson et al., 2001) and IRS2 (Kim et al., 2005) can also target these proteins for degradation to further modulate the insulin signal. It has also been suggested that IRS1 ubiquitin ligase may associate with a serine kinase, which acts on IRS1 (Zhande et al., 2002). A partial explanation for decreased insulin signaling in response to serine phosphorylation is proteasome mediated degradation of IRS proteins (Rui et al., 2001, Rui et al., 2002). Thus, phosphorylation of IRS proteins has been the subject of a large amount of research regarding peripheral insulin resistance.

I.I.a.i. Muscle insulin signaling

Insulin signaling in skeletal muscle is relatively well-established. It is important in the context of diabetes because skeletal muscle is responsible for more than 70% of glucose uptake (Bjornholm and Zierath, 2005) and muscle glucose uptake decreases as a result of insulin resistance. As mentioned, resistance to insulin occurs due to post-receptor events, namely, IRS serine phosphorylation due to increased activity of stress kinases. Our laboratory has shown that stress kinases play an important role in the impairment of insulin signaling in both diet-induced and aging models of insulin resistance (Gupte et al., 2008, Gupte et al., 2009).

In muscle, the primary function of insulin signaling is glucose transport. Glucose transport into the cell occurs through the glucose transporter (GLUT) family of proteins. To date, 14 GLUT isoforms have been characterized and vary in both tissue distribution and in their responsiveness to insulin (Augustin, 2010). GLUT1-GLUT4 comprise the “classic” glucose transporters and are the best characterized isoforms. GLUT1 is expressed

ubiquitously and the primary means of regulation for GLUT1 is through expression (Bunn et al., 1999). In the brain, GLUT1 is primarily found in microvessels (Maher et al., 1994). GLUT2 is present in beta cells and is responsible for glucose-sensing in the pancreas (Augustin, 2010), while GLUT3 is expressed highly in neurons (Maher et al., 1994) and is important for insulin-independent glucose uptake. The function of GLUT4 has been intensively studied due to its important role in skeletal muscle glucose uptake. It is contained intracellularly and exocytosed in response to the insulin signal, allowing for tight regulation of glucose uptake by insulin (Klip and Paquet, 1990).

I.I.a.ii. Brain insulin signaling

Unlike the role of insulin in skeletal muscle, relatively little is known about its effects in the brain. IRS1 and IRS2, PI3-K, and GLUT4 are all found in the brain, particularly in the basal ganglia (El Messari et al., 1998, Folli et al., 1994, Porte et al., 2005), suggesting a role for insulin signaling in this region. In the SN, insulin receptors co-localize with neurons containing tyrosine hydroxylase (Figlewicz et al., 2003, Moroo et al., 1994), and there is evidence that a dysfunction in insulin signaling may precede dopaminergic neuron death (Moroo et al., 1994). In addition, a study of human PD brains found that insulin receptor mRNA in the SN was markedly decreased in PD patients when compared to controls (Takahashi et al., 1996).

FIGURE 1.1.

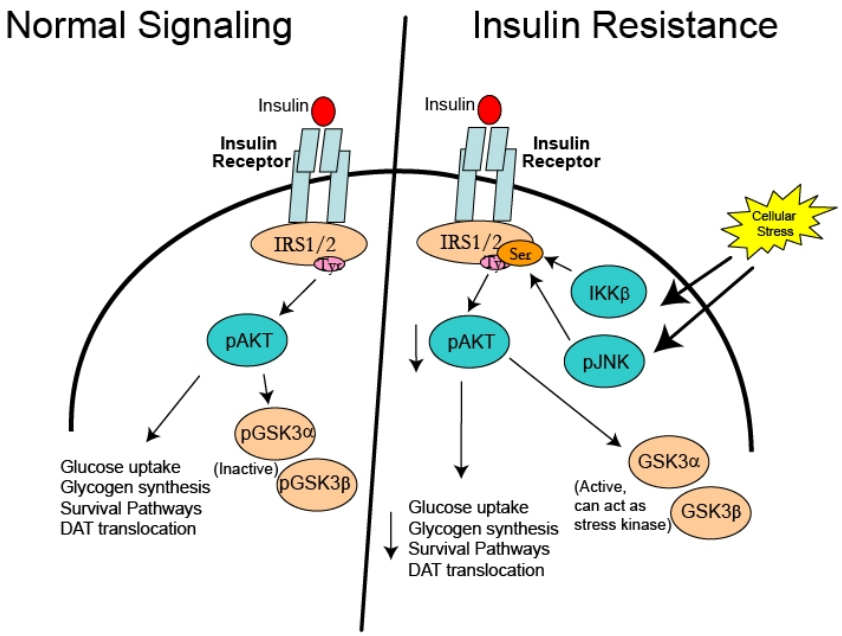

Figure 1.1. Schematic representation of insulin signaling. Under normal conditions, insulin binds to the insulin receptor, eliciting tyrosine phosphorylation of the insulin receptor substrate. This phosphorylation is communicated through PI3K and results in AKT phosphorylation. AKT phosphorylation has been linked to many diverse processes, including glucose uptake, activation of survival pathways, translocation of neurotransmitter transporters, and glycogen synthesis. Insulin resistance is a post-receptor defect. Cellular stress can activate stress kinases, such as c-Jun N-terminal kinase (JNK) and inhibitor of kappa B kinase beta (IKKβ). These kinases can serine phosphorylate IRS proteins, which sterically hinders tyrosine phosphorylation and decreases transmission of the insulin signal.

I.I.b. Additional roles of insulin

The presence of insulin receptors and proteins involved in insulin signaling in tissues where glucose uptake is not primarily dependent on insulin suggests that insulin signaling plays other cellular roles as well. In fact, insulin signaling is suggested to play a role in processes ranging from glycogen synthesis and lipid regulation to cellular survival. Evidence suggests that, in the CNS, insulin promotes cellular survival and that this effect is mediated through AKT (van der Heide et al., 2006). It is well-characterized that insulin can affect glycogen synthesis: glycogen synthase kianse 3 (GSK-3) is a downstream target of AKT (reviewed in (Manning and Cantley, 2007)). It should be noted that GSK-3 may also have direct relevance in neurodegenerative disease: active GSK-3 increases amyloid beta production and tau phosphorylation (Sims-Robinson et al., 2010). Insulin also promotes lipid synthesis and inhibits lipid degradation, possibly via steroid regulatory element-binding protein-1c (SREBP-1c) (Saltiel and Kahn, 2001). Furthermore, insulin can play a role in cellular dopamine and iron uptake, which will be discussed later (section I.3.b., 1.3.c).

I.I.c. Possible risk factors for T2D

There are several known risk factors for development of T2D. The most well-known risk factor for T2D is obesity. According to the Third National Health and Nutrition Examination Survey (NHANES), the prevalence of overweight or obesity in individuals with diagnosed diabetes was 85.2% from 1999-2002 (Eberhardt, 2004). Another well-known risk factor is aging. The prevalence of diabetes increases with age – in the United States, the prevalence of T2D is 7%, but increases to 20% in the elderly (Adler, 2008, Olefsky, 2001). This is of note, as the large population of baby boomers has reached middle age. Genetics also plays a role in the development of diabetes: some individuals are more likely to develop T2D based on their genetic makeup: many of these genes have only recently been identified

(McCarthy, 2010). Finally, the two most common neurodegenerative diseases, Alzheimer's disease and PD, have both been linked to T2D. Associations have been shown between dementia, AD, insulin resistance, and T2D, (Ott et al., 1996, Ronnemaa et al., 2008) (reviewed in (de la Monte, 2009, Sims-Robinson et al., 2010)) and insulin deficiency exacerbates amyloid pathology in mice (Wang et al., 2010). The potential link between T2D and PD is the subject of this dissertation and will be discussed in the following sections.

I.2. Parkinson's disease

Parkinson's disease (PD) is a chronic and progressive neurodegenerative disease. PD affects approximately 1.5 million individuals with 60,000 new diagnoses each year, and ranks second behind Alzheimer's disease regarding the number of individuals affected. The cardinal symptoms of PD include bradykinesia, muscle rigidity, gait disturbances, and resting tremor. Motor impairment occurs due to degeneration of dopamine (DA)-producing neurons in the substantia nigra pars compacta (SNpc) and the resulting depletion of DA from the striatum, the target region of these neurons. The preclinical phase of PD could last as long as 20 years (Savica et al., 2010). Clinical diagnosis most often occurs after the onset of motor symptoms.

The rate of PD misdiagnosis based on symptoms is estimated to be 10-25%, although functional imaging (i.e. PET and SPECT) increases the accuracy of diagnosis (Savitt et al., 2006). A PD diagnosis can be confirmed post-mortem. A hallmark of PD is a loss of DA neurons containing neuromelanin in the SNpc (Thomas and Beal, 2007). Many cases of PD also show a distinct staining for cytoplasmic inclusions called Lewy bodies in the SN. In 1997 alpha synuclein was identified as the primary component of lewy bodies (Polymeropoulos et al., 1997). The mechanism by which alpha-synuclein contributes to neurodegeneration remains contentious, with the most direct evidence for a role of the

protein in PD coming from clinical studies of genetic mutations. However, there are conflicting reports regarding the toxicity of overexpressed monomeric, wild-type alpha-synuclein (Waxman and Giasson, 2009). The role of the protein in PD is the subject of ongoing research and will be discussed later.

1.2.a. DA Systems and Neurotransmission

There are approximately one million DA-producing cells in the brain, and DA accounts for 80% of total brain catecholamine content. DA neurons are present in three main regions of the brain: the arcuate nucleus of the hypothalamus, the ventral tegmental area (VTA), and the SNpc. These DA neurons project to various termination nuclei via four primary pathways. DA neurons in the VTA project to the prefrontal cortex and the nucleus accumbens via the mesocortical and mesolimbic pathways, respectively. Hypothalamic DA neurons primarily project to the pituitary via the tuberoinfindibular pathway, and nigral DA neurons project to the caudate nucleus and putamen (humans) or striatum (rats) via the nigrostriatal pathway.

I.2.b. Nigrostriatal circuit

The primary DA pathway affected in PD is the nigrostriatal pathway. Within the nigrostriatal circuitry, DA neurons modulate movement through two pathways: the direct pathway and indirect pathway. The effect of DA on cell excitability is determined by post-synaptic receptor expression. Two main types of DA receptors exist on striatal medium spiny neurons (MSN's) and are important for understanding DA function in this region. D1 receptors are positively coupled to adenylate cyclase and, when activated, increase activity of L-type Ca^{2+} channels and current through the AMPA and NMDA receptors (Cepeda et al., 1998, Yan et al., 1999), reviewed in (Tang and Bezprozvanny, 2004)). In contrast, D2 receptors are negatively coupled to adenylate cyclase, and activation of these receptors *decreases* L-type Ca^{2+} channel current and activity of NMDA receptors (Kotecha et al.,

2002), causing cell hyperpolarization. Because MSN's projecting through the direct pathway express primarily D1 receptors, and MSN's projecting through the indirect pathway express primarily D2 receptors, DA affects these pathways differently.

Direct pathway

As mentioned, DA neurons originating in the SNpc excite GABA-ergic MSN's that express D1 receptor in the striatum. These neurons project to the internal segment of the globus pallidus (Gpi), inhibiting GABAergic inhibitory neurons in this region. Because the inhibitory GPi neurons project to the thalamus and inhibit excitatory neurons there, the net effect allows glutaminergic excitatory neurons in the thalamus to fire. Motor related thalamic neurons project to the cortex and output is communicated through the brainstem, spinal cord, and motoneurons, resulting in movement. Loss of DA neurons in PD results in disinhibition of inhibitory Gpi neurons, inhibiting the excitatory thalamic output to the cortex and downstream targets.

Indirect pathway

SNpc DA neurons also project to D2 expressing MSN's in the striatum, resulting in inhibition. Because these neurons synapse on inhibitory neurons in the external segment of the globus pallidus (GPe), GPe inhibitory neurons are disinhibited. This results in increased inhibition of excitatory glutaminergic neurons in the subthalamic nucleus (STN), decreasing excitation of GPi inhibitory neurons that project to the thalamus. This allows increased excitation of glutaminergic excitatory neurons in the thalamus, which promotes movement via output to the cortex. As in the direct pathway, loss of DA neurons ultimately increases inhibitory output from the GPi to the cortex due to increased activity of glutaminergic, excitatory input from the STN.

1.2.c. *DA synthesis and storage*

DA synthesis begins with the amino acid tyrosine. Tyrosine is converted to DOPA by the enzyme tyrosine hydroxylase and the cofactor tetrahydropterin. DOPA is subsequently converted to DA by the enzyme aromatic L-amino acid decarboxylase with the cofactor pyridoxal phosphate. DA is primarily stored in vesicles within a neuron, although a small amount of newly synthesized DA exists in the cytoplasm. Vesicular monoamine transporter 2 (VMAT2) is the primary protein responsible for vesicular DA packaging in the SNpc. It is coupled to an ATPase that pumps protons to the interior of the vesicle, creating both pH (vesicular pH 5.5 vs. cytoplasmic pH 7.0) and electrochemical gradients (Eiden et al., 2004). The cytoplasmic concentration of monoamines in nerve terminals is 10,000 fold less than vesicular concentrations (Parsons, 2000). This is extremely important, as accumulation of cytoplasmic DA increases production of reactive oxygen species (ROS) and quinones (Caudle et al., 2007).

Exocytosis of DA is triggered by a large calcium influx into the nerve terminal. Thus, it is not surprising that alterations in calcium regulation have been proposed to affect DA release (Reimann et al., 1993). Re-uptake of DA occurs against a concentration gradient and requires energy expenditure. Synaptic DA is taken up by the DA transporter (DAT) on the cell membrane. DA uptake is dependent on the electrochemical gradient created by the Na^+/K^+ ATPase (Storch et al., 2004). Intracellular transport of DA is coupled with transport of one Cl^- ion and two NA^+ ions and thus is driven via transport of Na^+ down its electrochemical gradient (Krueger, 1990). Once in the cell, the majority (90%) of DA is catabolized by monoamine oxidase (MAO) to generate 3,4-dihydroxyphenylacetic acid (DOPAC). The remainder is metabolized by catechol-O-methyltransferase (COMT). The ratio of DOPAC to DA is often used as an index of “DA turnover.” This data can be useful, because even if DA synthesis changes, tissue DA concentration may change little if the catabolism rate is also altered.

I.2.d. PD animal models

Several animal models of PD exist, all of which have strengths and weaknesses. Use of reserpine was the first model of Parkinson's disease that was developed. It results in long-lasting inhibition of VMAT and loss of DA storage capacity (Tolwani et al., 1999). This model is not selective for the DA system, as vesicular DA, NE, and 5-HT stores are depleted. Also, the effects are only transient and there are no degenerative changes. Alpha-methyl-p-tyrosine (AMPT) blocks the action of TH, which depletes DA and NE. Again, the effects are only temporary and there is no neuronal damage. 6-OHDA is a toxin model commonly used in rats that will be discussed extensively in the following chapters. This model results in large-scale nerve terminal degeneration. Selectivity for DA neurons can be introduced through pretreatement with desipramine, which blocks 6-OHDA transport into noradrenergic neurons, and/or targeted (stereotaxic) delivery to the region of interest. In unilateral 6-OHDA models, circling behavior in response to amphetamine is evident with higher depletion levels (Tolwani et al., 1999). Bilateral treatment is difficult due to effects such as severe bradykinesia and aphagia (Ungerstedt, 1968). A toxin commonly used in primates is 1-methyl-4-phenyl-1,2,3,6-tetrahydropyridine (MPTP). MPTP crosses the blood brain barrier and the site of toxicity is the mitochondria, where MPP+ is thought to block mitochondrial complex I and decrease synthesis of ATP (Nicklas et al., 1987).

I.2.e. PD treatment options

There are several treatment options available for PD patients. The "gold standard" for PD treatment is L-3,4-dihydroxyphenylalanine, or L-DOPA. Unlike DA itself, which cannot cross the blood brain barrier, the DA precursor L-DOPA can cross the blood brain barrier and thus can be given peripherally as a drug. Because the enzyme that converts L-DOPA to DA (DOPA decarboxylase) exists centrally and peripherally, L-DOPA is administered with a DOPA decarboxylase inhibitor to minimize conversion to DA before it

reaches the brain. Although L-DOPA is the most successful drug at treating PD, long-term L-DOPA administration commonly results in dyskinesias. Development of dyskinesia is a major drawback to L-DOPA therapy, as it increases the cost of patient care and decreases quality of life (Calabresi et al., 2010). DA agonists represent another group of compounds given to treat PD. These include drugs such as bromocriptine, ropinirole, and pramipexole (Schapira et al., 2009). Surgical procedures, such as Deep Brain Stimulation (DBS), pallidotomy, or thalamotomy, exist as treatment options for patients who do not respond or are no longer responsive to medications (Betchen and Kaplitt, 2003). DBS involves electrical stimulation of either the subthalamic nucleus or the globus pallidus. Unlike pallidotomy and thalamotomy, which destroy selected neuronal populations, DBS is reversible, making it the most attractive surgical treatment option available today.

I.3. Link between PD and T2D

I.3.a. Clinical evidence for comorbidity

As mentioned, clinical evidence suggests a mechanistic link between Parkinson's disease (PD) and Type 2 Diabetes (T2D). It has been shown that over 50% of PD patients exhibit abnormal glucose tolerance (Barbeau et al., 1961, Boyd et al., 1971) or diabetes (Lipman et al., 1974). The prevalence of T2D in the US is ~7% (Olefsky, 2001). The prevalence of T2D increases to 20% in elderly individuals (Adler, 2008), but this is still less than the prevalence in PD patients. PD patients also display increased immunoreactivity to insulin (Wilhelm et al., 2007) and PD patients with diabetes are often faced with increased motor symptom severity (Papapetropoulos et al., 2004) and cost of medical care (Pressley et al., 2003). Furthermore, hyperglycemia may decrease the effectiveness of L-DOPA therapy and increase motor dyskinesias in PD patients (Sandyk, 1993). L-DOPA therapy

may also exacerbate hyperinsulinemia and hyperglycemia in PD patients, (Boyd et al., 1971, Sirtori et al., 1972) possibly by diminishing peripheral glucose disposal in skeletal muscle (Smith et al., 2004) or affecting insulin release (Rubi et al., 2005).

The link between PD and T2D may extend further than altered peripheral metabolism in PD patients. It has been suggested that T2D may be a risk factor for PD. The most sobering finding comes from a large prospective clinical study, which found that patients with pre-existing T2D were 83% more likely to develop PD than their non-diabetic counterparts (Hu et al., 2007). A large study by Harvard Medical School found that diagnosed diabetes increased PD risk by 36% (Schernhammer et al., 2011), and an additional study found that diabetes resulted in 40% increased PD risk (Xu et al., 2011). Interestingly, the Harvard study found the highest risk between diabetes and early onset PD (odds ratio = 3.07) (Schernhammer et al., 2011). A clinical survey of elderly individuals has also found a positive correlation between T2D and PD based upon odds ratios (Pressley et al., 2003).

I.3.b. Clinical evidence against comorbidity

Although several studies support a link between PD and T2D, the clinical literature remains contentious as to whether a link exists and how it is mediated. One example is a 2008 prospective study that found increased PD risk in individuals with T2D. These authors stopped short of concluding that T2D was a preceding risk factor for PD, since in their study, increased T2D duration and severity did not increase PD risk (Driver et al., 2008). The highest PD risk was seen in short duration diabetes and it was suggested that PD may instead increase T2D risk. It should be noted that two clinical studies have found no correlation between the diseases (Becker et al., 2008, Simon et al., 2007) and another actually found an inverse relationship between the diseases (D'Amelio et al., 2009).

I.3.c. Importance of preclinical studies

The aforementioned clinical studies are very important because their findings make preclinical studies relevant. However, a weakness of these clinical studies is that important variables are not consistent from study to study. For example, study design varied – prospective studies, case-control studies, and surveys were all performed. Some studies were limited to men, others included both men and women. Some studies allowed self-reporting of disease, while others required clinical examination. These and other important differences likely contribute to the equivocal state of the clinical literature and underscore the importance of preclinical studies, where it is possible to tightly control potential confounding factors.

1.4. Potential mechanisms for a molecular link

There are several mechanisms that could account for a link between PD and T2D. It was unclear as to whether the link between these diseases is bidirectional, whether DA neuron degeneration in PD affected peripheral glucose metabolism, or whether peripheral hyperglycemia and hyperinsulinemia affected the brain. The potential mechanisms for these connections are discussed in the following paragraphs and analyzed in the following chapters.

I.4.a.The hypothalamus

The most direct mechanism for DA depletion in the central nervous system to affect peripheral metabolism is through the hypothalamus. The hypothalamus plays an essential role in regulating systemic autonomic and endocrine functions. Post-mortem examination of PD brains indicates Lewy body degeneration in the hypothalamus (Langston and Forno, 1978), and PD patients exhibit decreased TH reactive fibers, NE, and DA levels in this

region (Agid et al., 1973, Shannak et al., 1994). Thus, it is not surprising that PD patients exhibit many autonomic and endocrine deficiencies, including glucose intolerance (Sandyk and Iacono, 1987). Preclinical studies have shown that concentrations of monoamines, such as DA or NE, are decreased in the hypothalamus following unilateral or bilateral 6-OHDA administration into the medial forebrain bundle (Daniels et al., 1993, Jaffer et al., 1991, Jaffer et al., 1992, Sandyk, 1989) in rats, although studies that observed hypothalamic DA depletion reported much less depletion in this region than the striatum. In addition, the hypothalamus plays a role in regulation of hepatic glucose output (Uyama et al., 2004), and the autonomic nervous system is known to affect insulin release. In fact, parasympathetic nerves promote pancreatic insulin release, while sympathetic input to the pancreas is inhibitory to insulin release (Ahren, 2000, Migrenne, 2006, Teff, 2007). The autonomic nervous system is particularly important during the early phase of insulin secretion following a meal (Ahren, 2000), and in humans, insulin output during this phase has been correlated to blood glucose levels following a glucose tolerance test (Ahren and Holst, 2001).

I.4.b. Glucose and Insulin

It is possible that glucose levels can affect DA in the brain. Streptozotocin (STZ) treatment is used to model type 1 diabetes by destroying insulin-producing pancreatic beta cells and causing hyperglycemia (Szkudelski, 2001). Interestingly, STZ has been shown to decrease DA content in the nigrostriatal system (midbrain and striatum) (Gallego et al., 2003). Another group utilizing the STZ model found that in the striatum, diabetic rats had significantly decreased DA turnover rates. The degree of decreased DA turnover correlated with blood glucose levels (Shimomura et al., 1988). These studies indicate that peripheral hyperglycemia can affect DA function in the CNS. DA signaling can be affected by presynaptic factors, including DA synthesis, release, and reuptake, as well as postsynaptic factors, including expression and sensitivity of D1 and D2 DA receptors. DA reuptake occurs

primarily through the actions of DAT. In addition to glucose, evidence is accumulating for insulin as an important effector of pre- and post-synaptic DA function. *In vitro,* insulin promotes DAT cell surface expression and PI3-K inhibition causes DAT internalization (Carvelli et al., 2002). Furthermore, membrane DAT expression is controlled by basal activity of AKT, and insulin requires AKT for regulation of DAT surface expression (Garcia et al., 2005). AKT is a major downstream mediator of insulin signaling (van der Heide et al., 2006), and it has been suggested that DA negatively regulates AKT by postsynaptic actions on D2 receptors (Beaulieu et al., 2007). Finally, it has been shown that HF fed animals exhibit increased D2 DA receptor expression and decreased DAT density in the striatum compared to controls (South and Huang, 2008).

I.4.c. Iron

Iron is essential for proper brain function: it is necessary for neurotransmitter and myelin synthesis and is a cofactor in the electron transport chain (Lozoff et al., 2006). In the brain, iron is often stored in non-neuronal cell types, such as oligodendrocytes and microglia (Burdo et al., 1999, Lopes et al., 2008). In these cells, ferritin is most commonly used to store iron. In contrast, neurons primarily utilize neuromelanin to store iron and express lower levels of ferritin (Rhodes and Ritz, 2008). Neurons are vulnerable to both iron deficiency and iron excess. Iron is necessary many cellular functions, such as neurotransmitter synthesis, so decreased iron can be detrimental (Moos et al., 1998). However, because neurons also have more limited iron storage capacity than oligodendrocytes or microglia, excess iron can quickly contribute to oxidative stress and neuronal damage (LaVaute et al., 2001, Sengstock et al., 1992). Tight control of neuronal iron uptake is very important.

Several studies provide evidence implicating iron in the pathogenesis of T2D. Impaired glucose metabolism leads to increased iron stores in the periphery, while iron overload increases the risk of T2D (Fernandez-Real et al., 2002, Rajpathak et al., 2009,

Swaminathan et al., 2007). Conversely, animal studies report that iron deficiency leads to increased insulin sensitivity (Farrell et al., 1988). Dietary iron restriction and iron chelation therapy has been found to protect against diabetes and loss of beta cell function in the obese ob/ob leptin knockout mouse model of diabetes (Cooksey et al., 2010). In fat cells, transferrin receptors (which initiate vesicular iron import from the plasma into the cell) co-localize with glucose transporters and insulin-like growth factor receptors (Tanner and Lienhard, 1989). Insulin can stimulate iron uptake by redistributing transferrin receptors to the cell membrane (Davis et al., 1986). This is interesting, as iron metabolism and deposition are altered in PD (Rhodes and Ritz, 2008).

Numerous clinical studies have used a variety of techniques, such as histology, spectrophotometry, spectroscopy, and MRI to demonstrate increased nigral iron in PD patients (Dexter et al., 1987, Gorell et al., 1995, Jellinger et al., 1990, Riederer et al., 1989, Sofic et al., 1988), (Graham et al., 2000, Wallis et al., 2008). It has been suggested that iron can contribute to oxidative damage by participating in the Fenton reaction, as iron increases measures of oxidative stress (Harley et al., 1993, Jellinger et al., 1995). Insulin can cross the blood brain barrier (Banks, 2004), and insulin receptors exist in both the SN (where they co-localize with DA neurons) and striatum (Moroo et al., 1994, Morris et al., 2008). It is therefore possible that neuronal iron metabolism is affected by the hyperinsulinemia that results from a HF diet, leading to decreased nigrostriatal DA function and increased vulnerability to toxins in this pathway.

I.4.d. Oxidative stress

Oxidative stress has also been implicated as a contributing factor in the development of PD (Onyango, 2008, Thomas and Beal, 2007, Vali et al., 2008), and T2D (Evans et al., 2003, Robertson, 2006). A study of erythrocytes from 80 PD patients found altered levels and activity of several antioxidants when compared to controls (Younes-Mhenni et al.,

2007). Molecularly, DA loss and increased DA metabolites have been correlated with increased oxidized glutathione in the striatum (Spina and Cohen, 1989). Dopaminergic neurons may be inherently vulnerable to oxidative damage. Mitochondrial monoamine oxidases facilitate DA turnover and have high potential for H_20_2 generation (Andreyev et al., 2005). The high iron content of the SN and high H_20_2 concentration promotes the Fenton reaction, generating highly reactive oxygen species (ROS).

Oxidative stress also contributes to T2D. Increased oxidative stress due to insulin resistance and hyperglycemia can activate stress kinases such as c-Jun N-terminal kinase (JNK), glycogen synthase kinase 3 (GSK3), and IκB kinase β (IκBβ) (Aguirre et al., 2000, Bloch-Damti and Bashan, 2005, Werner et al., 2004, Zick, 2005). These kinases inhibit insulin signaling by phosphorylating IRS isoforms on serine residues and decreasing tyrosine phosphorylation (Aguirre et al., 2002, Evans et al., 2003, Hotamisligil, 2005, Saltiel and Kahn, 2001). Exacerbated insulin resistance and diabetes can result in oxidative stress and systemic mitochondrial oxidative damage in areas ranging from renal tissues to the brain (Kanwar et al., 2007, Moreira et al., 2007). Because it is involved in the pathogenesis of both PD and T2D, it is possible that oxidative stress could contribute to comorbidity of these diseases.

1.4.e. Mitochondrial dysfunction

It has been known for many years that dysfunction of mitochondrial complex I occurs in Parkinson's disease (Parker et al., 1989, Schapira et al., 1989). Interestingly, it is becoming increasingly accepted that mitochondria are also affected in T2D (Kelley et al., 2002, Mogensen et al., 2007, Ritov et al., 2010). In fact, a recent study specifically reported a functional change in mitochondrial complex I in the skeletal muscle of patients with T2D. In these individuals, mitochondrial complex I substrate sensitivity was increased, indicating that this complex was functioning closer to capacity compared to controls (Larsen et al., 2011).

However, the degree of mitochondrial dysfunction in T2D remains contentious. Some studies have reported no difference in skeletal muscle mitochondrial function between T2D groups and controls, either normally or after exercise training, after normalizing for mitochondrial content (Boushel et al., 2007, Hey-Mogensen et al., 2010). To further complicate matters, an additional study found individuals with T2D to exhibit decreased mitochondrial respiration only in leg muscle, but not arm muscle (Rabol et al., 2010). It is likely that the role of T2D in mitochondrial dysfunction, or vice versa, is complex. Our laboratory has noted increased mitochondrial protein expression, but slightly decreased mitochondrial enzyme activity, in a model of HF diet-induced insulin resistance (Gupte et al., 2009). In any case, the fact that studies have shown impaired mitochondrial function and alterations in mitochondrial complex I to be occur in both PD and T2D means that mitochondria should be considered when assessing the co-morbidity between these diseases.

I.4.f. Alpha synuclein

Due to its presence in Lewy bodies, alpha-synuclein has been implicated in PD for many years. Although the protein is primarily found in neurons, it is also located in glial cells. Alpha-synuclein is primarily found pre-synaptically (McLean et al., 2000) and is expressed in neuronal mitochondria in some brain tissues but not others (Liu et al., 2009). The role of endogenous alpha-synuclein remains unknown, but the protein may function as a chaperone (Ostrerova et al., 1999), interact with tubulin (Alim et al., 2002), contribute to vesicle transport (Cooper et al., 2006), or function as an anti-oxidant (Zhu et al., 2006). Although endogenous expression of alpha-synclein is necessary for essential cellular activities, mutation or overexpression of alpha-synuclein can contribute to aggregation, neurodegeneration, and motor deficits (Pandey et al., 2006, Plaas et al., 2008, Ulusoy et al., 2010).(Zhu et al., 2006). Iron, in addition to other metals, has been shown to induce alpha-

synuclein aggregation (Golts et al., 2002, Uversky et al., 2001) and fibrillation (Uversky et al., 2002). Moreover, recently it has been shown that alpha synuclein contains an IRE in its 5' UTR (Friedlich et al., 2007), meaning that cellular iron concentration may directly affect alpha-synuclein levels in addition to aggregation. The question of how iron actually accumulates in the SN is still unknown and is being actively investigated.

I.5. Research Questions

Using our knowledge of previous studies, we designed a project to increase our understanding of the potential link between nigrostriatal dopamine depletion and insulin resistance. Our primary goal was to determine the mechanism or mechanism behind this link, so that further studies could investigate therapeutic approaches. A HF diet animal model was used to determine the role of pre-diabetes in affecting DA function in the basal ganglia and iron dynamics in the substantia nigra. We also examined nigrostriatal DA depletion as a risk factor for insulin resistance using the 6-OHDA rat model of PD. Finally, a multiple hit model using HF feeding and 6-OHDA was used to determine whether toxin exposure could exacerbate the effects of a HF diet on the brain.

CHAPTER 2

EFFECTS OF HIGH FAT FEEDING ON NIGROSTRIATAL DOPAMINE FUNCTION

INSULIN RESISTANCE IMPAIRS NIGROSTRIATAL DOPAMINE FUNCTION

J.K. Morris, G.L. Bomhoff, B.K. Gorres, V.A. Davis, J. Kim, S-P Lee, W.B. Brooks, G.A. Gerhardt, P.C. Geiger and J.A. Stanford

Experimental Neurology (2011) [In Press]

Abstract

Clinical studies have indicated a link between Parkinson's disease (PD) and Type 2 Diabetes. Although preclinical studies have examined the effect of high-fat feeding on dopamine function in brain reward pathways, the effect of diet on neurotransmission in the nigrostriatal pathway, which is affected in PD and parkinsonism, is less clear. We hypothesized that a high-fat diet, which models early-stage Type 2 Diabetes, would disrupt nigrostriatal dopamine function in young adult Fischer 344 rats. Rats were fed a high fat diet (60% calories from fat) or a normal chow diet for 12 weeks. High fat-fed animals were insulin resistant compared to chow-fed controls. Potassium-evoked dopamine release and dopamine clearance were measured in the striatum using *in vivo* electrochemistry. Dopamine release was attenuated and dopamine clearance was diminished in the high-fat diet group compared to chow-fed rats. Magnetic resonance imaging indicated increased iron deposition in the substantia nigra of the high fat group. This finding was supported by alterations in the expression of several proteins involved in iron metabolism in the substantia nigra in this group compared to chow-fed animals. The diet-induced systemic and basal ganglia-specific changes may play a role in the observed impairment of nigrostriatal dopamine function.

Introduction

Although much is understood about Parkinson's disease (PD) pathophysiology, its etiology remains unknown. Genes involved in processes as diverse as organelle trafficking, degradation pathways, and mitochondrial or antioxidant function are affected in PD (Sulzer, 2007). In addition, non-genetic factors, such as aging (Hindle, 2010), pesticide exposure (Priyadarshi et al., 2001, Priyadarshi et al., 2000), diet (Anderson et al., 1999, Johnson et al., 1999, Logroscino et al., 1996), adiposity (Abbott et al., 2002, Hu et al., 2006) and diabetes (Hu et al., 2007, Schernhammer et al., 2011, Xu et al., 2011) have been linked to PD. It is likely that both environmental and genetic factors contribute to dopamine (DA) neuron degeneration in PD.

Several clinical studies link PD with Type 2 Diabetes or obesity (Abbott et al., 2002, Hu et al., 2007, Hu et al., 2006, Schernhammer et al., 2011, Xu et al., 2011). Because over 80% of individuals with diagnosed Type 2 Diabetes are overweight or obese (Eberhardt, 2004), a high fat (HF) diet is often used to model diabetes preclinically. We and others have shown that a HF diet makes DA-producing neurons in the substantia nigra (SN) more vulnerable to toxin exposure (Choi et al., 2005, Morris et al., 2010). Furthermore, motor symptoms of PD are worse in individuals with co-morbid Type 2 Diabetes (Papapetropoulos et al., 2004), and diabetes is associated with more severe parkinsonian signs in aged individuals without PD (Arvanitakis et al., 2007). However, little is understood about the mechanisms by which a HF diet or Type 2 Diabetes put the brain at risk and what factors may contribute. Studies provide evidence of increased circulating iron levels in Type 2 Diabetes (Fernandez-Real et al., 2002, Rajpathak et al., 2009, Swaminathan et al., 2007), which is interesting because iron levels are also increased in the SN in PD patients (Rhodes and Ritz, 2008). It is possible that iron accumulation in DA neurons may contribute to nigrostriatal vulnerability and impaired function. In addition, it has been shown that short and

long term HF feeding decreases DA release in striatal slices (Geiger et al., 2009, York et al., 2010). However, the extent to which a HF diet affects nigrostriatal DA function *in vivo* is unknown. Furthermore, important peripheral effects of HF feeding, such as glucose tolerance, insulin, or ghrelin levels, have not been characterized in the context of striatal DA function.

The purpose of this study was to analyze the degree to which HF diet-induced insulin resistance affects nigrostriatal DA function and iron deposition *in vivo.* In addition, we present a potential mechanism by which iron deposition could occur in this model. Measurement of potassium-evoked striatal DA release using *in vivo* electrochemistry allowed for calcium-dependent neurotransmitter release to be analyzed, mimicking normal neurotransmission, and for characterization of release dynamics across the dorsal striatum with a consistent stimulus in intact rats. Magnetic resonance imaging (MRI) permitted measurement of iron deposition *in vivo*, and iron transport proteins were measured in the SN using western blot. This study characterizes the role of HF-diet induced insulin resistance on nigrostriatal DA function and suggests a role for iron dysregulation in the SN.

Materials and Methods

Animals and Diet

Four-month-old male Fischer 344 rats were obtained from National Institutes on Aging colonies (Harlan). Rats were individually housed on a 12 hour light/dark cycle and provided food and water *ad libitum*. Rats in the control group (n=11) received chow (Harlan Teklad rodent diet 8604; 5% kCal from fat, 40% kCal from carbohydrate), while animals in the experimental group (n=15) received a HF diet (60% kCal from fat, 20% kCal from carbohydrate; Table 1) for 12 weeks. The composition of the HF diet has been described previously (Gupte et al., 2009). Food intake was measured every 2-3 days and body weight was measured weekly. Protocols for animal use were approved by the University of Kansas Medical Center Institutional Animal Care and Use Committee and adhered to the Guide for the Care and Use of Laboratory Animals (National Research Council, 1996).

Materials

Rat insulin, ferritin, and unacylated ghrelin ELISA kits were purchased from ALPCO diagnostics (Salem, NH), while a glutathione assay was obtained from Oxford Biomedical Research (Oxford, MI). Carbon fiber electrodes were purchased from Quanteon, Inc (Lexington, KY). Primary antibody corresponding to transferrin (Tf) was purchased from Enzo Life Sciences (Plymouth Meeting PA), while anti-transferrin receptor 1 (TfR1) was obtained from Invitrogen (Carlsbad, California). Anti-phospho-AKT and total AKT were obtained from Cell Signaling Technology (Beverly, MA), while actin antibodies were purchased from Abcam (Cambridge, UK). Anti-transferrin receptor 2 (TfR2), anti-divalent metal transporter 1 (DMT1), and anti-ferroportin were purchased from Alpha Diagnostic (San Antonio, TX). All other chemicals were obtained from Sigma-Aldrich (St. Louis, MO).

Intraperitoneal glucose tolerance test (IPGTT)

An intraperitoneal glucose tolerance test (IPGTT) was performed one week prior to tissue harvest following a 12-hour fast. Before glucose injection, serum samples were collected to analyze fasting insulin and unacylated ghrelin. Tubes used to collect blood for analysis of ghrelin were coated with EDTA prior to serum collection. Blood was placed on ice for 10 minutes before centrifugation (20 min at 4°C). Serum was aliquoted into fresh tubes for analysis using ELISAs specific to insulin or unacylated ghrelin (ALPCO). At time t=0, a 60% glucose bolus was administered at 2g/kg body weight. Glucose was quantified in tail blood using a glucometer at six timepoints over the following 2 hrs as previously described (Morris et al., 2010).

Magnetic resonance imaging (MRI) image processing and analysis

High resolution MRI was performed using a 9.4 T Varian system equipped with a 12 cm gradient coil (40 G/cm, 250 μs) (Varian Inc., Palo Alto, CA). Animals were imaged using a 6 cm volume transmit radio frequency (RF) coil and a detunable surface receive RF coil. Anesthesia was induced by 4% isoflurane mixed with 4 L/min air and 1L/min O_2 and maintained by 1-1.5% isoflurane. Body temperature was maintained at 37˚C using a circulating hot water pad and a temperature controller (Cole-Palmer, NY). Respiration was also monitored via a respiration pillow (SA Instruments, NY). T2 MRI was performed using a spin echo sequence with multiple echo times (TE). MRI parameters were TR/TE = 1200 / 13, 26, 39 and 52 ms, FOV = 3 × 3 cm, matrix = 256 × 256, slice thickness = 0.9 mm, number of averages = 4, and scan time per TE = 21 min. T2 maps were generated by fitting MR signal intensities to a mono-exponential function using a Simplex algorithm in ImageJ software (NIH) in a pixel-by-pixel basis.

Electrode preparation

Prior to the experiment, Ag/AgCl reference electrodes were plated by placing silver wire into a solution of 1M HCL saturated with NaCL while administering a current for 15

minutes. Reference electrodes were stored in 3M NaCl until use. Glass capillary micropipettes were prepared using a micropipette puller (KOPF instruments) and bumped to an inner diameter of 10 µm. Carbon fiber recording electrodes (30 µ O.D X 100 microns in length) were coated 2x with Nafion®, baked at 200°C for 4 minutes following each coat, and attached to a glass micropipette at a distance of 200 µm from electrode to micropipette tip with Stickywax. The morning of the experiment, recording electrodes were calibrated using stock solutions of 20mM DOPAC and 2mM DA added to 0.05M PBS (pH 7.4) to determine sensitivity and selectivity for DA. All electrodes used exhibited a selectivity for DA of >300:1 vs. DOPAC, limit of detection of <0.01 µM and were linear to DA additions.

In vivo electrochemistry

Animals were anesthetized using urethane (1.25g/kg) over the course of three injections and placed into a stereotaxic frame. A prepared Ag/AgCl reference electrode was placed into the brain in an area distal to the striatum and a burr hole was drilled at striatal stereotaxic coordinates of 1.0 A/P and 3.0 M/L. Each carbon fiber recording electrode was lowered using a microdrive at 0.5mm/min into the striatum. *In vivo* chronoamperometric measurements were made using the FAST-16 system (Quanteon, L.L.C.). A square wave of 0.0V (resting potential) to +0.55V (applied potential) vs. the reference electrode was applied with a pulse duration of 100ms. A filtered potassium chloride (KCl) solution (70mM KCl, 79mMNaCl, 2.5mM $CaCl_2$, pH 7.4) was pressure ejected using a Picospritzer III (Parker instrumentation) and the volume ejected was carefully monitored through a MEIJI scope with a 10mm reticule. DA responses were evoked every 0.5mm from 2.0 mm to 5.0 mm and were averaged for each animal. Data were analyzed using FAST analysis software version 2.1. We based our *in vivo* electrochemistry signal parameters on those previously published (Hoffman and Gerhardt, 1998). For each rat, we obtained the following signal parameters: 1) amplitude / volume, the amplitude of the signal normalized to the amount of KCl (nL)

infused to elicit the signal, 2) T_{80}, the time a signal decay to 80% of peak amplitude, and 3) T_c (clearance rate), the change in DA concentration between 20% (T_{20}) and 60% (T_{60}) of peak amplitude. It should be noted that T_{80} and T_c are specific to DA uptake and not diffusion or metabolism (Cass et al., 1993). Rise time for peak amplitude was also calculated for each signal in order to account for the potential influence of diffusion related to differences in parenchymal tortuosity between the two groups.

Measurement of circulating hormones and oxidative stress

Prior to tissue harvest, blood was collected for measurement of serum ferritin and oxidized and reduced glutathione. Blood for glutathione analysis was immediately stored at -80°C. Blood for serum ferritin analysis was allowed to clot for 10 minutes, centrifuged for 20 minutes and the serum was aliquoted into fresh tubes for further analysis. Serum collected for analysis of ferritin was analyzed using a ferritin ELISA (ALPCO). Blood samples for oxidative stress measurements were analyzed for reduced glutathione and oxidized glutathione using a microplate assay (Oxford Biomedical Research). To minimize oxidation of reduced glutathione, a thiol scavenger was added immediately to blood samples after collection.

High Pressure liquid chromatography (HPLC)

Brains were removed and immediately placed onto an ice-cold brain block. Striatal samples were carefully dissected, weighed, and frozen on dry ice for HPLC-EC analysis. Samples were prepared and analyzed using HPLC as described previously (Morris et al., 2008).

Western Immunoblotting

SN samples were carefully dissected from fresh brain, placed into centrifuge tubes, weighed, and frozen on dry ice. A 15x volume of cell extraction buffer (Invitrogen) with protease inhibitor cocktail (400uL, Invitrogen), sodium fluoride (200mM), sodium

orthovanodate (200 mM), and phenylmethanesulfonylfluoride (200 mM) was added based on tissue weight. Samples were briefly sonicated and protein extraction was allowed to occur on ice for 1 hour with intermittent vortexing. Tubes were centrifuged at 3,000 x g for 20 minutes to pellet cellular debris. Supernatant was collected into fresh tubes. A Bradford assay was performed on extracted supernatant to determine protein concentrations. Samples were prepared and analyzed using Western blot as previously described (Morris et al., 2010).

Statistical Analyses

Data for glucose tolerance were analyzed using two-way analyses of variance (ANOVA) with diet as the grouping variable and time as the repeated measure. All other data were analyzed using one-way ANOVA with diet as the grouping variable. Data were considered statistically significant at $p \leq 0.05$.

Results

HF diet induces glucose intolerance and oxidative stress

Initial body weight did not differ significantly between the two groups. As expected, a 12-week HF diet significantly increased body weight ($F=230.90$, $p<0.0001$) and epididymal fat ($F=83.40$, $p<0.001$) compared to a chow diet (Table 2). Food intake also differed between groups: as expected, HF-fed animals consumed more calories per day over the course of the experiment ($F=274.19$, $p<0.0001$; Table 2). We performed an IPGTT to analyze whole body glucose tolerance (Figure 1A). Glucose tolerance differed between groups over the course of the IPGTT ($F=5.496$, $p<0.05$), and HF-fed animals exhibited significantly greater area under the curve (AUC) ($F=5.12$, $p<0.05$; Table 2), indicating impaired glucose tolerance. Fasting blood glucose and serum insulin levels were also significantly higher in the HF group ($F=49.20$, $p<0.001$ and $F=F=9.67$, $p<0.01$, respectively), as increased insulin was not able to compensate for rising glucose levels (Table 2). The homeostatic model assessment of insulin resistance (HOMA-IR) is often used to obtain a global measure of insulin resistance (Wallace et al., 2004). The HOMA-IR is based on combined glucose and insulin values following an IGPTT. As expected, HOMA-IR was significantly increased in HF fed animals, indicating insulin resistance ($F=13.6$, $p<0.01$; Figure 1B). Impaired glucose tolerance was accompanied by increased measures of oxidative stress. HF feeding resulted in a significant decrease in serum reduced glutathione ($F=13.5$, $p<0.01$) and a decreased reduced:oxidized glutathione ratio ($F=5.15$, $p<0.05$), indicating less capacity to combat oxidative stress (Figure 1C, 1D). While these effects are not necessarily novel, they are included here to demonstrate insulin resistance resulting from the model. Serum levels of unacylated ghrelin and SN tissue expression of mitochondrial uncoupling protein 2 (UCP2) were also analyzed (Table 2), but did not differ significantly between groups.

HF diet impairs nigrostriatal DA release

Potassium-evoked striatal DA release was analyzed using *in vivo* electrochemistry. A representative plot of DA responses is shown in Figure 2A. The amplitude of striatal DA release was significantly less in HF-fed animals compared to chow-fed animals for the same KCl volume ($F=16.58$, $p<0.01$; Figure 2B). Signal rise times did not differ between the two groups (Table 2), ruling out possible differences in diffusion as an explanation. Interestingly, the amplitude of striatal DA release was positively correlated with HOMA-IR, as more insulin sensitive animals exhibited greater DA responsiveness ($p<0.01$, Figure 2C).

Measures of DA uptake and turnover are reduced by a HF diet

In addition, DA uptake was markedly slower in HF-fed rats: T_{80} was increased ($F=4.58$, $p<0.05$; Figure 3A), indicating that following HF feeding, the average time required for DA concentration to decay was greater. The effect on DA uptake is also evident when analyzing T_c, or clearance rate, which was decreased ($F=4.73$, $p<0.05$; Figure 3B). There was no statistical difference in DA content between the HF diet and chow diet groups (Figure 3C). However, in HF-fed animals, we observed a robust decrease in the DOPAC/DA ratio, which indicates decreased DA turnover ($F=5.84$, $p<0.05$; Figure 3D) and is consistent with *in vivo* electrochemical measures.

Iron deposition and transport is increased following HF feeding

The effect of a HF diet on iron deposition was also analyzed (Figure 4A). MRI T2 mapping of the SN revealed a significant difference in T2 values between HF and chow-fed rats ($F=5.14$, $p<0.05$ Figure 4B), indicating increased iron deposition. Altered expression of proteins involved in iron transport was also observed in the SN and further indicates increased iron deposition. The protein transferrin receptor 1 (TfR1) plays a role in cellular iron import, while ferroportin facilitates iron export. In HF-fed animals, ferroportin expression was increased ($F=5.021$, $p<0.05$, Figure 5A), while TfR1 was decreased ($F=4.253$, $p=0.05$,

Figure 5B), indicating that the cell may be compensating for increased iron load. We also observed differential expression of DMT1, another protein responsive to iron levels and involved in iron transport ($F=4.50$, $p<0.05$, Figure 5C). The protein transferrin (Tf) was significantly increased in this region ($F=4.42$, $p<0.05$, Figure 6A), and we observed a trend for increased transferrin receptor 2 (TfR2) expression ($p=0.07$, Figure 6B). Finally, we also measured hepcidin, which can regulate iron transport through modification of ferroportin. We observed a small but non-significant decrease in hepcidin expression (Table 2).

To determine whether circulating iron levels contributed to iron deposition, we analyzed levels of ferritin in serum. Serum ferritin did not differ between groups (Figure 7A), so it is unlikely that systemic iron levels were affected by diet. However, insulin signaling through the phosphoinositol 3-kinase (PI3-K) pathway increases cell-surface iron transporter expression and cellular iron transport in adipocytes (Davis et al., 1986, Ko et al., 2001). As an index of the PI3-K pathway, we measured phosphorylation of AKT on residue Ser473, which is representative of AKT activation (Alessi et al., 1996). $pAKT_{ser473}$ was increased in the SN ($F=7.23$, $p<0.05$), indicating increased AKT activation (Figure 7B). Because insulin signaling has been shown to increase iron transport in other tissues, it is possible that increased SN insulin signaling could increase iron transport in this region.

Discussion

In this study, a 12 week HF diet resulted in peripheral insulin resistance and oxidative stress. These changes were accompanied by impaired DA function in the dorsal striatum and impaired SN iron homeostasis. Specifically, *in vivo* electrochemical measures of DA neuron function revealed decreased potassium-evoked DA release, which correlated with the degree of insulin resistance. Further impairment of neuronal function was evident by decreased DA clearance in HF-fed animals compared to chow-fed controls. MRI showed a significant decrease in T2 values in the SN of HF-fed rats, indicating increased iron deposition, and expression of iron transport proteins was affected in the SN. Taken together, we have shown that HF diet-induced insulin resistance contributes to impaired function of nigrostriatal DA neurons and may play a role in increased iron deposition in the SN.

The purpose of this experiment was to sample the dorsal striatum as in previous microdialysis and electrophysiological studies (Stanford et al., 2001, Stanford and Gerhardt, 2004). We selected the dorsal striatum because it receives DA input from the SN, where we measured iron homeostasis. (Macdonald and Monchi, 2011). Our results are the first to demonstrate a substantial detrimental effect of a HF diet on specific parameters of DA function in this region of the nigrostriatal pathway. Stimulation with potassium evokes neurotransmitter release in a calcium-dependent manner, mimicking normal neurotransmission (West and Galloway, 1998). Our *in vivo* electrochemical analysis revealed that potassium-evoked DA release was robustly attenuated in HF-fed rats and correlated with HOMA-IR: decreased DA release was more evident in animals with a greater degree of insulin resistance. DA uptake was also impaired in HF-fed animals. The time required to clear DA (T_{80}) was significantly increased, while the rate of clearance (T_c) was decreased. Although striatal DA content was not different between groups, striatal DA turnover was substantially decreased, supporting the functional *in vivo* electrochemical

measures. The observed attenuation in striatal DA turnover in the nigrostriatal pathway may be a consequence of decreased membrane-associated DA transporter in the striatum (South and Huang, 2008). Our findings of impaired *in vivo* DA function in the dorsal striatum extend previous reports of dietary effects on mesolimbic neurons (nucleus accumbens) in brain slices (Davis et al., 2008, Geiger et al., 2009). In the context of parkinsonism, it is interesting to note that the effects of HF feeding on potassium-evoked striatal DA release and clearance in these young adult rats resemble the effects observed previously in senescent 2-year-old F344 rats (Hebert and Gerhardt, 1998).

Given the importance of iron in PD pathogenesis, MRI T2 mapping was performed to further investigate the effects of HF feeding on iron deposition in nigrostriatal neurons. MRI provides a non-invasive method to investigate iron deposition in PD (Graham et al., 2000, Wallis et al., 2008). Lower T2 values indicate increased iron deposition, as spin dephasing from magnetic fields surrounding iron deposits results in loss of signal (reviewed in (Schenck and Zimmerman, 2004)). It has been shown that iron deposition, as measured by T2 weighted MRI, is increased in many neurodegenerative diseases, including PD, as well as in normal aging (Brass et al., 2006). In our study, MRI revealed significantly lower T2 relaxation times in the SN of HF-fed animals compared to chow-fed animals, indicating increased iron levels. It is established that iron plays a role in the generation of highly reactive radicals through Fenton chemistry and may promote DA auto-oxidation (Bharath et al., 2002). Thus, increased iron deposition may be an early event that contributes to DA neuron dysfunction.

Altered expression of iron transport proteins in the SN provides additional evidence of increased iron deposition. Some proteins are responsive to iron levels and contain an iron response element. If the iron response element is contained in the 3' untranslated region, the transcript is stabilized in response to low iron or down-regulated in response to high iron

levels (Anderson and Vulpe, 2009, Kaur et al., 2009). The iron responsive proteins TfR1 and DMT1 contain an iron response element in the 3' untranslated region and were decreased in the SN of HF-fed animals. As TfR1 is involved in iron import, increased cellular iron content may contribute to the observed compensatory down-regulation of TfR1 expression in our study. Our observed downregulation of the isoform of DMT1 that contains a 3' IRE is logical in light of our other findings, but should not be overinterpreted. It has previously been shown that DMT1 expression is increased in the SN of PD patients (Salazar et al., 2008). However, our model is not an overt PD model, as we did not observe any DA depletion. In addition, there are four DMT1 isoforms, two of which do not contain an IRE. In the context of this study, decreased DMT1 can be interpreted as a marker of high iron content but the significance of this decrease remains unknown.

However, if the iron response element is contained in the 5' untranslated region, translation is blocked in conditions of low cellular iron and increased when iron is abundant (Anderson and Vulpe, 2009). Ferroportin is the primary iron exporter and contains an iron response element in the 5' untranslated region (Anderson and Vulpe, 2009). Studies have shown increased ferroportin mRNA and protein expression with increased iron (Aydemir et al., 2009, Yang et al., 2002). In our study, ferroportin expression was significantly increased in the SN of HF-fed rats, which is likely to result in increased iron export from the cell. We also measured SN levels of hepcidin, which can control ferroportin through post-translational modification (Nemeth and Ganz, 2006). We observed a non-significant decrease in hepcidin expression. Although this is in line with our observations of increased ferroportin, the non-significant effect on hepcidin suggests that in our study, control of ferroportin is primarily post-transcriptional, through the IRP/IRE system, rather than post-translational, via hepcidin. The differential regulation of TfR1 and ferroportin may represent a compensatory response by the SN to manage a higher iron load.

One outstanding issue in the field of iron homeostasis is how iron gets transported into mitochondria. Iron transport is essential for mitochondrial function (Richardson et al., 2010), but aberrant mitochondrial iron transport could be detrimental. It has been suggested that mitochondrial iron accumulation increases mitochondrial oxidative damage and dysfunction (Seo et al., 2008), and mitochondrial complex I function is impaired in PD (Beal, 2003, Schapira et al., 1989). One hypothesis regarding mitochondrial iron transport that has gained recent support involves Tf and TfR2. Both Tf and TfR2 are localized to mitochondria in DA neurons, are increased with rotenone treatment, and mediate mitochondrial iron transport (Mastroberardino et al., 2009). We observed a significant increase in Tf and a trend for increased TfR2 expression in the SN of HF-fed rats, which may indicate increased mitochondrial iron transport.

The iron storage protein ferritin can be used to gauge whole body iron levels (reviewed in (Wang et al., 2010)). We measured circulating ferritin to determine if systemic iron levels were affected by diet. Ferritin was not different between groups, so it is likely that tissue-specific iron transport, rather than systemic iron overload, contributes to iron dysregulation in the SN. Our 12-week HF diet resulted in impaired glucose tolerance and peripheral hyperinsulinemia. This is relevant because, interestingly, insulin affects iron metabolism (Fernandez-Real et al., 2002). In fat cells, Tf co-localizes with glucose transporters and insulin-like growth factor receptors in microsomes (Tanner and Lienhard, 1989) and insulin stimulates iron uptake by redistributing Tf receptors to the cell membrane (Davis et al., 1986). Because insulin can cross the blood brain barrier (Banks, 2004) and insulin receptors exist in the SN (Moroo et al., 1994), it is possible that iron transport was altered by the increased insulin levels produced by our HF diet. This is supported by our observation of increased AKT phosphorylation, an indicator of increased insulin signaling, in the SN. Insulin is known to activate (phosphorylate) AKT through the PI3-K pathway, and

insulin transport across the blood brain barrier is not saturated at plasma insulin levels observed in this experiment (Baura et al., 1993). Insulin stimulation has been shown to increase presentation of TfR by 60%, and this is likely mediated by PI3-K signaling, as PI3-K inhibition decreases cell surface TfR (Ko et al., 2001).

It should be noted that insulin is usually thought to be beneficial for the brain. Intranasal insulin has been consistently shown to improve memory, and insulin signaling can positively affect cell survival (Benedict et al., 2011, van der Heide et al., 2006). However, the effects of insulin in the brain are complex. Insulin receptor substrate 2 (IRS2), a main modulator of brain insulin signaling, can negatively regulate memory formation (Irvine et al., 2011), and calorie restriction (through decreased IRS2 mediated insulin signaling) has been linked to increased longevity (Taguchi et al., 2007). In the context of Alzheimer's disease, insulin has been shown to increase levels of the amyloid beta 42 (Craft, 2009), possibly by interfering with insulin degrading enzyme, which degrades amyloid beta (Qiu et al., 1997). It is likely that insulin can be detrimental at levels that are either chronically lower or higher than normal. We cannot conclude that insulin itself contributed to increased iron deposition in our study, but it is possible that insulin signaling may play a role in our observations of altered iron homeostasis. It would be interesting for future studies to directly measure the effects of insulin on expression of iron transport proteins in neurons.

Other factors that could compromise the function of DA neurons in the nigrostriatal pathway following HF feeding were also analyzed. Oxidative stress occurs peripherally in response to HF feeding, even prior to the onset of insulin resistance (Matsuzawa-Nagata et al., 2008). We observed a significant decrease in the level of reduced serum glutathione and the ratio of reduced to oxidized glutathione in HF-fed animals compared to the chow group, indicating peripheral oxidative stress. HF feeding increases markers of oxidative stress in multiple brain regions, including the SN (Fachinetto et al., 2005, Morrison et al., 2010,

Zhang et al., 2005), so it is likely that oxidative stress was also increased in the SN in our 12-week HF diet model. In line with our findings, oxidative damage decreases dopamine transporter expression and DA metabolite levels (Hatcher et al., 2007) so the contribution of oxidative stress to the observed deficits in DA function cannot be ruled out.

We also measured ghrelin, a hormone affected in obesity. Previous studies indicate that ghrelin can be neuroprotective against DA neuron-specific toxins and that this protection occurs via UCP2 (Andrews et al., 2009, Moon et al., 2009). Since decreased ghrelin could make cells more vulnerable to damage, we measured unacylated ghrelin, the most abundant form of ghrelin in serum (Delhanty et al., 2006) and UCP2 expression in the SN. In our study, we did not observe a significant difference in either ghrelin or UCP2 levels between groups, making it unlikely that decreased ghrelin contributes to the observed alterations in nigrostriatal DA function. One other potential player in our observations, specifically, the observed increase in AKT phosphorylation, is leptin. Leptin levels are elevated with increasing adiposity (Maffei et al., 1995) and both leptin and insulin can affect insulin signaling in neurons (Benomar et al., 2005). We did not measure leptin in this study and cannot discount this hormone as a potential player in our observed effects.

Conclusions

We have shown that HF diet-induced insulin resistance produces profound *in vivo* functional effects on nigrostriatal neurons. HF-fed rats exhibited attenuated DA release and uptake in the striatum, and insulin resistance correlated with decreased DA amplitude. Our findings are the first to characterize nigrostriatal DA function *in vivo* in the context of HF-diet induced insulin resistance. These same nigrostriatal neurons exhibited markers of increased iron deposition and a response to increased iron load in the SN. Although other mechanisms cannot yet be ruled out, alterations in iron homeostasis in response to a HF diet could impact nigrostriatal DA neuron function. These changes may precede neurodegeneration

and overt DA depletion. Future studies are needed to further investigate the role of iron and insulin signaling on DA neuron function.

Acknowledgments

We thank Susan Smittkamp and George Quintero for technical assistance. This work was supported by NIH grant AG026491 and P20 RR016475, Kansas Intellectual and Developmental Disabilities Research Center grant HD02528, the Kansas City Area Life Sciences Institute, and predoctoral National Research Service Award NS063492 awarded to J. K. Morris, with core support from MRRC and Hoglund Brain Imaging Center.

Table 2.1

High fat diet composition

Ingredients	**g/kg**
Casein	254
Sucrose	85
Cornstarch	169
Vitamin mix	11.7
Choline Chloride	1.3
Mineral mix	67
Bran	51
Methionine	3
Gelatin	19
Corn oil	121
Lard	218

Table 2.2

Additional metabolic and neuronal measures

Measure	Chow	High Fat
Final Body Weight (g)	372.1 ± 6.98	483.2 ± 4.19*
Food Intake (kCal / day)	61.3 ± 1.88	71.0 ± 1.49*
Iron intake (mg / day)	5.74 ± 0.057	5.36 ± 0.180*
Epididymal Fat (g)	9.88 ± 0.648	23.35 ± 0.503*
Fasting glucose (mg / dL)	104.8 ± 1.02	131 ± 3.13*
Fasting insulin (μU / mL)	12.15 ± 2.57	44.6 ± 8.48*
Unacylated Ghrelin (pg/mL)	1178.12 ± 87.0	1174.10 ± 42.8
UCP2 (SN)	0.554 ± 0.048	0.533 ± 0.033
Hepcidin (SN)	0.420 ± 0.031	0.360 ± 0.021
Rise time (sec)	12.3 ± 0.950	13.4 ± 0.589
IPGTT Area under curve (AUC)	20913.7 ± 1192	27306.9 ± 2007*

* $p<0.05$

FIGURE 2.1

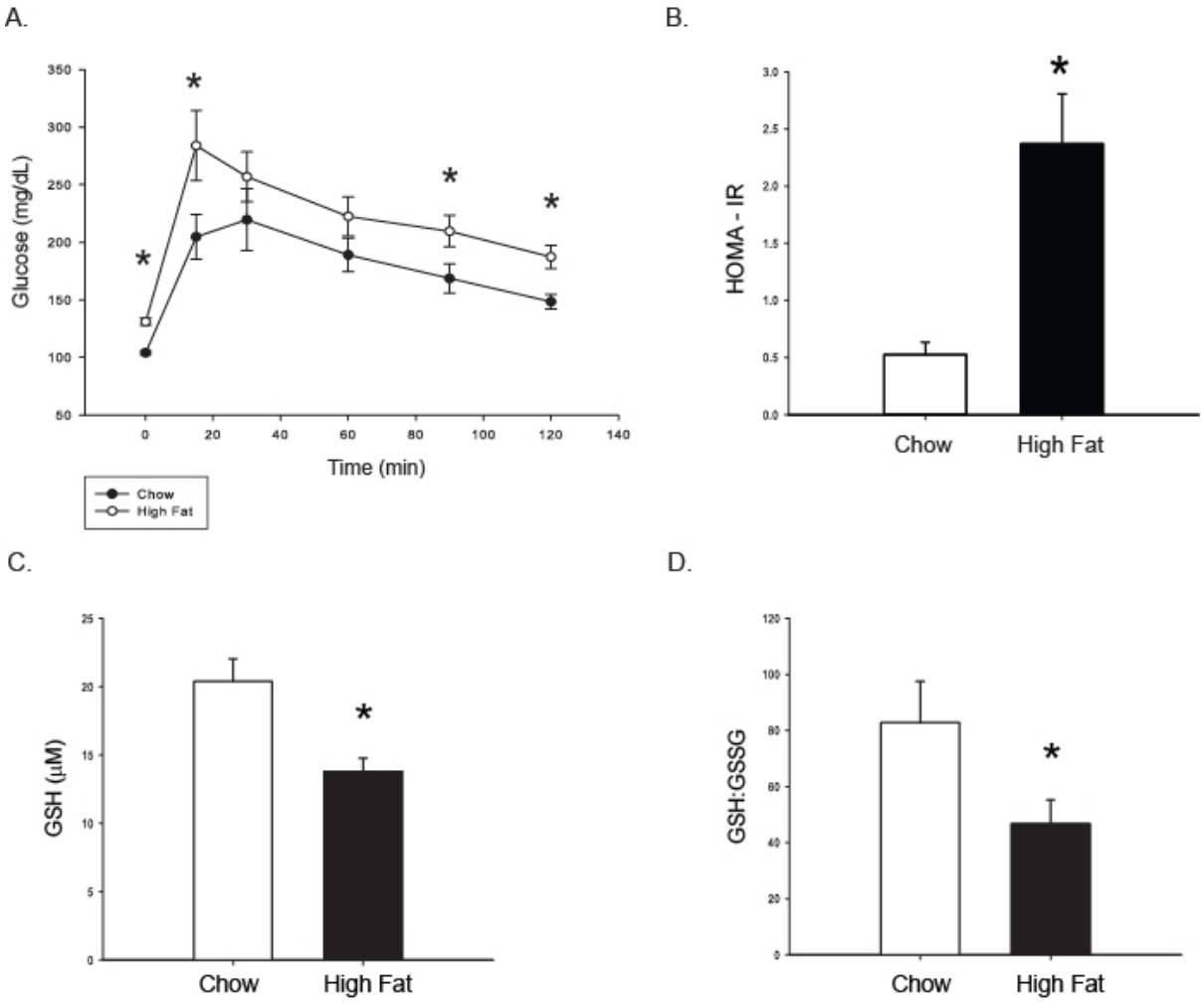
A.
B.
C.
D.
Glucose (mg/dL)
Time (min)
Chow
High Fat
HOMA - IR
GSH (μM)
GSH:GSSG
Chow
High Fat

Figure 2.1. Peripheral glucose tolerance and oxidative stress. After an overnight (12 hour) fast, an intraperitoneal glucose tolerance test was performed. A 60% glucose solution was administered intraperitoneally at 2g glucose/kg body weight. **(A)** Glucose was measured in tail blood at six time points: 0,15,45,60, 90, and 120 minutes after the glucose bolus (injection at t=0). Over the course of the test, glucose levels were higher in HF fed animals. HOMA-IR was also significantly increased **(B)**, indicating insulin resistance. Serum levels of reduced glutathione **(C)** and the ratio of reduced to oxidized glutathione **(D)** were measured to gauge diet-induced oxidative stress. HF-feeding decreased reduced glutathione levels and decreased the ratio of reduced to oxidized glutathione. Values are means ± SE for 11-15 rats per group. *P≤0.05 chow vs. HF.

FIGURE 2.2

A.

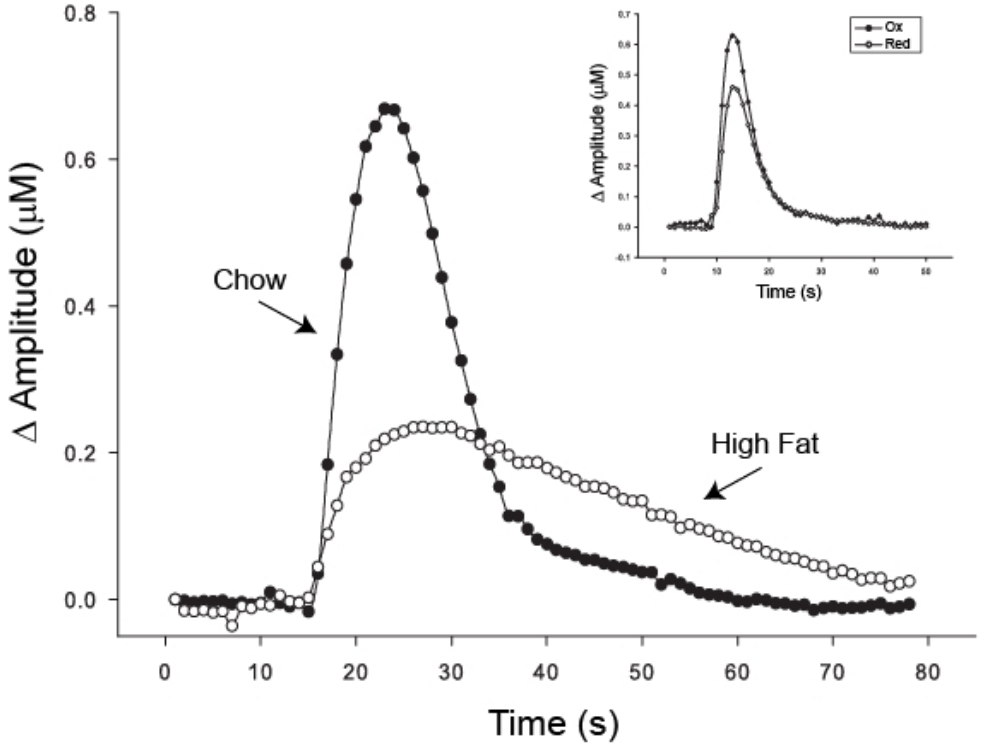

B.

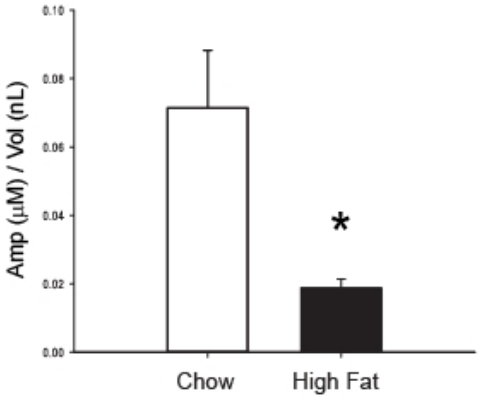

C.

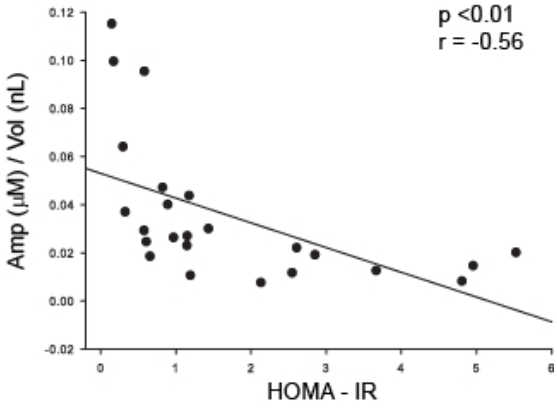

Figure 2. Diet-induced insulin resistance attenuates striatal DA release. *In vivo* electrochemistry was used to measure potassium-evoked DA release in the striatum. A representative plot of evoked DA signals seen in response to a 50nL KCl stimulus in a HF vs. Chow animal is shown **(A)**. A representative plot of redox ratios indicates specific detection of DA in our study (inset)**.** HF-feeding significantly decreased the amount of DA released per volume of stimulus **(B)**. The degree of insulin resistance (HOMA-IR) correlated negatively with the evoked DA concentration: more insulin resistant animals were less responsive to stimulus **(C)**. Values are means ± SE for 11-15 rats per group. *$p<0.05$ chow vs. HF.

FIGURE 2.3

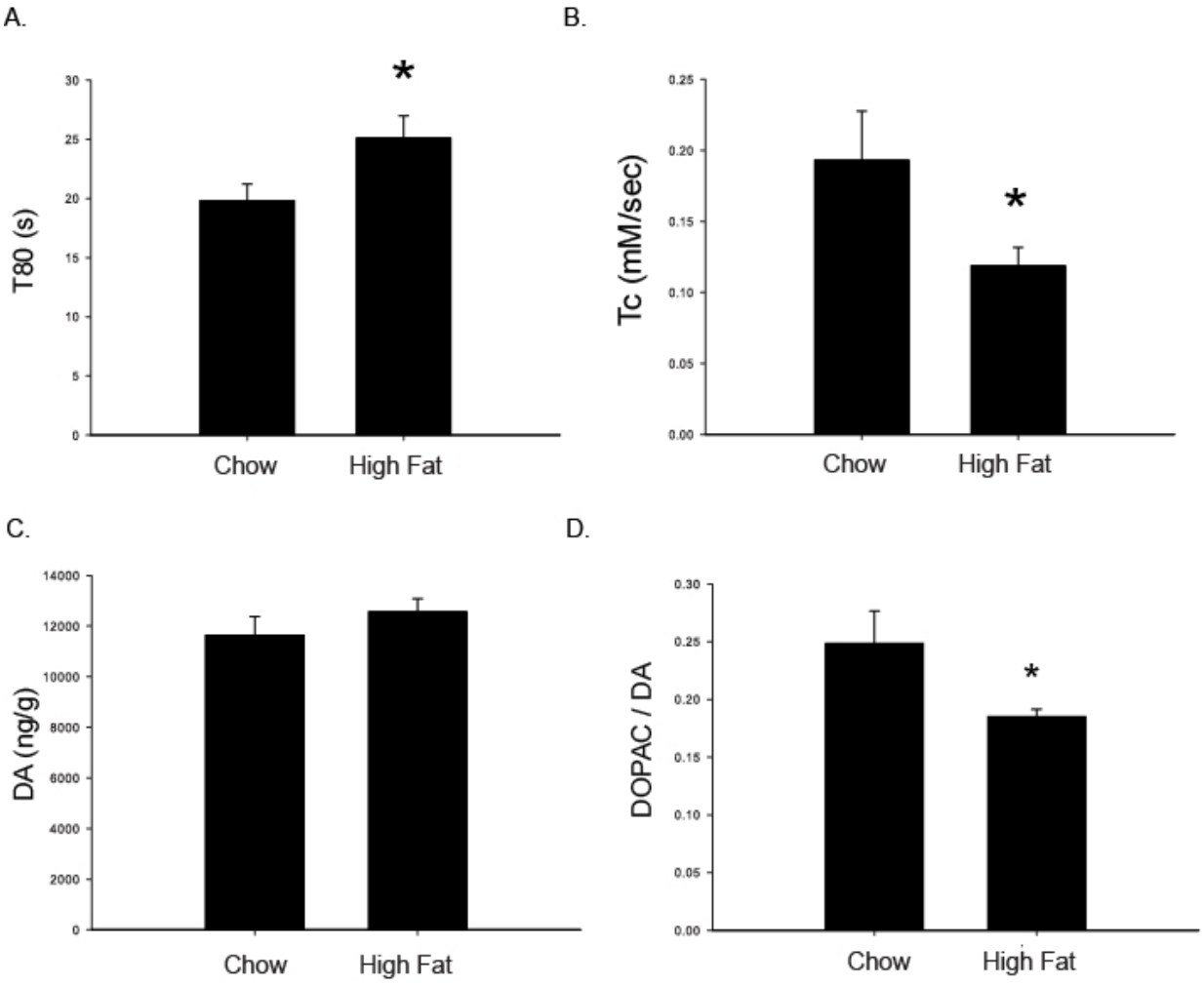
A.
T80 (s)
30
25
20
15
10
5
0
*
Chow
High Fat
B.
Tc (mM/sec)
0.25
0.20
0.15
0.10
0.05
0.00
*
Chow
High Fat
C.
DA (ng/g)
14000
12000
10000
8000
6000
4000
2000
0
Chow
High Fat
D.
DOPAC / DA
0.30
0.25
0.20
0.15
0.10
0.05
0.00
*
Chow
High Fat

Figure 2.3. Uptake and turnover mechanics are affected by diet. The rate of DA uptake was also affected by diet. The amount of time required to clear DA (T_{80}) was increased **(A)** and the rate of clearance (T_c) was decreased **(B)** with a HF diet. Although DA content was not affected **(C)**, the DOPAC/DA ratio **(D)**, which indicates decreased DA turnover, was significantly decreased in HF-fed animals. Values are means ± SE for 11-15 rats per group. *$p<0.05$ chow vs. HF.

FIGURE 2.4

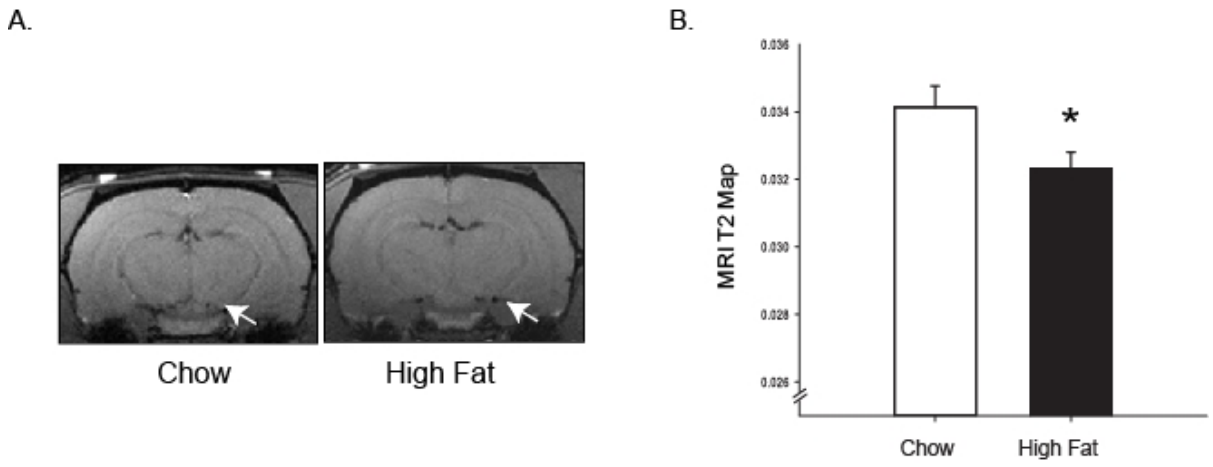
A.
B.
Chow
High Fat
MRI T2 Map
0.036
0.034
0.032
0.030
0.028
0.026
*
Chow
High Fat

Figure 2.4. Markers of iron deposition are increased with HF feeding. Magnetic resonance imaging (MRI) was performed on a subset of rats. MRI revealed hypointensity in the SN region, denoted by an arrow **(A)**. T2 values were significantly decreased with a HF diet **(B)**, indicating increased iron deposition. Values are means ± SE for 3 rats per group for MRI measures. *p<0.05 chow vs. HF.

FIGURE 2.5

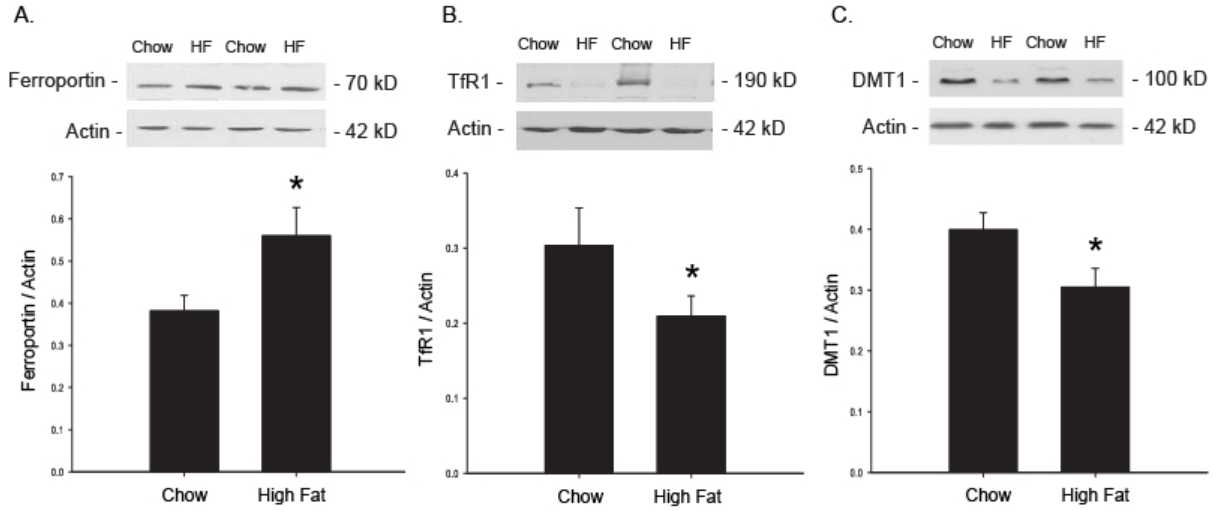
A.
Chow HF Chow HF
Ferroportin -
- 70 kD
Actin -
- 42 kD
Ferroportin / Actin
Chow
High Fat
B.
Chow HF Chow HF
TfR1 -
- 190 kD
Actin -
- 42 kD
TfR1 / Actin
Chow
High Fat
C.
Chow HF Chow HF
DMT1 -
- 100 kD
Actin -
- 42 kD
DMT1 / Actin
Chow
High Fat

Figure 2.5. Expression of IRE-regulated proteins in the SN. Expression of proteins involved in iron transport was also affected in the SN. Ferroportin was significantly increased **(A),** while TFR1 **(B)** and DMT1 **(C)** were significantly decreased, suggesting increased intracellular iron content. Values are means ± SE for 11-15 rats per group. *$p<0.05$ chow vs. HF.

Figure 2.6.

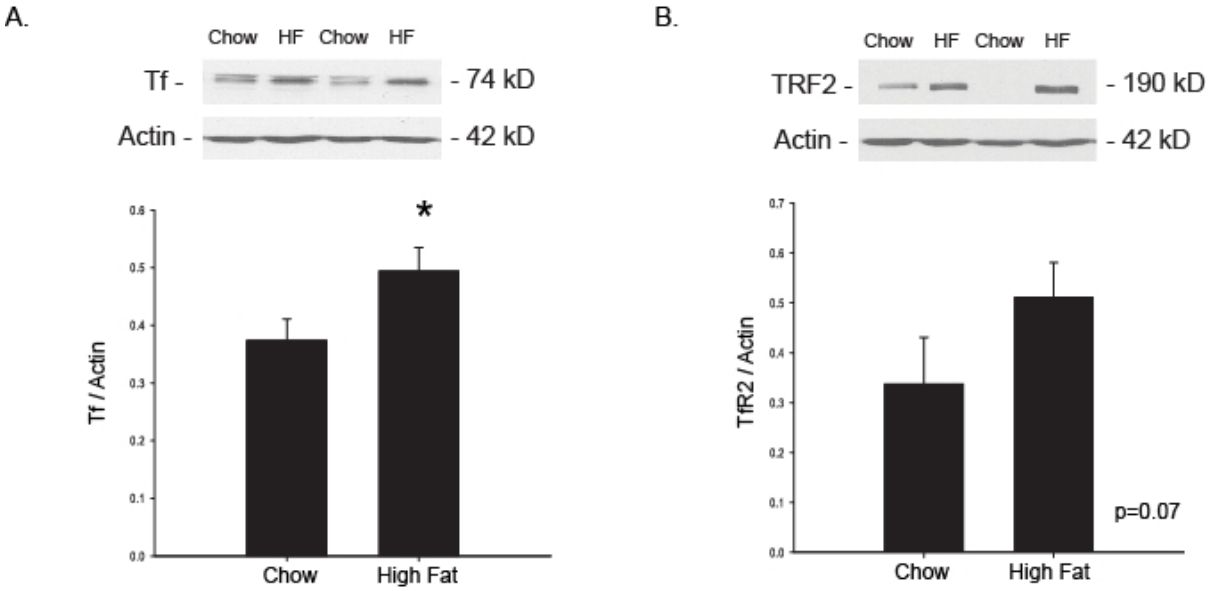
A.
Chow HF Chow HF
Tf -
- 74 kD
Actin -
- 42 kD
Tf / Actin
*
Chow
High Fat
B.
Chow HF Chow HF
TRF2 -
- 190 kD
Actin -
- 42 kD
TfR2 / Actin
p=0.07
Chow
High Fat

Figure 2.6. Expression of non-IRE regulated proteins in the SN. The expression of other proteins involved in iron transport was affected as well. Tf was increased **(A)** and a trend for increased TfR2 was observed **(B),** indicating further effects of increased iron. Values are means ± SE for 11-15 rats per group. *p<0.05 chow vs. HF.

Figure 2.7.

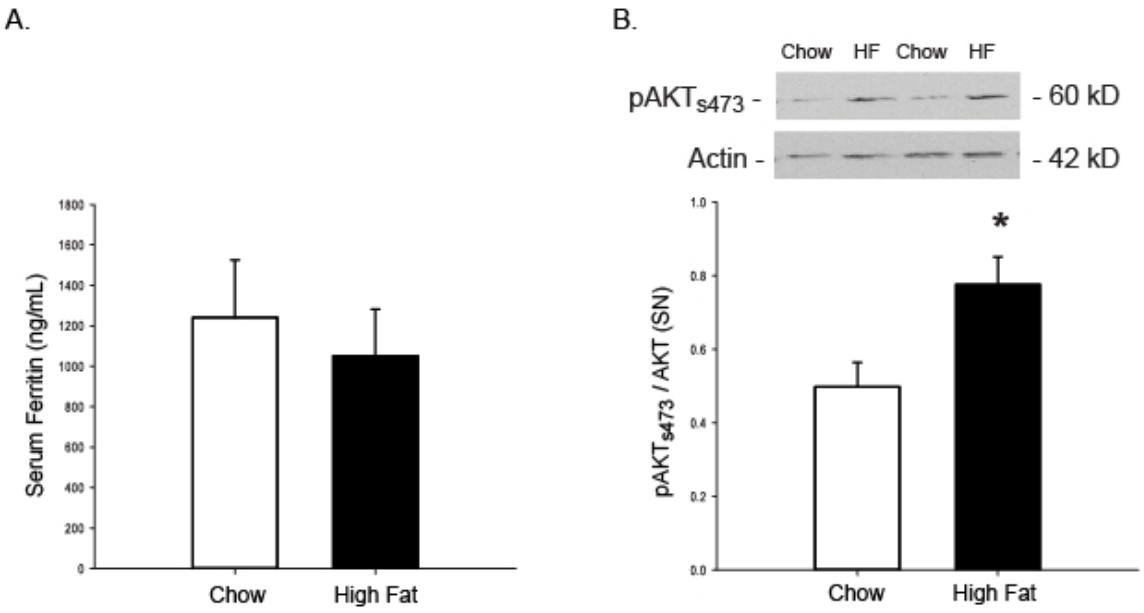
A.
Serum Ferritin (ng/mL)
1800
1600
1400
1200
1000
800
600
400
200
0
Chow
High Fat
B.
Chow HF Chow HF
pAKTs473 -
- 60 kD
Actin -
- 42 kD
pAKTs473 / AKT (SN)
1.0
0.8
0.6
0.4
0.2
0.0
*
Chow
High Fat

Figure 2.7. Mechanisms for increased iron deposition. (A). Ferritin levels were not different between groups, indicating that effects on iron transport may be tissue specific and not due to increased circulating iron. Activation of AKT via phosphorylation was analyzed using Western blot **(B)** and indicates upregulation of PI3-K pathway signaling, which has been implicated in iron transport. Serum ferritin levels were analyzed to determine if whole-body iron stores were affected by diet. Values are means ± SE for 11-15 rats per group. *$p<0.05$ chow vs. HF.

Chapter 3

EFFECTS OF 6-HYDROXYDOPAMINE ON BRAIN AND PERIPHERAL INSULIN SIGNALING

Overview

Although some clinical studies show a link between PD and T2D, it is unclear whether this relationship is bidirectional, whether DA neuron degeneration in PD affects peripheral glucose levels, or whether T2D affects DA function in the brain. To further investigate this relationship, we analyzed the effect of 6-OHDA administration and DA depletion on insulin signaling in the brain and periphery. In the first study, 6-OHDA was administered to young rats, yielding a range of DA depletion levels. With severe striatal DA depletion, impairments in insulin signaling were observed in the striatum, but peripheral glucose tolerance and insulin signaling in muscle were not affected. A follow-up study was performed in middle aged rats, because aging is a risk factor for both diseases. Once again, impaired insulin signaling was observed in the striatum, but animals still did not exhibit peripheral insulin resistance. However, small changes were observed in the insulin curve throughout a glucose tolerance test. These findings suggest that any changes in glycemia following 6-OHDA are likely due to altered insulin secretion and not glucose disposal into muscle. Taken together, the findings of these two experiments do not suggest that the unilateral 6-OHDA model is a good model for studying the effects of DA neurodegeneration in peripheral glucose metabolism and instead indicate that a bilateral model may produce a greater effect.

MEASURES OF STRIATAL INSULIN RESISTANCE IN A 6-HYDROXYDOPAMINE MODEL OF PARKINSON'S DISEASE

J.K. Morris, H. Zhang, A.A. Gupte, G.L. Bomhoff, J.A. Stanford, and P.C. Geiger.

Brain Research (2008) 1240:185-95

ABSTRACT

Clinical evidence has shown a correlation between Parkinson's Disease (PD) and Type 2 Diabetes (T2D), as abnormal glucose tolerance has been reported in >50% of PD patients. The development of insulin resistance and the degeneration of nigrostriatal dopamine (DA) neurons are both mediated by oxidative mechanisms, and oxidative stress is likely a mechanistic link between these pathologies. Although glucose uptake in neuronal tissues is primarily non-insulin dependent, proteins involved in insulin signaling, such as insulin receptor substrate 2 (IRS2) and glucose transporter 4 (GLUT4), are present in the basal ganglia. The purpose of this study was to determine whether nigrostriatal DA depletion affects measures of insulin resistance in the striatum. Six weeks after 6-hydroxydopamine (6-OHDA) infusion into the medial forebrain bundle, rats were classified as having either partial (20-65%) or severe (90-99%) striatal DA depletion. Increased IRS-2 serine phosphorylation, a marker of insulin resistance, was observed in the DA depleted striatum. Additionally, severe depletion resulted in decreased total IRS-2, indicating possible degradation of the protein. Decreased phosphorylation of AKT and expression of the kinase glycogen synthase kinase-3 alpha (GSK3-α) was also measured in the striatum of severely DA depleted animals. Finally, expression of heat shock protein 25 (hsp25), which is protective against oxidative damage and can decrease stress kinase activity, was decreased in the striatum of lesioned rats. Together, these results support the hypothesis that nigrostriatal DA depletion impairs insulin signaling in the basal ganglia.

Introduction

Parkinson's disease (PD) is characterized by degeneration of dopaminergic neurons projecting from the substantia nigra pars compacta (SNpc) to the striatum. This degeneration results in decreased striatal dopamine (DA) content, aberrant neurotransmission throughout the basal ganglia, and motor dysfunction. PD patients also exhibit autonomic and endocrine deficits, such as glucose intolerance and diabetes (Barbeau and Pourcher, 1982, Boyd et al., 1971, Lipman et al., 1974). Insulin resistance, often characterized by impaired insulin signal transduction, diminished glucose uptake, and dysregulated energy metabolism, is frequently preceded by glucose intolerance and can lead to the development of Type 2 Diabetes (T2D).

Clinical studies have revealed a high incidence of glucose intolerance (>50%) in PD (Sandyk, 1993). It has been shown that patients with PD exhibit increased autoimmune reactivity to insulin (Wilhelm et al., 2007), and that PD patients with diabetes have increased PD disease severity (Papapetropoulos et al., 2004). Co-morbidity of PD and T2D is also correlated with a significant increase in the cost of care of affected individuals (Pressley et al., 2003). Hyperglycemia has been suggested to decrease the effectiveness of levodopa (L-DOPA) therapy and increase motor dyskinesias experienced by PD patients (Sandyk, 1993). Further, L-DOPA therapy may exacerbate hyperinsulinemia and hyperglycemia in PD patients (Boyd et al., 1971, Sirtori et al., 1972), possibly by diminishing peripheral glucose disposal in skeletal muscle (Smith et al., 2004). An early marker for the development of peripheral glucose intolerance may be insulin resistance in neural tissues. Hypothalamic parasympathetic nerves affect insulin release by beta cells, while sympathetic nerves act directly on the liver to affect hepatic glucose metabolism (reviewed in (Uyama et al., 2004)). Thus, it is important to understand the mechanistic link between nigrostriatal DA depletion and CNS insulin signaling.

Studies indicate a role for insulin signaling in the basal ganglia. Insulin receptors co-localize with neurons containing tyrosine hydroxylase in the SNpc (Figlewicz et al., 2003, Moroo et al., 1994), and mRNA for insulin receptor is present in human SN (Takahashi et al., 1996). Insulin receptor substrate 2 (IRS2) is also present in the CNS and functions to couple insulin receptor activation to signaling via the IRS-PI3K pathway (Porte et al., 2005). Finally, localization of the insulin-dependent glucose transporter GLUT4 to the brain, including basal ganglia nuclei (El Messari et al., 1998), suggests an important role for insulin signaling in neuronal function. Despite these findings and their clinical implications, preclinical studies examining relationships between nigrostriatal DA depletion and insulin resistance in animal models are lacking.

The purpose of the current study was to test the hypothesis that nigrostriatal dopamine depletion following unilateral 6-hydroxydopamine (6-OHDA) infusion would impair insulin signaling in the basal ganglia. The unilateral 6-OHDA-treated rat is perhaps the most widely studied preclinical model of PD, and the effects of this model on nigrostriatal DA are well documented (Schober, 2004, Yuan et al., 2005). Because insulin resistance has been tied to a post-insulin receptor defect in insulin signaling (Fink et al., 1983), in the current study we measured the expression and activation of proteins involved in post-receptor insulin signaling, including IRS2, AKT, JNK, GSK3-α/β, and Hsp25. To our knowledge, this study is the first to assess brain insulin signaling in the 6-OHDA preclinical model of PD.

Materials and methods

Animals

Twenty male 4 month old Fisher 344 rats were obtained from National Institutes on Aging colonies (Harlan). Rats were housed two per cage, maintained on a 12 hour light/dark cycle, and provided food and water ad libitum. Protocols for animal use were approved by the University of Kansas Medical Center Institutional Animal Care and Use Committee and adhered to the Guide for the Care and Use of Laboratory Animals (National Research Council, 1996).

Materials

Antibodies against phospho-SAPK/JNK(T183/Y185), total SAPK/JNK, phospho-AKT, total AKT, and phospho-GSKα/β (Ser21/9) were obtained from Cell Signaling (Beverly, MA). Anti-phospho-Hsp 25 and anti-Hsp 25 were purchased from Stressgen (Victoria, BC, Canada). Anti-phospho-Ser307-IRS-1 and total GSK3-α/β were obtained from Upstate (Lake Placid, NY), while total IRS-1 was purchased from BD Biosciences (Franklin Lakes, NJ). Antibodies against phospho-Ser731-IRS-2 (corresponding to rat phospho-Ser233) and Actin were obtained from Abcam (Cambridge, MA). Goat-anti-rabbit HRP-conjugated secondary antibodies were purchased from Santa Cruz Biotechnology (Santa Cruz, CA). Goat anti-mouse HRP-conjugated secondary antibodies were obtained from Bio-Rad (Hercules, CA). Chemicals used in HPLC-EC (DA, DOPAC, DHBA) were obtained from Sigma-Aldrich (St. Louis, MO). Enhanced chemiluminescence reagents were purchased from Amersham (Little Chalfont, Buckinghamshire, UK).

6-OHDA Infusion

The 6-OHDA lesion procedure was based on previously published studies (Enna et al., 2006). Rats were anesthetized with Nembutal (50mg/mL) at 1mL/kg body weight prior to surgery and placed into a stereotaxic frame. Rats in the lesion group (n=14) were infused

with 4uL of 6-OHDA in 0.9% NaCl with 0.02% ascorbate into the right medial forebrain bundle (stereotaxic coordinates with respect to bregma: M/L 1.3, A/P -4.4, and D/V -7.8) at a dose of 2.25mg/mL. The infusion rate was 0.25uL/minute over a period of 16 minutes, a flow rate that will limit local tissue damage. The cannula was withdrawn 1 minute after infusion was completed. Identical surgical procedure was followed for rats receiving a sham lesion (n=6), except that sham rats received saline (0.9% NaCl with 0.02% ascorbate) instead of 6-OHDA. Rats were allowed to recover for six weeks post-surgery. The six-week timepoint is a somewhat arbitrary timepoint that was chosen to ensure that the oxidative stress and apoptotic and neurodegenerative processes in the nigrostriatal pathway following 6-OHDA administration were completed.

Intraperitoneal glucose tolerance test (IPGTT)

An IPGTT was performed 48 hours before animals were sacrificed. Animals were fasted overnight (12 hours) prior to the IPGTT. A 60% glucose bolus of D-(+)-Glucose (Sigma) in saline was administered intraperitoneally at t=0. A glucometer (AccuCheck Active) was used to analyze glucose levels in tail blood at timepoints 0,15, 30, 60, 90, and 120 minutes following glucose administration. Tail blood samples (~400µL) were taken at each timepoint and allowed to clot on ice for 30 minutes before being centrifuged at 3,000 x g for 1 hour. Serum was immediately extracted and aliquoted into fresh tubes. Serum insulin was measured using an Insulin (rat) EIA kit (Alpco Diagnostics). Rats were anesthetized with Nembutal (50mg/mL) at 1mL/Kg body weight 45 minutes prior to the IPGTT.

HPLC-EC analysis of Dopamine Content

The HPLC-EC system consisted of a Coulochem III electrochemical detector (ESA), Model 5011A high-sensitivity analytical coulometric cell (ESA), LC-10AS single plunger pump (Shimadzu), and 3µm CAPCELL PAK reversed phase C-18 column (Shiseido). The composition of citrate acetate mobile phase (pH 4) was as follows: octane sulfonic acid

(0.0738 g/L), ethylenediaminetetraacetic acid (0.05 g/L), sodium acetate trihydrate (13.8 g/L), citric acid (14 g/L), triethylamine (0.01%), and methanol (4%). Mobile phase was made using filtered water from a Milli-Q purification system (Millipore) and the solution was subsequently filtered through a 0.2µm nylon membrane filter (Whatman).

Six weeks post-lesion, rats were sacrificed and brains were removed. Bilateral striatum samples were dissected, weighed, and frozen on dry ice to be processed for HPLC-EC and Western blot analysis. Striatal sections were processed for HPLC through sonication in burnt, filtered citrate acetate mobile phase with 50uL DHBA (0.1mM) added to each sample. Following sonication, tubes were centrifuged in a Hermle Z400K refrigerated centrifuge (Midwest Scientific) for 10 minutes at 12,000 x g at 4°C. Supernatants were extracted and placed into Microcon Ultracel YM-10 centrifugal filter devices (Amicon), and centrifuged at 12,000 x g for 1 hour at 4°C. Eluent was collected and used for HPLC analyses. DA depletion values were obtained from HPLC measures by dividing the DA content of the striatum on the lesioned (right) side by the DA content of the striatum on the non-lesioned (left) side of the brain. Rats receiving a lesion were further divided into two groups (partial and severe DA depletion) based upon DA depletion levels.

Western Immunoblotting

Protein samples were processed as previously described (Geiger et al., 2007, Gupte et al., 2008). Frozen striatum samples to be processed for protein analysis were diluted 10x in cell extraction buffer (Invitrogen) with protease inhibitor cocktail (500µL, Invitrogen), sodium flouride (200mM), sodium orthovanodate (200mM) and phenylmethanesulphonylfluoride (200mM) added. Tissue was homogenized using a hand homogenizer, and samples were placed on ice for 1 hour with intermittent vortexing to allow protein extraction to occur. Samples were centrifuged at 3,000 x g at 4°C for 20 minutes. Supernatants were extracted and placed into fresh tubes.

A Bradford assay was performed to determine sample protein concentrations. Samples were analyzed in triplicate using working strength Bradford reagent, diluted 5x from Bradford dye concentrate (BioRad) with filtered distilled water. Based upon protein concentrations, samples were diluted with HES buffer (20mM HEPES, 1mM EDTA, 250M Sucrose, pH 7.4) and reducing sample buffer (0.3M Tris-HCL, 5% SDS, 50% glycerol, 100mM dithiothreitol, Thermo Scientific) to obtain samples of constant concentration for analysis using SDS-PAGE. Due to the large molecular weight of the IRS proteins, samples analyzed for IRS1 and IRS2 phosphorylation and expression were run on 7.5% gels. When examining all other proteins of interest, samples were run on 10% gels.

For SDS-PAGE, the largest number of samples were run on the same gel as possible. After SDS-PAGE, samples were transferred to nitrocellulose membranes. Due to the high molecular weight of IRS2, gels to analyze IRS2 total protein and serine phosphorylation were transferred for 90 minutes at 400mA. All other proteins were transferred for 60 minutes at 200mA. Nitrocellulose membranes were blocked in 5% nonfat dry milk for 1 hour and incubated with primary antibody diluted 1:1000 in 1% milk overnight at 4°C. Secondary antibody corresponding to the host primary antibody of interest was used at a dilution of 1:10,000 in 1% milk for 1 hour at room temperature. Upon exposure, films were scanned at high resolution to obtain digital images. Densitometry analyses were performed using Image J software. Images were normalized for background and repeated densitometry measurements were averaged for each band of interest. All bands of interest shown in figures are taken from the same gel. For analysis of results, phosphorylated protein levels were normalized to total protein levels, while total protein expression was normalized to the loading control actin.

Statistical analysis

Two-way analysis of variance (ANOVA) with striatal hemisphere and experimental group as factors was used to analyze differences in protein expression and activation between sham, partial, and severe lesion groups. No protein expression or activation differences between lesioned and non-lesioned hemispheres were observed for any measure analyzed, so measurements from the left and right striatal hemisphere were averaged to obtain one data point for each animal. ANOVA was used to analyze IRS2 serine phosphorylation and expression, and when appropriate this was followed by a post hoc comparison using the least-significant difference test. Low tissue weights of several animals from the partial depletion group resulted in a lower partial lesion group n-value (N=3) for other proteins analyzed. To account for this, we used nonparametric statistics (Kruskal-Wallis One-Way Analysis of Variance) to analyze measures other than phosphorylated and total IRS2. Multivariate repeated measures analysis was used to compare insulin and glucose levels over the course of an IPGTT, and an unpaired Student's t-test was used to analyze differences between groups at individual time points during the IPGTT. For all analyses, statistical significance was set at $P \leq 0.05$.

Results

Body weight

The Fisher 344 rats used in this experiment had an average initial body weight of 306.3 ± 8.3g. All three groups gained weight over a period of 6 weeks post-lesion. On average, the percent weight gain was 6.2% for sham lesioned rats, 4.9% for rats with partial DA depletion, and 5.5% for rats with severe DA depletion. The between-groups differences in weight gain were not significant at 6 weeks post-lesion ($p>0.05$).

DA depletion

Values for DA and its metabolite dihydroxyphenylacetic acid (DOPAC) in the striatum of animals in each group are given in Table 3.1. Striatal DA depletion following 6-OHDA ranged from 20-99% (Figure 2.1). This range is consistent with previous studies using this protocol (Hudson et al., 1993). As previous studies have done (Skitek et al., 1999), we assigned individual rats to groups based on striatal DA depletion levels. Rats exhibiting partial DA depletion (20-65%) were included in the "partial depletion" group (n=6). This group was compared to rats with DA depletions of greater than 90% (n=8), the "severe depletion" group (Figure 3.1). The mean DA depletion for the partial depletion group was 37.6% ± 13.9, while the mean DA depletion for the severe depletion group was 98% ± 2.7%.

Intraperitoneal glucose tolerance test (IPGTT)

An IPGTT was performed to determine if severe DA depletion affects peripheral glucose tolerance six weeks post-lesion. An IPGTT was not performed on partially lesioned animals. Both serum insulin levels (Figure 3.2A) and blood glucose levels (Figure 3.2B) were measured. A multivariate repeated measures analysis showed no difference in either insulin or glucose levels between groups over the course of the test. However, at one timepoint, (15 minutes), the severely depleted group exhibited an increase in serum insulin

that approaches significance (p=0.06) that is reflected by a significant decrease in blood glucose (p=0.04). No differences were observed between groups at any other timepoint.

Serine phosphorylation of IRS1 and IRS2

Six weeks post-lesion, rats exhibiting severe DA depletion showed a 69% increase in striatal IRS2 serine phosphorylation (F=4.238, p=0.03) when compared to both sham lesioned controls (Figure 3.3A). IRS2 serine phosphorylation was also increased with partial DA depletion, although this increase was not significant when compared to the control group. Serine phosphorylation of IRS1 was not significantly different between sham lesion control rats and rats in either lesion group (Figure 3.4A).

IRS1 and IRS2 protein levels

Serine phosphorylation of IRS1 and IRS2 proteins can result in protein degradation (Kim et al., 2005, Rui et al., 2001). Thus, we evaluated the three experimental groups for total IRS protein content. As expected, the severe DA depletion group that exhibited increased serine phosphorylation also displayed a 47% decrease in total IRS2 protein compared to sham lesioned control rats and a 49% decrease when compared to partially depleted animals (F=3.603, p=0.05) (Figure 3.3B). IRS2 protein content was not significantly different between the control group and rats exhibiting partial DA depletion. IRS1 total protein levels were not significantly different between any groups (Figure 3.4B).

Downstream insulin signaling affects

Protein kinase B (AKT) is a major mediator of insulin signaling that functions downstream of IRS proteins (van der Heide et al., 2006). AKT is activated by phosphorylation in response to insulin, and AKT phosphorylation can be used to gauge insulin sensitivity. We observed a 59% decrease in AKT phosphorylation in severely depleted rats compared to sham lesioned controls, (Figure 3.5A) which was statistically

significant (H=6.224, p=0.04). No significant difference in AKT phosphorylation was observed between partially depleted rats and sham lesioned controls.

Measures of cellular stress

Activation of stress kinases, such as c-Jun N-terminal kinase (JNK) or glycogen synthase kinase 3 (GSK3) in response to a 6-OHDA lesion could contribute to the observed increase in serine phosphorylation in lesioned rats. Lesioned rats exhibiting high levels of DA depletion showed a non-significant increase in JNK phosphorylation six weeks post-lesion (Figure 3.5B). Phosphorylation of GSK3-α and GSK3-β isoforms was also examined. Decreased GSK3 phosphorylation indicates increased kinase activity (Henriksen et al., 2003). A non-significant decrease in GSK3-α and GSK3-β phosphorylation was observed in both partial and severe depletion groups (Figures 3.6A and 3.6C). However, a significant decrease in GSK3-α protein expression (H=6.353, p=0.04) was observed in rats exhibiting both partial and severe DA depletion (Figure 3.6B). GSK3-β expression was not statistically different between either depletion group and control rats (Figure 3.6D). Both depletion groups showed a significant decrease (H=8.894, p=0.02) in Hsp25 expression. Hsp25 was decreased by 43% in severely depleted rats and 59% in partially depleted animals compared with control rats (Figure 3.7).

Discussion

We report here effects on insulin signaling pathways in the basal ganglia following nigrostriatal DA depletion. Signs of impaired insulin signaling in the basal ganglia in rats with severe DA depletion included increased serine phosphorylation of IRS2, decreased IRS2 protein content, and decreased AKT phosphorylation. Decreased GSK3-α and Hsp25 expression were also observed in this group. Animals in the partial depletion group exhibited decreased GSK3-α and Hsp25 expression without a significant effect on IRS2 phosphorylation or expression or AKT phosphorylation. Additionally, a non-significant increase in JNK activation was observed with severe DA depletion, and a non-significant increase in GSK3-α and GSK3-β activation was observed in both depletion groups. At six weeks, no difference in peripheral glucose or insulin levels existed between severely depleted rats and controls over the course of an IPGTT, indicating that a dysfunction in brain insulin signaling may precede changes in peripheral glucose tolerance.

The mechanisms and pathways involved in insulin signal transduction are similar for the periphery and the brain (Reagan, 2005). Insulin signaling requires interactions between IRS proteins and insulin receptor, and these interactions are mediated by the phosphorylation of IRS proteins on tyrosine residues (White, 1998). This process also allows for the binding of effector proteins. Although four IRS isoforms exist, IRS3 and IRS4 are thought to play only minor roles in insulin signaling (Sykiotis and Papavassiliou, 2001) and were not measured in the current study. Conversely, IRS1 and IRS2 are expressed in most tissues and modulate the majority of the insulin signaling in the body (White, 2002). IRS1 is most important in skeletal muscle signaling (Sykiotis and Papavassiliou, 2001), where it has been extensively characterized. Studies have shown IRS2 likely plays a more prominent signaling role in tissues such as liver, pancreas, and brain (Dong et al., 2006, Lin et al., 2004, Taguchi et al., 2007), where its role has been most thoroughly characterized in the

hypothalamus (Morton et al., 2007, Pardini et al., 2006, Porte et al., 2005). IRS2 employs an additional interaction with the insulin receptor via its kinase regulatory loop binding domain, allowing discernment between IRS1 and IRS2 signals (Sawka-Verhelle et al., 1997). Serine phosphorylation of IRS1 and IRS2 impairs IRS interaction with the insulin receptor and decreases the ability of these proteins to propagate the insulin signal by undergoing tyrosine phosphorylation (Aguirre et al., 2002, Paz et al., 1997). Our observation of a DA depletion-related increase in IRS2 serine phosphorylation, with little change in serine phosphorylation of IRS1 between either lesion group and sham lesion controls, implicates IRS2 in neural insulin resistance in parkinsonism.

In addition to inhibiting tyrosine phosphorylation, serine phosphorylation of IRS1 and IRS2 can target these proteins for degradation (Kim et al., 2005, Pederson et al., 2001), providing another mechanism by which insulin signaling can be modified. It has been suggested that IRS1 ubiquitin ligase may associate with a serine kinase which acts on IRS1 (Zhande et al., 2002), and that a partial explanation for decreased insulin signaling in response to serine phosphorylation is proteasome mediated degradation of IRS proteins (Rui et al., 2001, Rui et al., 2002). Our finding of a significant decline in total IRS2 protein in rats with severe DA depletion, but not partial DA depletion, is consistent with increased serine phosphorylation in severely depleted rats. Because IRS2 degradation occurs only with severe and chronic IRS2 serine phosphorylation, it is likely that the non-significant increase in IRS2 serine phosphorylation in the partial depletion group was not sufficient to trigger significant IRS2 degradation. The fact that we observed no difference in total IRS1 protein between lesion and sham lesion groups is consistent with our negative findings regarding expression and activity of IRS1 following DA depletion.

A major mediator of insulin signaling that functions downstream of IRS proteins is AKT (van der Heide et al., 2006). AKT phosphorylation occurs in response to insulin and

can be used to gauge insulin sensitivity. AKT activity promotes translocation of the glucose transporter GLUT4 to the plasma membrane (Wang et al., 1999), which allows glucose uptake, and AKT activation is tied to cellular survival (van der Heide et al., 2006). Basal AKT activity also influences DAT expression on the plasma membrane (Garcia et al., 2005). Because of the multifaceted roles of AKT, we analyzed AKT activation in the striatum of 6-OHDA lesioned animals. AKT phosphorylation was significantly decreased in severely depleted rats when compared to sham lesioned controls, indicating a defect in signaling. No significant difference was observed between partially depleted rats and controls.

To investigate a mechanism for increased IRS2 serine phosphorylation, we analyzed two well characterized stress kinases: c-Jun N-terminal kinase (JNK) and glycogen synthase kinase 3 (GSK3). JNK is activated via phosphorylation in response to cellular stress (Bloch-Damti and Bashan, 2005). Specifically, active JNK may contribute to serine phosphorylation of IRS proteins and inhibit insulin signaling (Aguirre et al., 2002, Werner et al., 2004, Zick, 2005). The JNK pathway has also been linked to PD (Peng and Andersen, 2003). JNK contributes to apoptosis of dopaminergic neurons in response to paraquat and rotenone, two neurotoxins used in animal models of PD (Klintworth et al., 2007). Conversely, inhibiting JNK activation facilitates survival of dopaminergic neurons in a 6-OHDA animal model of PD (Rawal et al., 2007). Thus, JNK plays a role in both modulation of insulin signaling and PD pathogenesis. Our data reveal a non-significant increase in active (phosphorylated) JNK in the striatum of severely lesioned rats six weeks post-lesion.

GSK3 is classically known for its role in inhibiting glycogen synthesis by phosphorylating glycogen synthase under basal conditions. Insulin stimulation causes GSK3 phosphorylation, inactivating its kinase activity and allowing glycogen synthesis to occur (Lee and Kim, 2007). However, GSK3 activity has also been suggested to contribute to serine phosphorylation of both IRS1 and IRS2 (Liberman et al., 2008, Sharfi and Eldar-

Finkelman, 2008) in rodent models. Two isoforms of GSK3 exist, GSK3-α and GSK3-β. Using Western blot analysis, we measured the phosphorylation levels of both isoforms. A non-significant increase in GSK3-α and GSK3-β activation (decreased phosphorylation) was observed in both depletion groups. GSK3-α expression was significantly decreased in both groups, although no difference in GSK3-β expression was observed. GSK3-β is highly expressed in the central nervous system, where it localizes to neurons (Leroy and Brion, 1999). A previous study reported that 6-OHDA treatment inhibits GSK3-β phosphorylation in a human dopaminergic neuroblastoma cell line and induces GSK3-β dephosphorylation in two additional cell lines (Chen et al., 2004), activating its kinase activity. The role of GSK3- α in the brain has not been as clearly defined but likely exhibits some redundant actions of GSK3-β. GSK inhibition is associated with activation of neuronal survival pathways (Garcia-Segura et al., 2007), and stimulation of glucose transport (Henriksen et al., 2003), and both isoforms have been implicated in tau phosphorylation in Alzheimer's disease (Baum et al., 1996).

Previous studies have shown Hsp25 (the rodent form of human Hsp27) to be protective against oxidative stress (Escobedo et al., 2004). Specifically, Hsp25 protects against damage to mitochondrial complex I (Downs et al., 1999), which is damaged in PD (Beal, 2003). In addition to its protective role against oxidative damage, Hsp25 has been shown to bind the stress kinase inhibitor of kappa kinase beta (IkKβ), decreasing its activity (Park et al., 2003). Because IkKβ is another stress kinase that is suggested to contribute to serine phosphorylation of IRS proteins and is linked to insulin resistance (Bloch-Damti et al., 2006, Gupte et al., 2008), a decrease in Hsp25 expression could be also linked to IRS serine phosphorylation. We observed a decrease in the expression of Hsp25 in rats exhibiting both partial and full DA depletion. This could indicate increased vulnerability to oxidative stress, even in the absence of altered phosphorylation levels. Because the pool

from which activated Hsp25 can be drawn is decreased, it is possible that the Hsp response upon exposure to stress conditions will be impaired, resulting in cellular and mitochondrial damage.

When given an IPGTT, severely depleted rats exhibited a nearly significant increase in serum insulin levels and a significant drop in blood glucose levels 15 minutes post-bolus compared to controls. Chronic hyperglycemia is often preceded by increased metabolic demand for insulin and compensation by beta cells to produce more insulin. This state of hyperinsulinemia typically precedes glucose intolerance (Smiley and Umpierrez, 2007). The changes we observe at 15 minutes post-bolus may indicate that changes in peripheral glucose tolerance are beginning to occur six weeks post-lesion. However, severely depleted rats are not glucose intolerant, as glucose and insulin levels are not different between groups at any other timepoint or over the course of the test. It is thus possible that changes in brain insulin signaling precede peripheral glucose intolerance.

Our statistical analyses revealed no effect of striatal hemisphere on any protein measures addressed here. Although we did not measure diffusion, it is highly unlikely that unilaterally administered 6-OHDA diffused into the contralateral hemisphere. Our findings therefore suggest that the between-groups differences in expression and activation of proteins involved in insulin signaling in this experiment are due to DA depletion rather than direct effects from the toxin. It has been shown that the contralateral striatum is affected by a unilateral 6-OHDA lesion even when DA projections to the contralateral striatum remain intact (Cadet et al., 1991, Lawler et al., 1995, Nikolaus et al., 2003). The effects of unilateral DA depletion are thus not necessarily restricted to the lesioned hemisphere, and the bilateral effects that we observe here warrant further investigation. Furthermore, 6-OHDA induced oxidative stress has been shown to return to pre-lesion levels within 7 days after administration (Sanchez-Iglesias et al., 2007). It is therefore also unlikely that a sufficient

level of residual oxidative stress persists from 6-OHDA administration to affect these measures 6 weeks post-lesion.

Overall, our results demonstrate a bilateral increase in measures of striatal insulin resistance in rats exhibiting severe DA depletion, with some effects in animals with partial depletion. These novel findings suggest a direct effect of nigrostriatal DA depletion on insulin signaling in the basal ganglia. Although we cannot completely rule out a general neurotoxic effect of 6-OHDA on insulin signaling, several factors argue against this alternative hypothesis. The first two are that 6-OHDA is highly selective for catecholamines such as DA (Schober, 2004), and that DA terminals comprise less than 5% of striatal tissue content (Bennett and Wilson, 2000), where the measures of insulin resistance were made. Furthermore, measures of insulin resistance exhibited a “dose-dependent” effect, with the severely DA-depleted group exhibiting greater effects than the partially depleted group. These findings nevertheless warrant investigation of insulin signaling in other brain areas and in other preclinical models of PD. Because the hypothalamus provides a direct connection to peripheral metabolism, future studies of whether this region is affected in the 6-OHDA model are also warranted. The extent of brain insulin resistance beyond basal ganglia nuclei could shed more light on the question of how PD can be a risk factor for peripheral glucose intolerance.

FIGURE 3.1

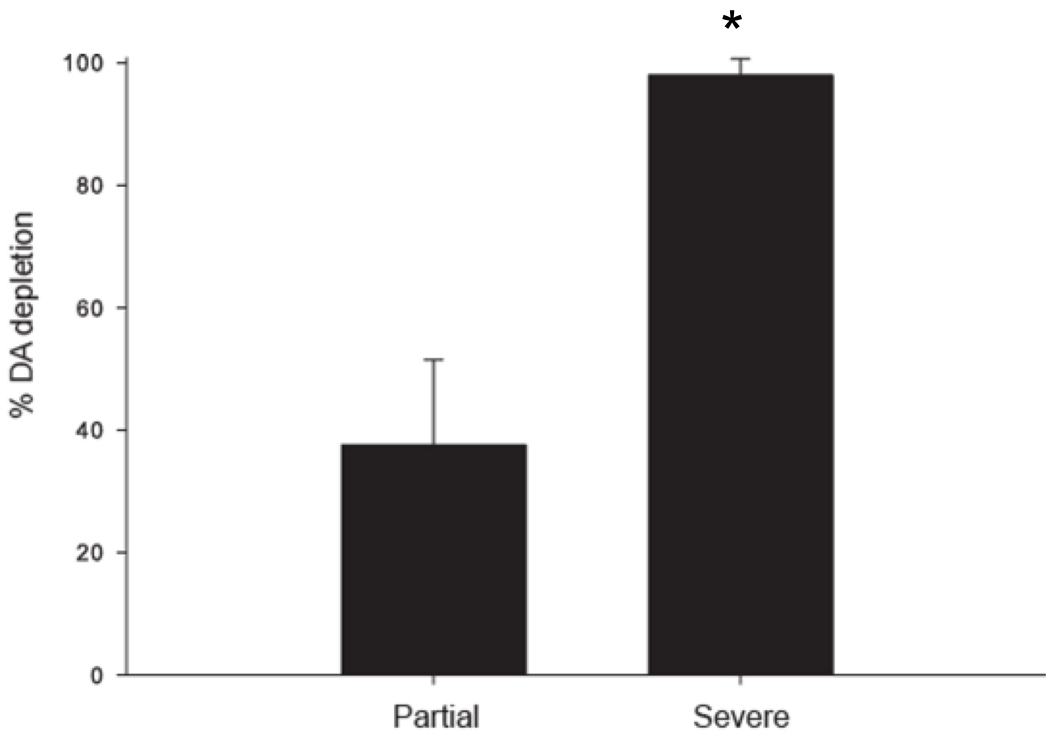

FIGURE 3.1. DA depletion levels for partially and severely depleted rats. DA content in the right (lesioned) striatum was divided by DA levels in left (nonlesioned) striatum to obtain a percent depletion for each lesioned rat. The average depletion level for rats with partial DA depletion was 37.6% ± 13.9, while rats in the severe DA depletion group exhibited a mean depletion of 98% ± 2.7%. Values are mean ± SE for 7-8 animals per group. *P≤0.05.

FIGURE 3.2

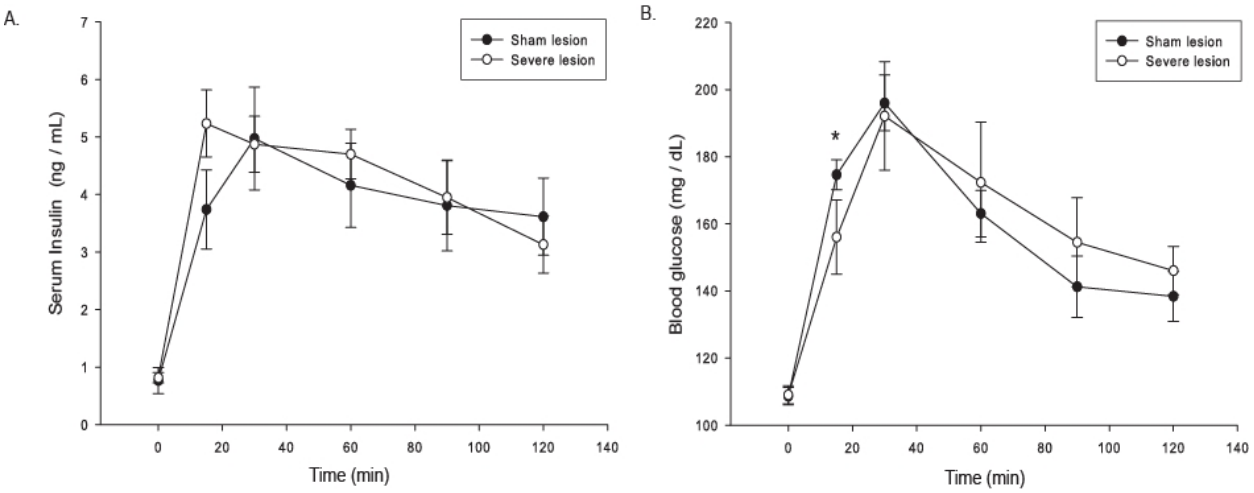
A.
Sham lesion
Severe lesion
Serum Insulin (ng / mL)
Time (min)
B.
Sham lesion
Severe lesion
Blood glucose (mg / dL)
*
Time (min)

FIGURE 3.2. Intraperitoneal glucose tolerance test (IPGTT). After an overnight (12 hour) fast, an intraperitoneal injection of 60% glucose was administered at 2g glucose/kg body weight. Insulin **(A)** and glucose **(B)** were measured in tail blood at six time points: 0,15,45,60, 90, and 120 minutes after the glucose bolus (injection at t=0). Fifteen minutes following the bolus, an increase in insulin that approaches significance ($p=0.06$) is reflected by a significant decrease in glucose ($p=0.04$). However, neither insulin nor glucose levels were significantly different between groups over the course of the test or at any other timepoint, indicating that severely depleted rats were not glucose intolerant six weeks postlesion. *$P \leq 0.05$.

FIGURE 3.3

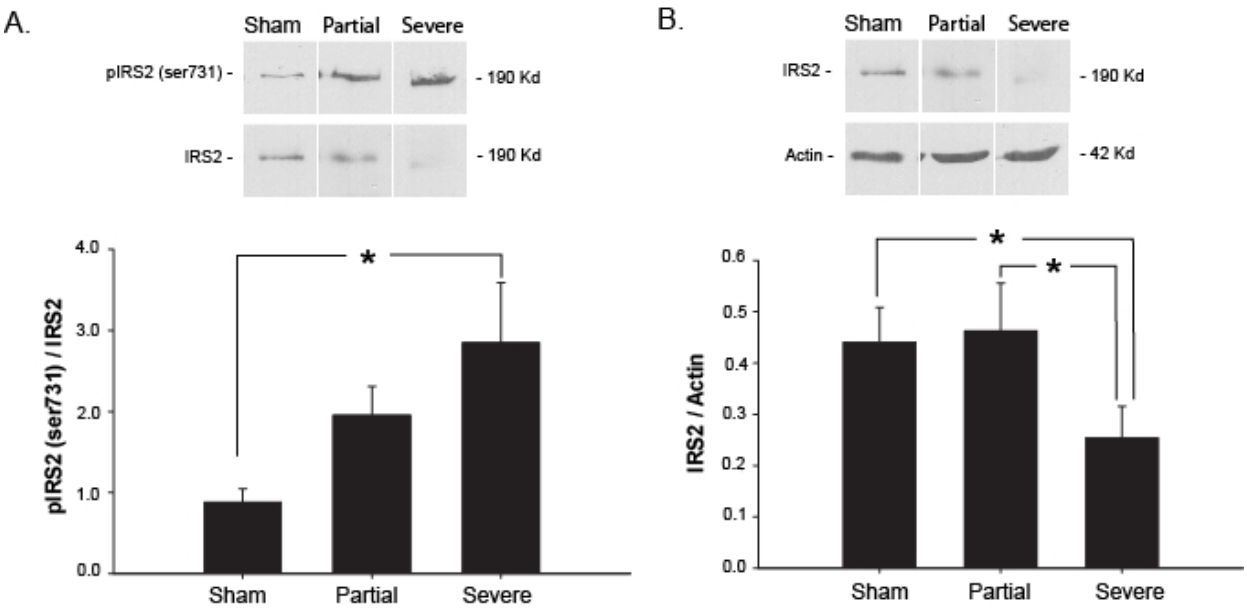
A.
Sham
Partial
Severe
pIRS2 (ser731) -
- 190 Kd
IRS2 -
- 190 Kd
pIRS2 (ser731) / IRS2
4.0
3.0
2.0
1.0
0.0
*
Sham
Partial
Severe
B.
Sham
Partial
Severe
IRS2 -
- 190 Kd
Actin -
- 42 Kd
IRS2 / Actin
0.6
0.5
0.4
0.3
0.2
0.1
0.0
*
*
Sham
Partial
Severe

Figure 3.3. Effect of 6-OHDA lesion on IRS2 activation and protein content. Homogenized striatal lysates were analyzed by Western blot for pIRS2 **(A)**, normalized to total IRS2, and total IRS2 **(B)**, normalized to actin. There was a DA depletion-related increase in pIRS2, while total IRS2 was diminished in the severe lesion group. Values are means ± SE for 6-8 samples per group. *P≤0.05.

FIGURE 3.4

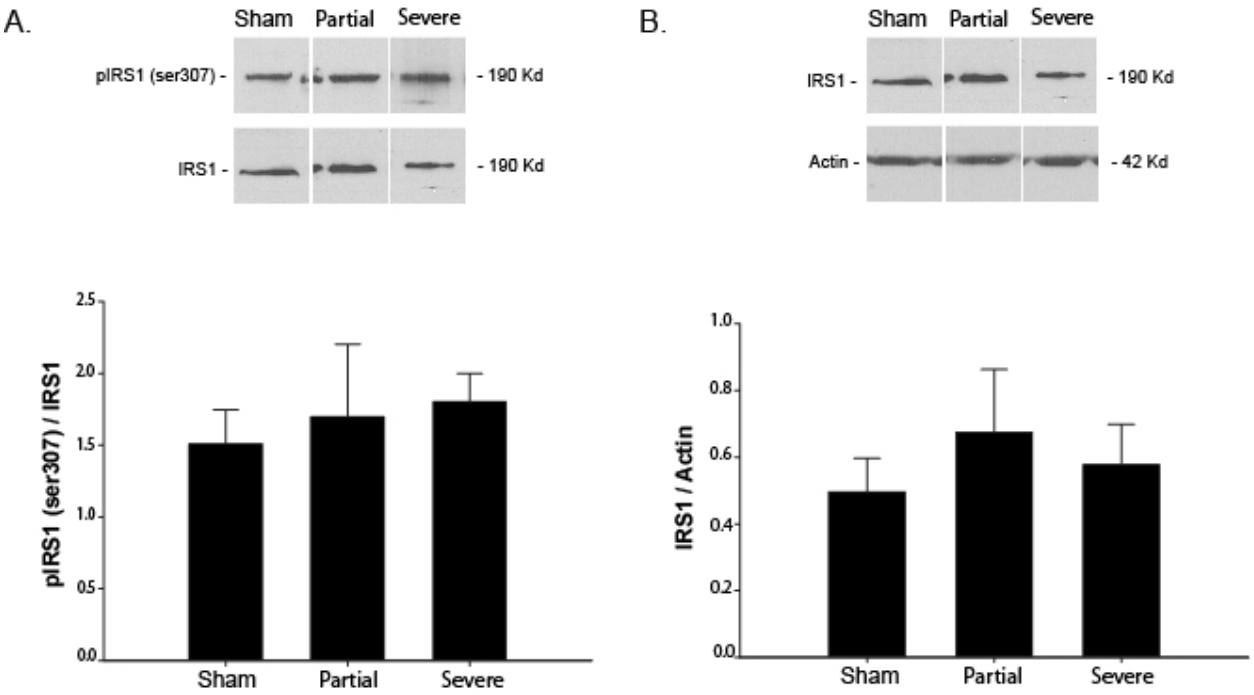
A.
Sham
Partial
Severe
pIRS1 (ser307) -
- 190 Kd
IRS1 -
- 190 Kd
pIRS1 (ser307) / IRS1
2.5
2.0
1.5
1.0
0.5
0.0
Sham
Partial
Severe
B.
Sham
Partial
Severe
IRS1 -
- 190 Kd
Actin -
- 42 Kd
IRS1 / Actin
1.0
0.8
0.6
0.4
0.2
0.0
Sham
Partial
Severe

Figure 3.4. Protein expression and phosphorylation of IRS1. Homogenized striatal lysates were analyzed by Western blot for pIRS1 **(A)**, normalized to total IRS1, and total IRS1 **(B)**, normalized to actin. There was no significant difference between phosphorylated IRS1 or total IRS1 protein between any groups tested. Values are means ± SE for 3-8 samples per group.

FIGURE 3.5

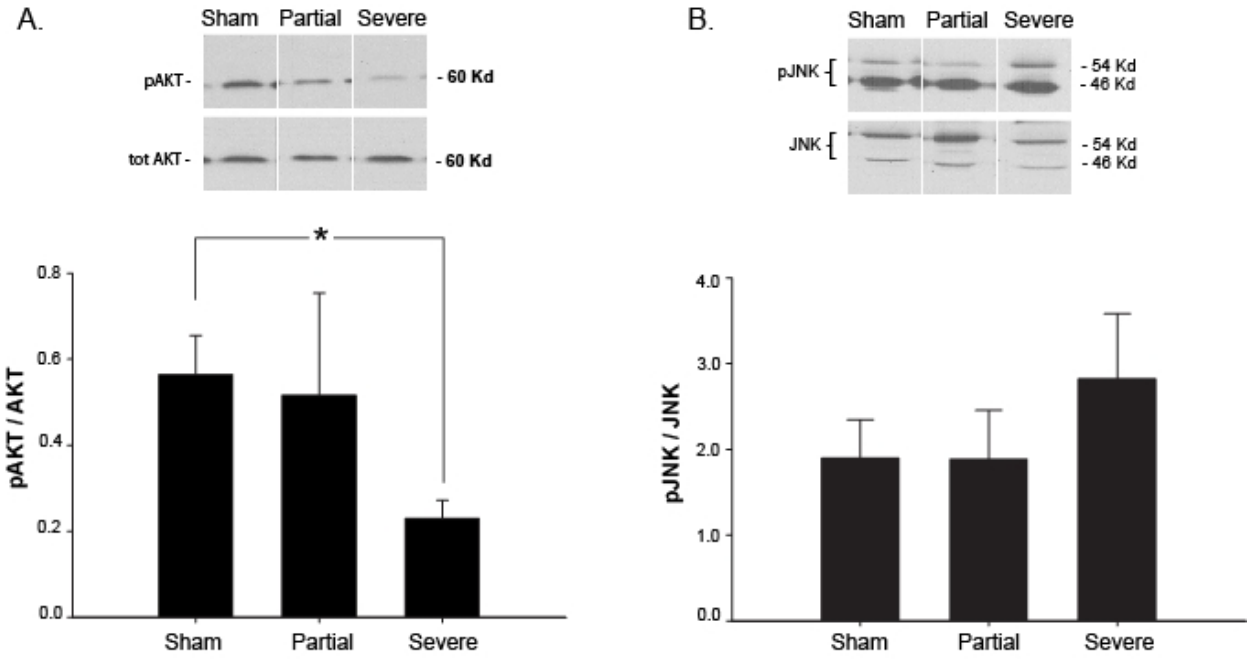
A.
Sham
Partial
Severe
pAKT -
- 60 Kd
tot AKT -
- 60 Kd
*
pAKT / AKT
0.8
0.6
0.4
0.2
0.0
Sham
Partial
Severe
B.
Sham
Partial
Severe
pJNK
- 54 Kd
- 46 Kd
JNK
- 54 Kd
- 46 Kd
pJNK / JNK
4.0
3.0
2.0
1.0
0.0
Sham
Partial
Severe

Figure 3.5. Activation of AKT and JNK. Homogenized striatal lysates were analyzed by Western blot for pAKT **(A)**, normalized to total AKT, and pJNK **(B)**, normalized to total JNK. pAKT was significantly decreased with a severe lesion when compared to sham lesion controls. Severely depleted rats also exhibited a non-significant increase in JNK phosphorylation. Values are means ± SE for 3-8 samples per group. *P≤0.05.

FIGURE 3.6

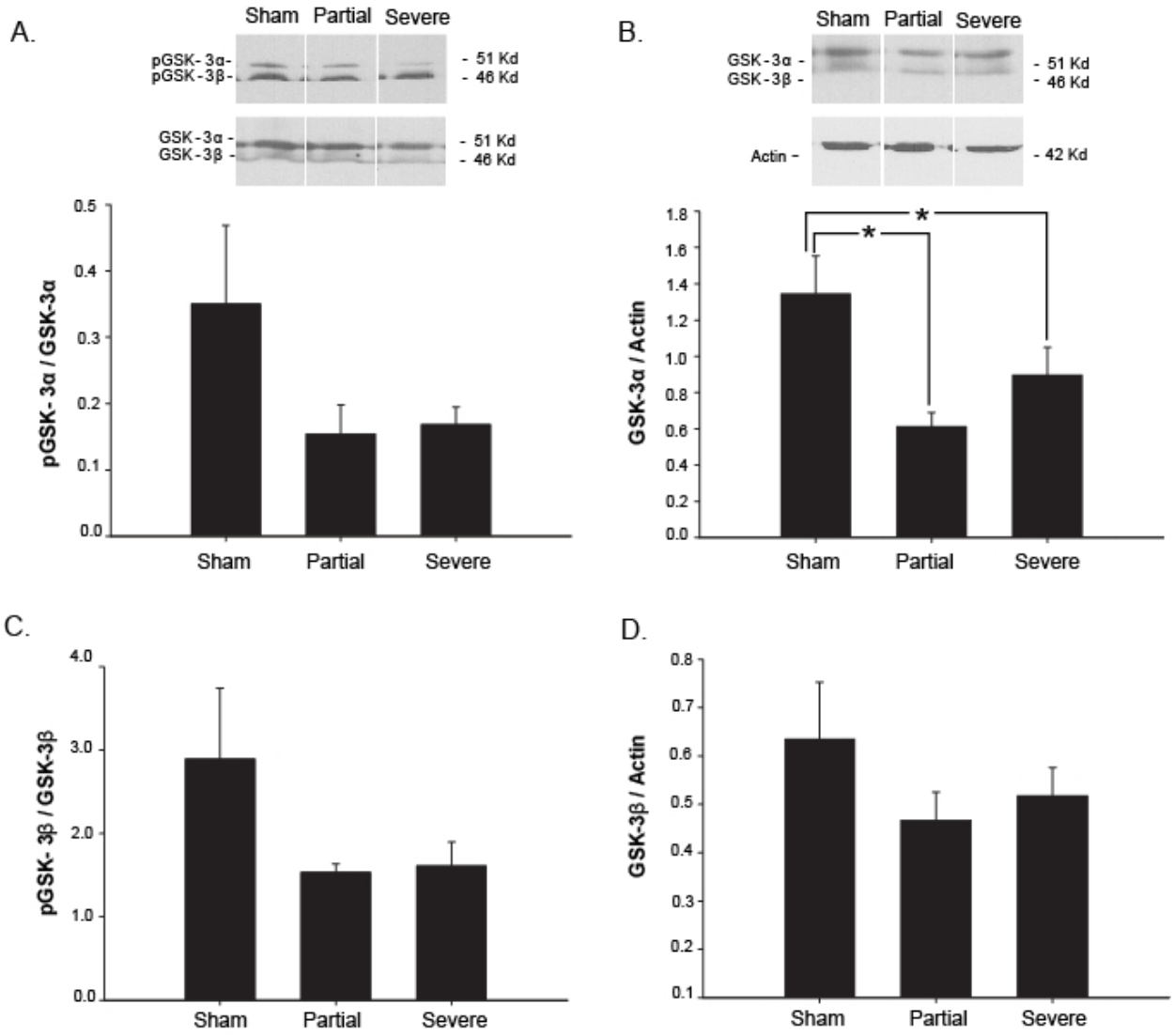
A.
Sham Partial Severe
pGSK-3α-
pGSK-3β-
- 51 Kd
- 46 Kd
GSK-3α -
GSK-3β -
- 51 Kd
- 46 Kd
pGSK-3α / GSK-3α
0.5
0.4
0.3
0.2
0.1
0.0
Sham
Partial
Severe
B.
Sham Partial Severe
GSK-3α -
GSK-3β -
- 51 Kd
- 46 Kd
Actin -
- 42 Kd
GSK-3α / Actin
1.8
1.6
1.4
1.2
1.0
0.8
0.6
0.4
0.2
0.0
*
*
Sham
Partial
Severe
C.
pGSK-3β / GSK-3β
4.0
3.0
2.0
1.0
0.0
Sham
Partial
Severe
D.
GSK-3β / Actin
0.8
0.7
0.6
0.5
0.4
0.3
0.2
0.1
Sham
Partial
Severe

Figure 3.6. Activation of GSK3 isoforms in response to DA depletion. Homogenized striatal lysates were analyzed by Western blot for pGSK3-α **(A)**, normalized to total GSK3-α, GSK3-α **(B)**, normalized to actin, pGSK3-β **(C)**, normalized to total GSK3-β, and total GSK3-β **(D)**, normalized to actin. Total GSK3-α was decreased significantly in both the partial and severe lesion groups. Although pGSK3-α, pGSK3-β, and total GSK3-β were decreased in the lesioned groups, these effects did not reach significance. Values are means ± SE for 3-8 samples per group. *P≤0.05.

FIGURE 3.7

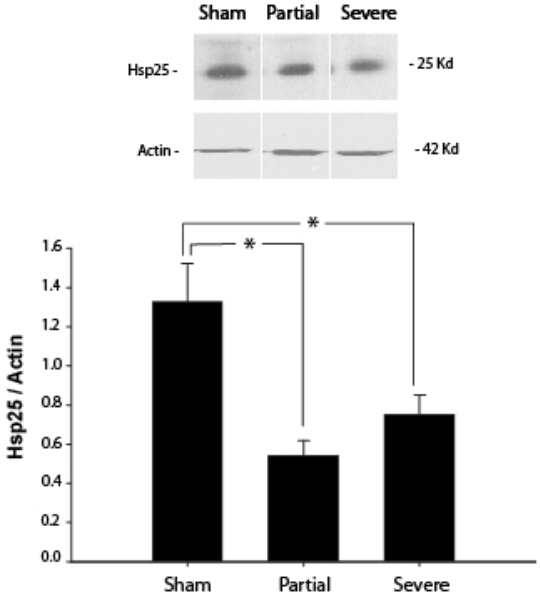
Sham
Partial
Severe
Hsp25 -
- 25 Kd
Actin -
- 42 Kd
*
*
Hsp25 / Actin
1.6
1.4
1.2
1.0
0.8
0.6
0.4
0.2
0.0
Sham
Partial
Severe

Figure 3.7. Expression of Hsp25 in response to a 6-OHDA lesion. Homogenized striatal lysates were analyzed for Hsp25 normalized to actin**.** Hsp25 was decreased significantly in both the partial and the severe lesion groups when compared to sham lesioned controls. Values are means ± SE for 3-8 samples per group. *P≤0.05.

Table 3.1

Mean (+/- S.E.M.) striatal DA and DOPAC values for experimental groups

	DOPAC (ng/g)		DA (ng/g)	
	Left Striatum	Right Striatum	Left Striatum	Right Striatum
Sham	1357.8 ± 130.3	1343.8 ± 117.4	4964.4 ± 383.4	4108.3 ± 584.3
Partial	1965.4 ± 419.4	2825.9 ± 597.2	4659.6 ± 1057.0	2891.9 ± 693.8
Severe	1558.3 ± 169.9	85.3 ± 54.5	6852.8 ± 2450.9	210.4 ± 124.8

EFFECTS OF 6-OHDA ON PERIPHERAL GLUCOSE TOLERANCE AND INSULIN SIGNALING IN MIDDLE AGED RATS

Morris, J.K., Seim, N.L., Geiger, P.C., and J.A. Stanford

Submitted

Abstract

Clinical studies have indicated an increased rate of Parkinson's disease in patients with Type 2 Diabetes, and impaired glucose tolerance in individuals with Parkinson's disease. It is unclear how Parkinson's disease can affect glucose tolerance. The purpose of this study was to analyze peripheral glucose tolerance in an established PD animal model, the 6-hydroxydopamine lesion model. Our aim was twofold: to analyze glucose tolerance following severe unilateral dopamine depletion and to determine whether peripheral insulin signaling was affected. Six weeks following unilateral 6-hydroxydopamine treatment, we observed severe unilateral dopamine depletion in the striatum and substantia nigra. Markers of striatal insulin resistance were evident. However, although serum insulin levels differed significantly between groups over the course of a glucose tolerance test, no significant effect on glucose tolerance or insulin signaling was observed. Together, these data suggest that although 6-OHDA may affect serum insulin levels, the unilateral 6-OHDA lesion model does not induce glucose intolerance or insulin resistance.

Introduction

Glucose intolerance or diabetes has been shown to occur in individuals with Parkinson's disease (PD) (Barbeau et al., 1961, Boyd et al., 1971, Lipman et al., 1974). It is important to investigate the mechanism of glucose intolerance in this disease, as glucose intolerance or diabetes has been suggested to decrease the effectiveness of L-DOPA therapy (Sandyk, 1993), increase cost of medical care (Pressley et al., 2003), and increase motor symptom severity (Papapetropoulos et al., 2004).

In a previous study, our laboratory showed that 6-OHDA administration into the MFB impaired striatal insulin signaling in young rats (Morris et al., 2008). However, peripheral glucose and insulin levels were not affected. We sought to determine if 6-OHDA would affect peripheral glucose tolerance in middle-aged rats, since aging is a risk factor for both PD and insulin resistance (Supiano et al., 1993, Vanitallie, 2008), and T2D onset often occurs during middle age.

Material and Methods

Sixteen male 16 month old Fisher 344 rats were obtained from National Institutes on Aging colonies (Harlan). Protocols for animal use were approved by the University of Kansas Medical Center Institutional Animal Care and Use Committee and adhered to the Guide for the Care and Use of Laboratory Animals (National Research Council, 1996). Rats were divided arbitrarily to obtain two experimental groups of similar average body weight. The 6-OHDA lesion procedure was based on previously published studies (Morris et al., 2008). Nembutal (50mg/mL) was given at 1mL/kg body weight. Rats were placed into a stereotaxic frame. Animals receiving a 6-OHDA lesion (n=8) were infused with 12µL of 6-OHDA in 0.9% NaCl with 0.02% ascorbate into the right medial forebrain bundle (stereotaxic coordinates with respect to bregma: M/L 1.3, A/P -4.4, and D/V -7.8) at a dose of 2.25mg/mL. The infusion rate was 0.75µL/min over a period of 16 min and the cannula was

withdrawn 1 min following infusion. Sham (saline) infused rats received the same surgical procedure was followed for rats receiving a sham lesion (n=8), with saline (0.9% NaCl with 0.02% ascorbate) substituted for 6-OHDA. Tissue harvest was performed 6 weeks post-lesion.

Food intake and body weight were measured weekly. Two days prior to sacrifice, blood glucose and serum insulin levels were measured during an intraperitoneal glucose tolerance test (IPGTT) as previously described (Morris et al., 2008). Prior to tissue harvest, muscles were dissected and incubated with insulin *in vitro* to determine insulin sensitivity (Gupte et al., 2008). Animals were deeply anesthetized and soleus (slow-twitch) and EDL (fast-twitch) muscles were carefully dissected. Muscles from each side were split longitudinally and incubated in a recovery solution for 90 min at 39°C. One half of each muscle was removed into a solution containing 1 mU/mL insulin for 10 min at 39°C (insulin-stimulated) while the other half (basal) remained in the recovery solution. Muscles were then clamp-frozen and stored at -80°C for Western blot analysis. At tissue harvest, adiposity was measured by weighing epididymal fat from animals in each group. Gastrocnemius muscles were dissected and weighed to determine whether muscle atrophy had occurred.

Striatal sections were dissected for HPLC-EC and for Western blotting. For HPLC-EC analysis, striatal tissue was processed and analyzed as previously described (Morris et al., 2008). DA and NE levels were also analyzed in the SN and the hypothalamus. These samples were prepared identically to striatal samples, except the volume of burnt citrate acetate mobile phase was reduced to 250µL and DHBA concentration was reduced to 10^{-7}M due to the smaller size of these tissues. Striatal sections for Western blotting were dissected freehand and frozen on dry ice. Brain and muscle samples were prepared and analyzed for western blot as previously described (Gupte et al., 2008, Morris et al., 2010).

Data for food intake, body weight and glucose tolerance were analyzed using two-way analyses of variance (ANOVA) with diet as the grouping variable and time as the repeated measure. Neurotransmitter depletion was analyzed using one-way ANOVA with diet as the grouping variable. Western blot data was analyzed using student's t-test. No protein expression or activation differences between lesioned and non-lesioned hemispheres were observed for any protein measures, so data from the left and right striatal hemisphere were pooled for each animal. When necessary, post-hoc analyses were performed using student's t-test. Data were considered statistically significant at $p<0.05$.

Results and Discussion

Although groups lost weight after surgery, the 6-OHDA group lost more weight overall ($F=7.18$, $p<0.05$; Table 3.2). This group experienced a greater drop in food intake immediately following surgery (weeks 1-4, $F= 19.76$, $p<0.01$; Table 3.2). However, food intake almost completely normalized by the end of the experiment (weeks 5-6). Lesioned animals also had less fat mass at tissue harvest ($F=7.09$, $p<0.05$; Table 1). Gastrocnemius muscle weight did not differ between groups, indicating that weight differences were primarily due to loss of fat mass and not contralateral muscle atrophy following the lesion.

Administration of 6-OHDA into the MFB had a dramatic effect on DA concentration in the striatum, where a significant group ($F=74.21$, $p<0.001$), side ($F=64.57$, $p<0.001$) and group by side interaction ($F=13.103$, $p<0.01$) were observed, as DA concentration was reduced by ~95% in the lesioned hemisphere. Surprisingly, sham (saline) infusion also decreased striatal DA concentration (~25%) in the saline-infused hemisphere. This is likely due to neuronal damage from a higher infusion rate and larger infusion volume than used in our previous study (Morris et al., 2008). DA concentration ipsilateral to the saline-infused hemisphere was approximately the same as that in the control (contralateral) hemisphere of 6-OHDA infused animals. A bilateral decrease in striatal DA concentration in 6-OHDA treated rats is consistent with our observation of bilateral effects on striatal insulin signaling in both this and the previous study.

As expected, the 6-OHDA lesion group also had significant DA depletion in the SN. ($F=14.78$, $p<0.001$; Table 3.3). Saline-infused animals did not exhibit DA depletion in this region, while 6-OHDA treatment elicited approximately 50% DA depletion. Because 6-OHDA induces retrograde terminal degeneration (Ries et al., 2008), it is not surprising that we observed greater DA depletion in the striatum. In the hypothalamus, 6-OHDA did not cause DA depletion in either hemisphere. Because 6-OHDA can also damage noradrenergic

neurons, we also analyzed NE levels in all three tissues. There was no significant effect of 6-OHDA on NE levels in the striatum or SN. However, in the hypothalamus, there was a large depletion of NE in the 6-OHDA treated group ($F=28.9$, $p<0.001$; Table 3.3). Although a bilateral decrease in NE was observed with 6-OHDA treatment, post-hoc analysis also revealed a significant decrease in DA depletion between the lesioned and nonlesioned hemisphere in the toxin-infused group.

As previously noted in a study with younger animals, insulin signaling was impaired in the striatum following 6-OHDA mediated DA depletion. Serine phosphorylation of IRS2, which is inhibitory to insulin signaling (White, 2002), was increased in the lesion group ($p<0.05$; Figure 3.8A). Long term serine phosphorylation can result in IRS degredation (Kim et al., 2005, Pederson et al., 2001), and we observed a strong trend ($p=0.06$) for decreased protein content in lesioned animals (Figure 3.8B). The protein AKT is activated by phosphorylation, which occurs in response to normal insulin signaling to promote glucose uptake (Gonzalez and McGraw, 2006). As expected, we observed decreased pAKT in the striatum ($p<0.05$), in line with increased serine phosphorylation of IRS2 (Figure 3.8C).

Although we observed effects on brain insulin signaling, in this study, peripheral glucose tolerance was not affected. However, the insulin response to a glucose bolus did differ between groups over the course of an IPGTT ($F=3.93$, $p<0.01$; Figure 3.9A). Post-hoc analysis showed that 6-OHDA lesioned animals exhibited a greater initial increase in insulin (15 min), but were not able to maintain this increased level and insulin was significantly less at the final timepoint (120 min). Over the course of the test, blood glucose levels did not differ between groups (Figure 3.9B), but lesioned animals did exhibit higher glucose values at the final timepoint. Although this does not indicate an outright impairment in glucose tolerance, these subtle changes in insulin action may precede a larger-scale effect. To determine whether glucose uptake was affected, insulin signaling in skeletal muscle was

analyzed. Even with severe nigrostriatal DA depletion, insulin signaling, as measured by AKT phosphorylation, was not affected in either slow (Soleus) or fast (EDL) muscle (Figure 2C,2D).

It is possible that the increase in serum insulin levels early in the IPGTT may help maintain normal glycemia. In support of this possibility, higher blood glucose levels were observed at 120 minutes in the 6-OHDA treated group, when insulin levels had dropped significantly. Another possibility is that insulin release was affected by decreased input of the sympathetic nervous system. NE is the primary neurotransmitter used in the sympathetic nervous system (Hall, 1990), and in this study we did observe hypothalamic NE depletion. Sympathetic nerves inhibit insulin secretion (Ahren, 2000), and a decrease in the activity of these sympathetic nerves would lessen their inhibitory effect. However, control of insulin release by the autonomic nervous system is complex and involves reciprocal sympathetic and parasympathetic inputs (Teff, 2007). We did not directly measure autonomic nervous system function, and thus cannot further speculate on the role of these neurons in the altered insulin response.

Conclusions

This study confirms previous work describing striatal insulin resistance in young rats following 6-OHDA and expands these findings to a middle aged model and analysis of peripheral insulin signaling. Although serum insulin levels differed over the course of a glucose tolerance test, no effect on glucose tolerance or peripheral insulin signaling was observed. We cannot conclude that aging increases the risk of developing peripheral glucose tolerance following unilateral 6-OHDA treatment. However, the observed alterations in serum insulin levels are interesting and warrant further study.

Figure 3.8

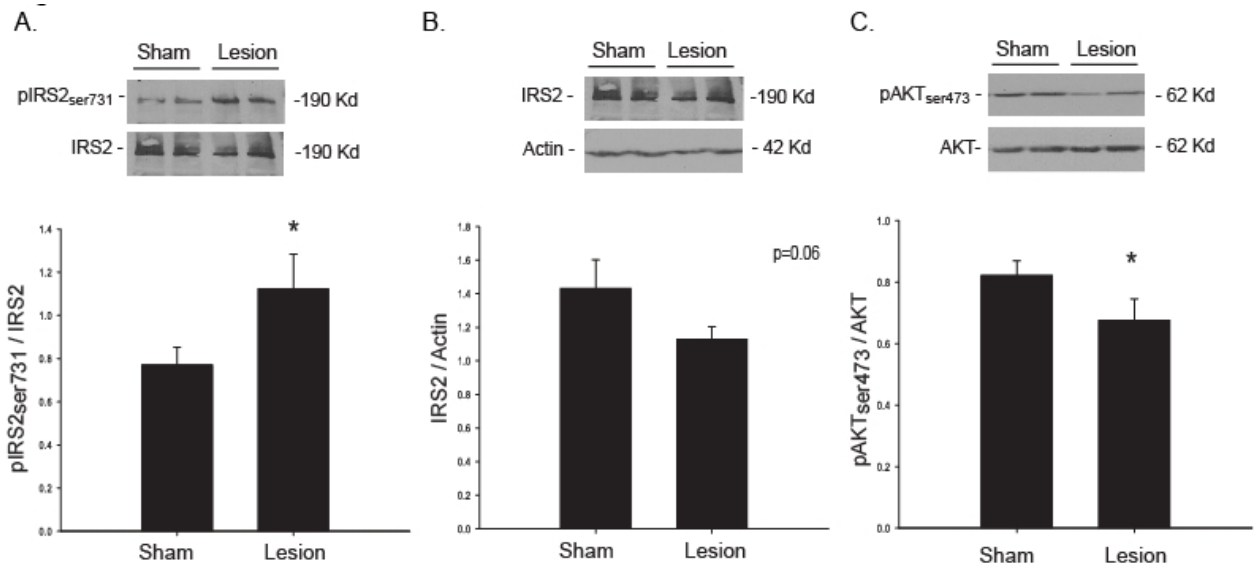
A.
Sham
Lesion
pIRS2ser731 -
-190 Kd
IRS2 -
-190 Kd
pIRS2ser731 / IRS2
*
Sham
Lesion
B.
Sham
Lesion
IRS2 -
-190 Kd
Actin -
- 42 Kd
p=0.06
IRS2 / Actin
Sham
Lesion
C.
Sham
Lesion
pAKTser473 -
- 62 Kd
AKT-
- 62 Kd
pAKTser473 / AKT
*
Sham
Lesion

Figure 3.8. Striatal Insulin signaling in 6-OHDA treated middle aged rats. Treatment with 6-OHDA significantly increased serine phosphorylation of IRS2 (A), indicating insulin resistance. A trend for decreased IRS2, which has been shown to occur with chronic serine phosphorylation, was observed in the severely depleted group. In line with these findings, serine phosphorylation of the downstream protein AKT, which is a positive indicator of insulin signaling, was significantly decreased in the lesion group. Values are means ± SE for 5-8 samples per group. *$p<0.05$ sham vs. lesion.

FIGURE 3.9

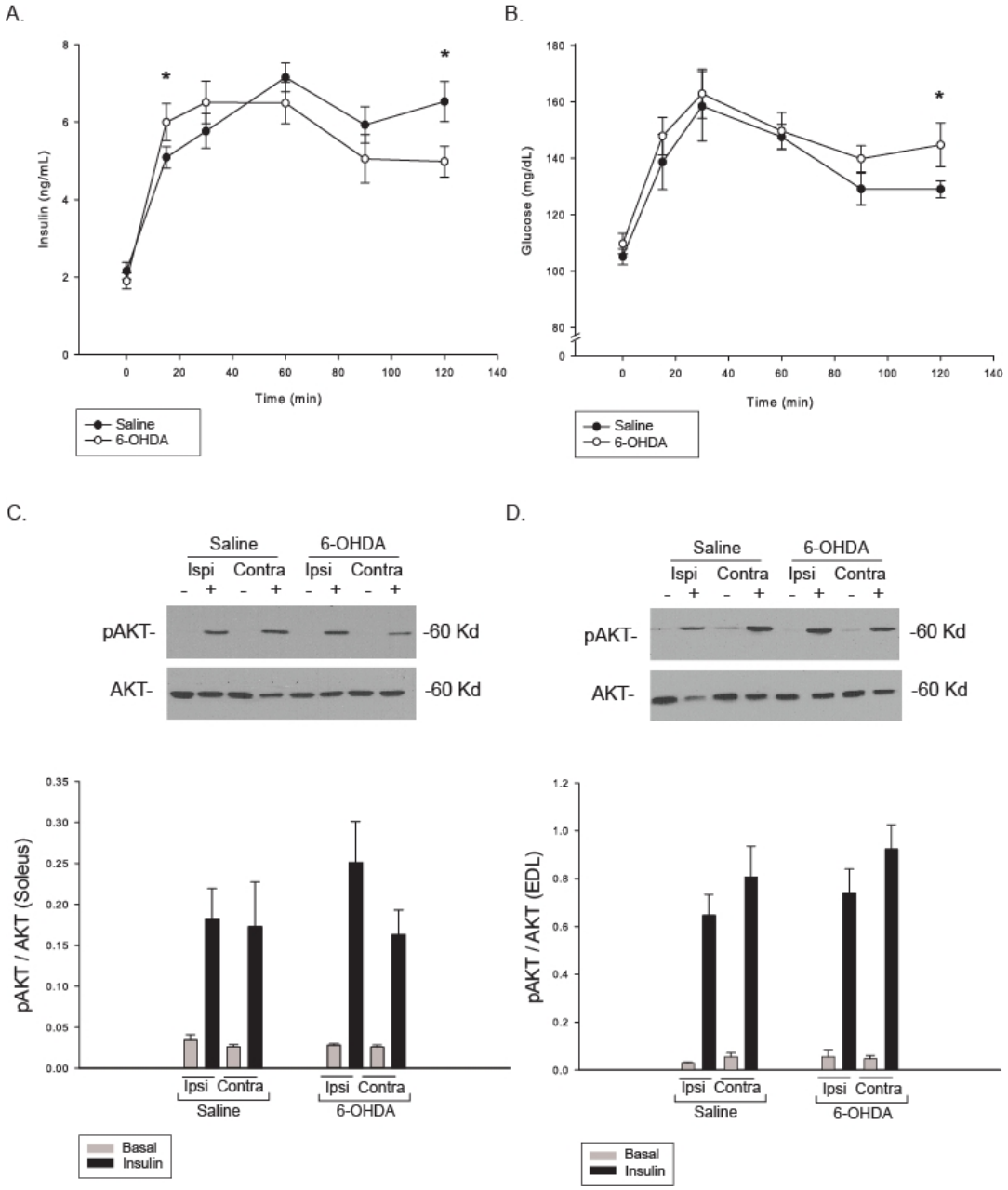
A.
Insulin (ng/mL)
Time (min)
Saline
6-OHDA
B.
Glucose (mg/dL)
Time (min)
Saline
6-OHDA
C.
Saline
6-OHDA
Ispi Contra Ispi Contra
pAKT-
AKT-
-60 Kd
-60 Kd
pAKT / AKT (Soleus)
Ipsi Contra
Saline
Ipsi Contra
6-OHDA
Basal
Insulin
D.
Saline
6-OHDA
Ispi Contra Ipsi Contra
pAKT-
AKT-
-60 Kd
-60 Kd
pAKT / AKT (EDL)
Ipsi Contra
Saline
Ipsi Contra
6-OHDA
Basal
Insulin

Figure 3.9. Peripheral glucose tolerance and skeletal muscle insulin signaling. An intraperitoneal glucose tolerance test (IPGTT) was performed following a 12 hour overnight fast, A glucose bolus (60% glucose, 2g glucose/kg body weight) was injected intraperitoneally at t=0. **(A)** Appoximately 400uL of whole blood was collected at six time points: 0,15,45,60, 90, and 120 minutes, for analysis of serum insulin (A). Blood glucose (B) was also measured at these timepoints using a glucometer. Basal (gray bars) and insulin-stimulated (black bars) AKT phosphorylation was measured by western blot in soleus (C) and EDL (D) muscles as an indicator of insulin signaling. No difference in insulin-stimulated pAKT was observed, indicating the absence of skeletal muscle insulin resistance. Values are means ± SE for 8 muscles per group. *$p<0.05$ chow vs. HF.

Table 3.2

	Control	6-OHDA
Pre-lesion BW (g)	466.1 ± 6.6	466.4 ± 13.3
Final BW (g)	457.7 ± 6.75	407.7 ± 19.4*
Pre-lesion food intake (Kcal/day)	75.1 ± 2.2	89.5 ± 2.3*
Food intake (wk 1-4) (Kcal/day)	69.2 ± 2.0	47.5 ± 5.1*
Food intake (wk 5-6) (Kcal/day)	78.1 ± 5.2	77.3 ± 5.4
Contralateral Gastroc wt (g)	1.86 ± 0.05	1.77 ± 0.06
Ipsilateral Gastroc wt (g)	1.88 ± 0.05	1.76 ± 0.07
Fat Mass (g)	14.86 ± 0.68	10.96 ± 1.3*

*$p<0.05$ 6-OHDA vs. control

Table 3.3

		Sham		6-OHDA	
Tissue	Analyte	Contralateral	Ipsilateral	Contralateral	Ipsilateral
Striatum	DA	7376.5 ± 664	5490.71 ± 494$^{\#}$	5243.5 ±302	266.21 ± 111$^{*\#\dagger}$
	NE	116.4 ± 17	88.0 ± 17	104.3 ± 26	123.9 ± 54
Substantia Nigra	DA	1064.2 ± 166	1185.0 ± 146	801.6 ±99.0	441.7 ± 95.9$^{*\#}$
	NE	547.3 ± 67	692.5 ± 76	534.7 ± 109	609.2 ± 198
Hypothalamus	DA	916.4 ± 323	1110.7 ± 392	751.2 ± 265	615.1 ± 232
	NE	26503.1 ± 9370	28525.6 ± 10085	13888.9 ± 4910	6876.2 ± 2431$^{*\#}$

*p< 0.05 6-OHDA vs. Sham
$^{\#}$p<0.05 Ipsilateral vs. Contralateral
†p<0.05 Group x Side interaction

CHAPTER 4

HIGH FAT FEEDING EXACERBATES TOXIN-MEDIATED DOPAMINE DEPLETION

NEURODEGENERATION IN AN ANIMAL MODEL OF PARKINSON'S DISEASE IS EXACERBATED BY A HIGH FAT DIET

J.K. Morris, G.L. Bomhoff, J.A. Stanford, and P.C. Geiger

Am J Physiol Regul Integr Comp Physiol (2010)299(4): R1082-90.

Abstract

Despite numerous clinical studies supporting a link between Type 2 Diabetes (T2D) and Parkinson's disease (PD), the clinical literature remains equivocal. We therefore sought to address the relationship between insulin resistance and nigrostriatal dopamine (DA) in a preclinical animal model. High fat feeding in rodents is an established model of insulin resistance, characterized by increased adiposity, systemic oxidative stress, and hyperglycemia. We subjected rats to a normal chow or high fat diet for five weeks before infusing 6-hydroxydopamine (6-OHDA) into the medial forebrain bundle. Our goal was to determine whether a high fat diet and the resulting peripheral insulin resistance would exacerbate 6-OHDA-induced nigrostriatal DA depletion. Prior to 6-OHDA infusion, animals on the high fat diet exhibited greater body weight, increased adiposity and impaired glucose tolerance. Two weeks after 6-OHDA, locomotor activity was tested and brain and muscle tissue was harvested. Locomotor activity did not differ between the groups nor did measures of muscle atrophy. High fat-fed animals exhibited higher homeostatic model assessment of insulin resistance (HOMA-IR) values and attenuated insulin-stimulated glucose uptake in fast-twitch muscle, indicating decreased insulin sensitivity. Animals in the high fat group also exhibited greater DA depletion in the substantia nigra and the striatum, which correlated with HOMA-IR and adiposity. Decreased phosphorylation of HSP27 and degradation of IκBα in the substantia nigra indicate increased tissue oxidative stress. These findings support the hypothesis that a diet high in fat and the resulting insulin resistance may lower the threshold for developing PD, at least following DA-specific toxin exposure.

Introduction

Clinical studies suggest a link between Type 2 Diabetes (T2D) and Parkinson's disease (PD) (Hu et al., 2007, Pressley et al., 2003), and between fat intake or adiposity and PD (Abbott et al., 2002, Hu et al., 2006, Johnson et al., 1999). Moreover, it was reported over forty years ago that greater than 50% of PD patients exhibit abnormal glucose tolerance (Barbeau et al., 1961, Boyd et al., 1971) or diabetes (Lipman et al., 1974). Despite this information, very little is known regarding the relationship of these diseases and the impact of co-morbidity on their pathogenesis. T2D is estimated to impact 300 million individuals by 2025 (Seidell, 2000) with the elderly at greatest risk (Wild et al., 2004), the population also at greatest risk for neurodegenerative diseases like PD. For these reasons, understanding the potential for T2D, obesity, high dietary fat intake, and insulin resistance to contribute to PD is critical. Although the exact cause of PD is unknown, various environmental factors such as aging, diet, and environmental toxin exposure have been implicated in contributing to its development (Hindle, Johnson et al., 1999, Thiruchelvam et al., 2000). The idea that "multiple hits" play a role in PD degeneration is supported by the fact that 80% of dopamine (DA) producing neurons must be lost for symptoms to appear (Sulzer, 2007). While diabetes and PD do not invariably coincide, several studies suggest that obesity may potentiate neuronal dysfunction or even neurodegeneration (reviewed in (Bruce-Keller et al., 2009)). High fat diet-induced insulin resistance could make DA neurons in the substantia nigra (SN), the origin of DA producing neurons that degenerate in PD, more susceptible to environmental insults.

While it is possible that a diet high in fat may contribute to the development of PD, much about this relationship remains unknown. In animal models, most studies have focused on the effect of obesity or high fat (HF) feeding on the mesolimbic DA pathway (Davis et al., 2008, Fulton et al., 2006, Geiger et al., 2009), which modulates response to

reward and is likely affected in obese individuals. However, few studies have addressed this issue in the nigrostriatal DA pathway, which is involved in the production of movement and affected in PD. Although best known for its role in movement disorders, the nigrostriatal pathway has also been shown to play an important role in feeding behavior (Palmiter, 2007) and may also be affected by obesity or HF feeding. Although it is possible that HF feeding may make DA neurons more vulnerable to environmental insults, such as neurotoxins, only one preclinical study has investigated the effect of a HF diet on DA neurodegeneration (Choi et al., 2005). These authors found that treatment with the neurotoxin MPTP (used to model PD) produced greater striatal DA depletion in HF-fed mice than in chow-fed controls.

We wanted to further characterize the effect of a high fat diet on toxin-induced nigrostriatal DA depletion using the 6-hydroxydopamine (6-OHDA) rat model of PD. Unlike MPTP, 6-OHDA may play a role as an endogenous neurotoxin (reviewed in (Blum et al., 2001)). Iron is abundant in the SN and can react in a fenton-type reaction with DA and hydrogen peroxide (produced extensively by monoamine oxidase during DA turnover) to produce 6-OHDA (Pezzella et al., 1997), which in turn can increase iron release from ferritin (Linert et al., 1996). This suggests that 6-OHDA may play an important role in perpetuating this damaging endogenous cycle. In addition, 6-OHDA is increased in the urine of patients treated with L-DOPA (Andrew et al., 1993, Jellinger et al., 1995), the most common and effective treatment of PD, and L-DOPA treatment in rodents increases 6-OHDA production in the striatum (Borah and Mohanakumar). To determine if HF-fed animals were indeed more sensitive to 6-OHDA mediated DA depletion, we administered equal amounts of 6-OHDA to HF-fed, insulin resistant rats and chow-fed controls. We observed that the HF diet group exhibited significantly greater levels of DA depletion in the SN, the origin nucleus of DA neurons in the nigrostriatal pathway, and the striatum, the termination point of this

pathway. These results support an exacerbating role for dietary fat, and consequent insulin resistance, in vulnerability to toxin-induced nigrostriatal DA depletion.

Materials and Methods

Animals and Diet

Sixteen-month-old Fisher 344 rats were obtained from National Institutes on Aging colonies (Harlan). Rats were individually housed, maintained on a 12 hour light/dark cycle, and provided food and water ad libitum. Rats in the chow group (n=10) received normal chow (Harlan Teklad rodent diet 8604), while animals in the HF diet group (n=8) received a diet with 60% calories from fat. The composition of the HF diet has been described previously (Gupte et al., 2009). During the seven weeks of the experiment, food intake was measured every 2-3 days. Body weight was measured weekly. Protocols for animal use were approved by the University of Kansas Medical Center Institutional Animal Care and Use Committee and adhered to the Guide for the Care and Use of Laboratory Animals (National Research Council, 1996).

Materials

Chemicals used in high pressure liquid chromatography (HPLC) (norepinephrine, DA, 3,4-dihydroxyphenylacetic acid (DOPAC), and 3,4-Dihydroxybenzylamine) and D-(+)-Glucose were obtained from Sigma-Aldrich (St. Louis, MO). [^{14}C]mannitol and 2-deoxy [1,2-^{3}H] glucose were purchased from American Radiolabeled Chemicals (St. Louis, MO). Rat insulin ELISA kits were obtained from Alpco diagnostics (Salem, NH). Cholesterol E and LDL-C kits were purchased from Wako Diagnostics (Richmond, VA). Antibodies against actin were obtained from Abcam (Cambridge, MA). Anti-phospho-Hsp 25 and anti-Hsp 25 were purchased from Stressgen (Victoria, BC, Canada), while IkBα antibody was purchased from Cell Signaling Technology (Beverly, MA).

Pre-lesion glucose tolerance analysis

Three days prior to surgery, animals were administered an intraperitoneal glucose tolerance test (IPGTT) as described previously (Morris et al., 2008). Animals were fasted

overnight (~12 hours) at which time they were anesthetized with Nembutal (50mg/mL) at 1mL/kg body weight. To begin the test, an intraperitoneal injection of 60% of D-(+)-Glucose (Sigma) at 2g/kg body weight was given. Blood glucose was measured using a glucometer at 0, 15, 30, 60, 90, and 120 minutes following injection, and 400uL of tail blood was collected at each timepoint for measurement of serum insulin. Blood samples were placed on ice for 30 minutes and centrifuged for 1 hour at 3,000 × g and serum was aliquoted into fresh tubes for serum insulin analysis.

6-OHDA Infusion

Five weeks after beginning the diet, all animals received a unilateral 6-OHDA lesion in the medial forebrain bundle. This procedure was modified from previous studies published by our laboratory (Morris et al., 2008)**.** Anesthesia was induced with 5% isoflurane. Anesthetized rats were placed in a stereotaxic frame and maintained at 3% isoflurane anesthesia during surgery. Animals were infused with 3µg 6-OHDA (4µL of 0.75 mg/mL 6-OHDA in 0.9% NaCl with 0.02% ascorbate) into the right medial forebrain bundle (stereotaxic coordinates with respect to bregma: M/L 1.3, A/P -4.4, and D/V -7.8). The infusion rate was 0.5µL/minute over a period of 8 minutes. The cannula was withdrawn 1 minute after infusion was completed. Animals were allowed to recover for two weeks post-surgery. After two weeks and prior to tissue harvest, animals were placed onto a force plate actometer (Stanford et al., 2002) in a dark room for 30 minutes so that spontaneous locomotor activity could be measured.

Glucose, insulin, and cholesterol measures

Prior to sacrifice following an overnight (12 hour) fast, animals were anesthetized with sodium pentobarbital (60 mg/kg). Tail blood was harvested for fasting blood glucose and insulin measurements at the end of the experiment. Glucose measurements were made using a glucometer, while serum samples were collected as previously described (Morris et

al., 2008) and analyzed using a rat insulin ELISA (ALPCO). Serum samples were also analyzed for total cholesterol levels using a Cholesterol E kit (Wako diagnostics) and low density lipoprotein cholesterol (LDL-C) levels using an L-type LDL-C kit (Wako diagnostics). HOMA-IR was calculated for rats as described previously (Cacho et al., 2008) using fasting glucose and fasting insulin values. This method has been validated in rodents and is consistent with other measures of insulin sensitivity (Cacho et al., 2008, Wallace et al., 2004).

Epididymal fat and gastrocnemius muscle atrophy measures

To measure fat accumulation, epididymal fat was dissected and weighed. In addition, to analyze if any muscle atrophy occurred due to disuse of the contralateral muscle post-lesion, gastrocnemius muscles were carefully dissected tip to tip and weighed.

Muscle incubations

Soleus and extensor digitorum longus (EDL) muscles both ipsilateral and contralateral to the lesioned hemisphere were quickly dissected from anesthetized animals. Glucose transport was measured as previously described by our laboratory (Gupte et al., 2009, Gupte et al., 2009) Each muscle was cut in half horizontally to avoid diffusion limitation and allow assessment of both basal and insulin-stimulated glucose transport. Both halves were placed into 2mL of Recovery buffer (8mM glucose, 32mM mannitol, and 0.01% BSA in KHB) for 30 minutes at 35°C. One muscle half (insulin-stimulated) was incubated in 8mM glucose, 32mM mannitol, 1mU/mL insulin, 0.01% BSA in KHB for 1 hour at 35°C while the other muscle half (basal) was retained in recovery buffer. Each muscle half was then rinsed in 40mM mannitol and 0.01% BSA in KHB for 10 minutes at 29°C. Finally, the insulin stimulated muscle half was placed into 4mM 2-[1,2-^{3}H]deoxyglucose (2-DG) (1.5 µCi/ml), 36mM, [^{14}C]mannitol (0.2 µCi/ml), 0.01%BSA in KHB containing 1mU/mL insulin at 29°C. The other half was placed into the same buffer without insulin. After 20 minutes both

muscles were immediately removed, trimmed, and clamp-frozen. A gas phase of 95%O_2 /5%CO_2 was maintained during all incubations. Muscles were processed as previously described (Young et al., 1986), and analyzed in a scintillation counter to determine intracellular 2-DG content (^{3}H dpm) and extracellular space (^{14}C dpm).

HPLC-EC analysis of Whole Tissue Dopamine Content

Following muscle harvest, brains were immediately removed and placed on an ice-cold brain block. Striatum and SN samples were dissected from each hemisphere, weighed, and frozen on dry ice to be processed for HPLC-EC and Western blot analysis. For HPLC-EC analysis, burnt citrate acetate mobile phase was added to samples from each tissue. For striatum tissue, 450µL of burnt mobile phase and 50µL DHBA (1e-6M) was added to each sample. Because the size of the SN is smaller than the striatum, SN samples were diluted in 250µL of burnt mobile phase and 50µL DHBA (1e-7M) for maximum analyte detection. Samples were then prepared and analyzed by HPLC as described previously (Morris et al., 2008).

Western Immunoblotting

For protein extraction, frozen pellets from SN samples that were processed for HPLC were diluted 15x in cell extraction buffer (Invitrogen) with protease inhibitor cocktail (500µL, Invitrogen), sodium flouride (200mM), sodium orthovanodate (200mM) and phenylmethanesulphonylfluoride (200mM) added. Samples placed on ice for 1 hour and vortexed every 15 minutes to allow for protein extraction. Samples were centrifuged at 3,000 x g at 4°C for 20 minutes before supernatants were collected. Protein concentration was determined using a Bradford assay. Bradford dye concentrate was diluted 5x in water to obtain working reagent and used to analyze samples in triplicate. Samples were diluted with HES buffer (20mM HEPES, 1mM EDTA, 250M Sucrose, pH 7.4) and reducing sample buffer (0.3M Tris-HCL, 5% SDS, 50% glycerol, 100mM dithiothreitol, Thermo Scientific) based on

protein concentration to generate samples of the same concentration for analysis using SDS-PAGE.

Samples were run on 10% SDS-PAGE gels and transferred to nitrocellulose membranes at 200mA for 60 minutes. After membranes were blocked for 1 hour in 5% milk, they were incubated overnight with primary antibody at 4°C (1:1,000 dilution in 1% BSA). Secondary antibody was used at a dilution of 1:10,000 in 1% milk for 1 hour at RT and corresponded to the host primary antibody of interest. Films were scanned at high resolution and densitometry measurements were analyzed using Image J software. Repeated measurements were taken for each band of interest. Protein content was normalized to the loading control actin.

Statistical Analyses

Data for body weight and food intake were analyzed using two-way analyses of variance (ANOVA) with diet as the grouping variable and time as the repeated measure. Glucose transport and DA turnover were analyzed using one-way ANOVA with diet and side (ipsilesional vs contralesional) as grouping variables. Correlations were assessed using Pearson's method. All other data were analyzed using one-way ANOVA with diet as the grouping variable. Data were considered statistically significant at $p \leq 0.05$.

Results

Body weight and food intake

Analysis of body weight (Fig. 4.1A) yielded significant main effects for both group ($F=7.915$, $p=0.01$) and time ($F=25.5$, $p<0.0001$), as well as a significant interaction effect ($F=16.57$, $p<0.0001$). As expected, HF-fed animals gained more weight than chow-fed animals, and both groups lost weight post-lesion during the recovery period. Statistical analysis of food intake revealed significant main effects for group ($F=16.15$, $p<0.001$) and time ($F=14.43$, $p<0.001$), and a significant interaction effect ($F=10.51$, $p<0.001$, Fig. 4.1B). Initially, animals in the HF diet group consumed far more calories than chow-fed animals, although this difference became less pronounced after several weeks of feeding. Food intake dropped in both groups post-lesion but rebounded during the recovery period, and was virtually the same between groups post-lesion.

Systemic effects of HF feeding

An intraperitoneal glucose tolerance test (IPGTT) was performed on a subgroup of rats after 5 weeks of feeding, prior to the 6-OHDA lesion. Glucose measurements revealed a significant effect of group ($F=4.84$, $p=0.04$) and time ($F=22.27$, $p<0.001$; Figure 4.2A). Glucose levels increased in response to the glucose bolus and HF-fed animals exhibited higher glucose values over the course of the test than chow fed animals. Over the course of the test, serum insulin measurements (Figure 4.2B) revealed a strong trend for a difference between group ($p=0.07$), a significant effect of time ($F=22.3$, $p<0.0001$), and a significant interaction effect of group and time ($F=2.73$, $p=0.03$). Serum insulin levels increased in both groups in response to insulin, but remained high in HF-fed animals well after insulin levels had returned to normal in the chow-fed group at the end of the IPGTT. Analysis of serum for total cholesterol and LDL-C levels revealed no statistical difference between groups.

When spontaneous locomotor activity was assessed 4 days prior to tissue harvest, total distance traveled did not differ significantly between the two groups (Table 4.1). This indicates no difference in activity level between groups. Fasting blood glucose and serum insulin were measured on the last day of the experiment prior to tissue harvest and values are given in Table 4.1. HF diet-fed animals exhibited significantly higher fasting glucose levels compared to chow animals. ($F=12.0$, $p=0.003$). HF animals also exhibited a non-significant ($p=0.07$) trend toward greater fasting serum insulin levels compared to the chow group. To determine whether the lesion caused peripheral muscle atrophy, gastrocnemius muscles were dissected bilaterally tip-to-tip and weighed. Gastrocnemius muscle weights did not differ significantly between the ipsilesional and contralesional sides, nor did they differ significantly between the two groups (Table 4.1).

Glucose uptake

The majority of glucose uptake in the body occurs in skeletal muscle. Thus, to analyze the degree of insulin resistance, we assayed 2-deoxyglucose uptake into two different skeletal muscles: the EDL (fast-twitch glycolytic fiber type) and soleus (slow-twitch oxidative fiber type). Because there was no difference in glucose transport between muscles ipsilateral or contralateral to the lesion, muscles for each rat were pooled for these analyses. In the EDL, insulin exposure affected the diet groups differently: glucose uptake was greatly increased in chow-fed animals in response to insulin (Figure 4.3A), but only a slight increase from basal was observed in HF animals. This led to a significant effect of insulin ($F=18.4$, $p=0.0001$) and a significant interaction between group and insulin ($F=7.25$, $p=0.01$). The decrease in insulin action due to HF feeding is characteristic of insulin resistance. Basal glucose uptake did not differ significantly between groups. In the soleus muscle, insulin significantly increased glucose uptake from basal in both groups ($F=24.7$, $p<0.0001$). No

significant difference was observed for either basal or insulin stimulated glucose uptake between groups in the soleus (Figure 4.3B).

DA depletion

In the SN, DA depletion was 48.8 ± 7.2% in the HF group compared to 27.8 ± 6.1% in the chow-fed group (Fig. 4.4A), a difference that was statistically significant ($F=4.96$, $p=0.04$) . Likewise, striatal DA depletion was also significantly higher in the HF diet group ($F=4.986$, $p=0.04$), averaging 28.3 ± 4.6% for chow animals and 49.0 ± 8.3% for HF animals (Fig. 4.4B). Average analyte values for DA and DOPAC in each region are provided in Table 4.2.

DA depletion and systemic effects of HF feeding

When HOMA-IR was analyzed to take into account both fasting glucose and fasting insulin values (Cacho et al., 2008, Wallace et al., 2004), HF animals exhibited values that were significantly greater than chow-fed animals ($F=4.23$, $p=0.05$), indicating decreased insulin sensitivity (Figure 4.5A). Interestingly, we observed a significant positive correlation between this index of insulin resistance and DA depletion levels in both the SN ($p=0.03$, Figure 4.5B) and striatum ($p=0.02$, Figure 4.5C). Epididymal fat mass was measured to determine differences in body fat composition and overall adiposity. As expected, HF rats exhibited far greater fat mass than chow fed rats ($F=38.56$, $p<0.001$); Figure 4.5D). A significant positive correlation also existed between fat mass and DA depletion in the SN ($p=0.04$, Fig. 5E) and striatum ($p=0.01$, Figure 4.5F).

Dopamine turnover

To estimate whether diet-induced differences in depletion levels affected DA metabolism, we analyzed the ratio of DOPAC to DA (a measure of DA turnover). In the SN of HF animals, DA turnover was increased in the lesioned hemisphere compared to the nonlesioned hemisphere, while chow animals exhibited a decrease in the lesioned

hemisphere (Figure 4.6A). This led to a significant main effect for group (F=10.9, p=0.002) and a significant interaction between group and hemisphere (F=9.97, p=0.004). In the striatum, there were no significant effects for hemisphere or group with regard to DA turnover (Figure 4.6B).

Protein effects in the substantia nigra

We measured activation of heat shock protein 27 (Hsp27) and protein levels of (IkBα) to indirectly assess oxidative stress in the SN. Hsp27 is activated by phosphorylation, and phosphorylated Hsp27 was significantly decreased in the HF-diet group compared to chow-fed controls (F=8.01, p=0.01; Figure 4.7A). The stress kinase IKKβ is activated by cellular stress, such as oxidative stress and insulin resistance (Gloire et al., 2006, Yuan et al., 2001) and degrades the protein inhibitor I kappa B alpha (IkBα) when active. Thus, protein levels of IkBα can be used to gauge stress kinase activity (Hacker and Karin, 2006). We observed a strong trend for decreased IkBα protein levels in HF fed rats compared to chow rats (F=4.02. p=0.056), indicating increased stress kinase activity (Figure 4.7B).

Discussion

We report here that HF-fed, insulin resistant rats exhibited enhanced nigrostriatal DA depletion following 6-OHDA. These changes occurred in the absence of altered cholesterol levels, diminished locomotor activity or muscle atrophy. Our results support an exacerbating role for dietary fat, and consequent insulin resistance, in vulnerability to toxin-induced nigrostriatal DA depletion. If 6-OHDA is produced endogenously even in small amounts, the increased vulnerability of DA neurons in response to HF diet-induced insulin resistance could put the nigrostriatal pathway at greater risk of damage during chronic HF feeding.

HF feeding in rodents has been previously characterized by our laboratory to cause weight gain, impaired insulin signaling, and glucose intolerance (Gupte et al., 2009). In the current study, an IPGTT indicated that HF-fed animals were insulin resistant prior to 6-OHDA administration. Skeletal muscle accounts for the vast majority of glucose uptake in the body (DeFronzo et al., 1985), and muscle glucose uptake decreases as a result of insulin resistance. Thus, to further analyze the extent of insulin resistance in these animals, glucose uptake was measured in two muscles: the EDL (fast-twitch glycolytic) and soleus (slow-twitch oxidative) muscles. In the EDL, insulin action was impaired with HF feeding: insulin exposure elicited a much greater increase in glucose transport in chow animals compared to HF-fed rats. However, in the soleus, insulin-stimulated glucose transport did not differ significantly between the two groups. This may be due to different metabolic adaptations to a HF diet between muscle types (Gupte et al., 2009), or different levels of heat shock proteins, which protect tissues against oxidative stress (Gupte et al., 2008).

The fact that HF-fed animals exhibited significantly greater DA depletion than chow-fed animals in both the SN and the striatum after 6-OHDA treatment supports a relationship between insulin resistance and PD. Neurons in the SN exist under a high oxidative load due

to DA metabolism. Both enzymatic and non-enzymatic DA metabolism generates reactive oxygen species (Martin and Teismann, 2009), and in this manner DA can cause both intracellular and extracelluar damage to local neurons (Yokoyama et al., 2008). The SN also has a very high iron content (Snyder and Connor, 2009), which may further exacerbate oxidative damage by reacting with byproducts of DA metabolism to generate highly reactive radicals (Coyle and Puttfarcken, 1993). Although the nature of DA neuron degeneration in PD is unclear, it is likely that reactive oxygen species play a role in early disease progression (reviewed in (Jenner, 2003). It is possible that the HF diet may exacerbate further DA depletion in this region because it is already highly vulnerable to damage. Because neurons in the SN project to the striatum and release DA, it follows that DA depletion would be evident in this tissue as well.

Interestingly, DA depletion in both the SN and striatum correlated significantly with HOMA-IR values. HOMA-IR is a widely used assessment of beta cell function and insulin resistance that accounts for both fasting glucose and fasting insulin levels (Wallace et al., 2004). As expected, HF-fed animals exhibited significantly higher epididymal fat weight was compared to the chow group. HF feeding and increased adiposity have been shown to increase levels of free fatty acids (Chess et al., 2009), which are known to contribute to insulin resistance in skeletal muscle (Boden, 2008). Like HOMA-IR, epidydymal fat content also correlated significantly with nigral and striatal DA depletion.

It is possible that increased oxidative stress contributes to SN vulnerability in the HF diet group. As an indirect measure of oxidative stress occurring in the SN, we measured activation (phosphorylation) of Hsp27 and protein levels of IkBα. We chose to analyze Hsp27 because, when active, it can protect against oxidative stress and mitochondrial complex I damage (Downs et al., 1999, Escobedo et al., 2004), which occurs in PD (Beal, 2003). Hsp27 also binds and sequesters the stress kinase IkKβ, in turn decreasing its

activity (Park et al., 2003). We observed a significant decrease in protective Hsp27 activity (pHsp27) in the SN of HF-fed rats, indicating an impaired stress response in this group. Because the stress kinase IkKβ degrades the downstream protein IkBα, analysis of IkBα levels is used as an indicator of IkKβ activity (Gupte et al., 2009, Hacker and Karin, 2006). The HF group exhibited a strong trend for decreased IkBα protein levels, likely due to increased activity of IkKβ.

Altered DA turnover (indicated by the ratio of DOPAC to DA in whole tissue) is a measure of DA metabolism (Altar et al., 1987) and reflects a functional response to nigrostriatal degeneration. In the SN, DA turnover was greater in HF-fed animals compared to the chow fed animals. Previous studies have shown that DA turnover is dependent on the extent of DA depletion, with greater DA depletion resulting in increased turnover [42, 43]. In our study, DA turnover was significantly increased in the lesioned compared to nonlesioned SN in HF rats, the group that exhibited nearly 50% DA depletion. Increased DA turnover could be a compensatory mechanism for maintenance of normal synaptic DA levels following DA neuron loss (Zigmond et al., 1990), and in a progressive MPTP model, DA turnover increases with greater DA depletion (Bezard et al., 2001). However, the chow group in our study actually exhibited decreased DA turnover in the lesioned vs. nonlesioned SN. It is possible that, with much lower (~30%) DA depletion, decreased turnover could also be a compensatory effect to keep existing DA in the synapse for an extended time period. It is clear that the low depletion level in chow animals was not sufficient to trigger an increase in DA turnover, as occurred in the HF group. In addition, there was no significant effect of group or hemisphere for this measure in the striatum. This suggests either that alterations occurring “upstream” in the SN occur first, or that the partial DA depletions in the chow-fed rats did not reach the threshold necessary to produce these compensatory effects in the terminal region.

Although our results support an exacerbating role for a HF diet on toxin-induced DA depletion, other effects of a HF diet may also contribute. Increased inflammatory signaling, adipokine levels, oxidative or nitrostative stress, mitochondrial dysfunction, and lipid metabolism have all been shown to occur with HF feeding (Cano et al., 2009, Gupte et al., 2009), reviewed in (Uranga et al., 2010). Some of these peripheral effects, such as oxidative stress, also occur in the brain following HF feeding (Fachinetto et al., 2005, Morrison et al., 2010, Zhang et al., 2005). Although specific contributions of additional effects of the HF diet cannot be ruled out, our findings support a role for insulin resistance in mediating increased toxin-induced DA depletion.

In conclusion, our results suggest that a HF diet can increase 6-OHDA-induced DA depletion in the nigrostriatal pathway. This study supports the findings of a previous study reporting enhanced MPTP toxin-induced nigrostriatal DA depletion in mice following a HF diet (Choi et al., 2005) and extends these findings to a different model and species. Our novel findings regarding 6-OHDA are particularly of interest in light of the fact that 6-OHDA is likely produced endogenously by DA metabolism. These findings, which support a "multiple hit" hypothesis regarding insulin resistance and neurotoxin exposure in vulnerability to PD, warrant further investigation into the mechanisms by which DA depletion is increased by a HF diet and insulin resistance.

FIGURE 4.1

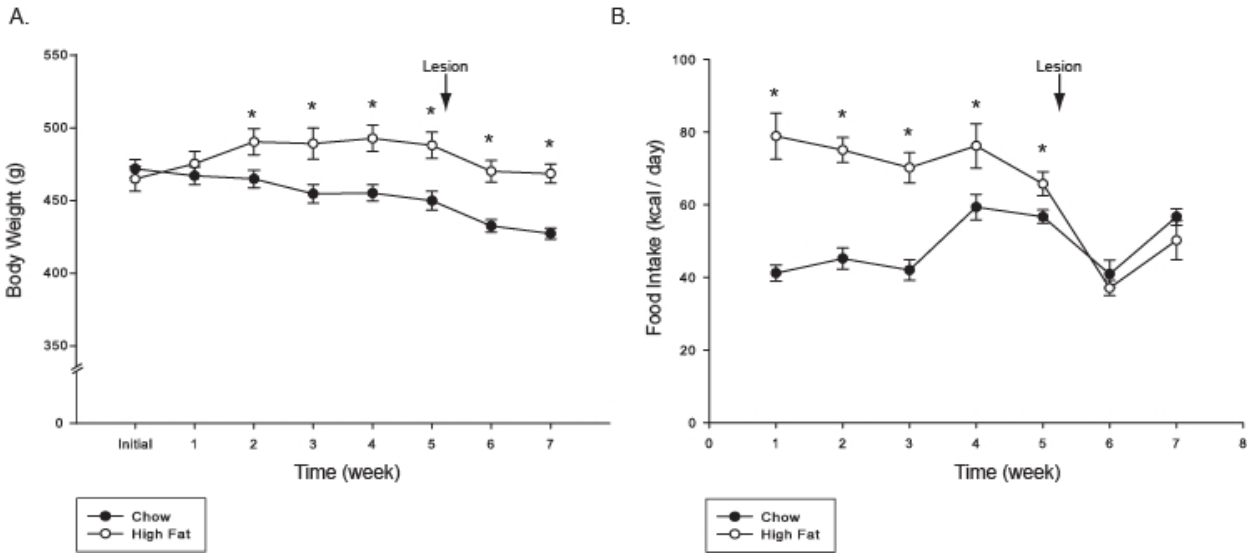
A.
Body Weight (g)
550
500
450
400
350
0
Lesion
Initial
1
2
3
4
5
6
7
Time (week)
Chow
High Fat
B.
Food Intake (kcal / day)
100
80
60
40
20
0
Lesion
0
1
2
3
4
5
6
7
8
Time (week)
Chow
High Fat

Figure 4.1. Food intake and body weight. HF feeding affected body weight **(A)**, and food intake **(B).** HF-fed animals weighed more than chow-fed rats, although food intake in the HF group was increased only initially and was affected to a greater extent by the lesion. Values are means ± SE for 8-10 rats per group. *$p<0.05$ Chow vs. HF.

FIGURE 4.2

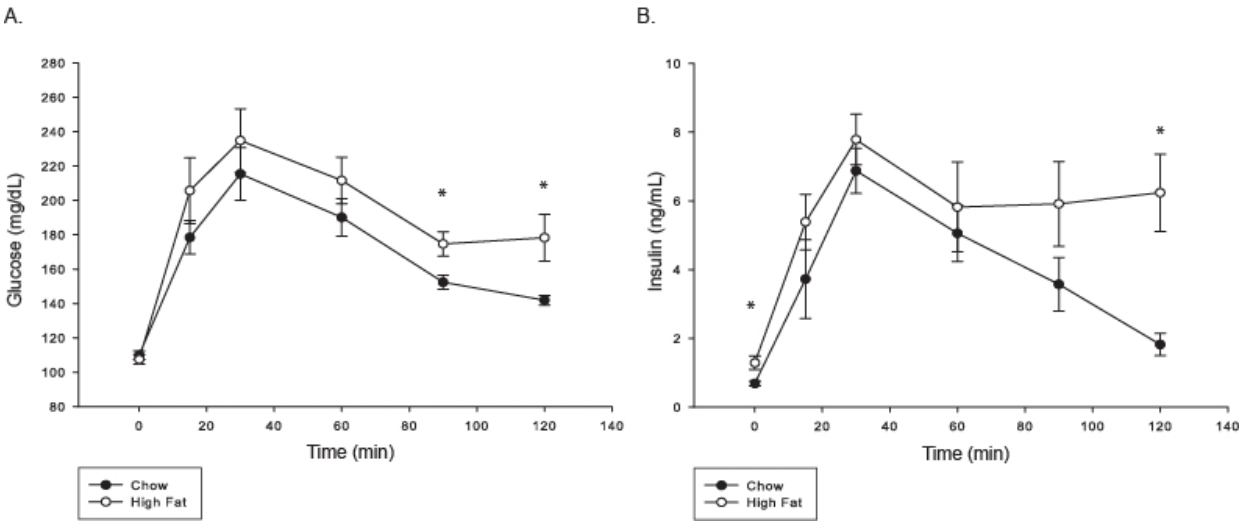
A.
Glucose (mg/dL)
280
260
240
220
200
180
160
140
120
100
80
0
20
40
60
80
100
120
140
Time (min)
Chow
High Fat
B.
Insulin (ng/mL)
10
8
6
4
2
0
Time (min)
Chow
High Fat

Figure 4.2. Intraperitoneal glucose tolerance test (IPGTT). After an overnight (12 hour) fast, an intraperitoneal injection of 60% glucose was administered at 2g glucose/kg body weight. Insulin **(A)** and glucose **(B)** were measured in tail blood at six time points: 0,15,45,60, 90, and 120 minutes after the glucose bolus (injection at t=0). The HF group exhibited significantly higher glucose values 90 and 120 minutes following the bolus. Serum insulin levels were significantly higher at the fasting (0) time point and 120 minutes post-bolus. *P≤0.05.

FIGURE 4.3

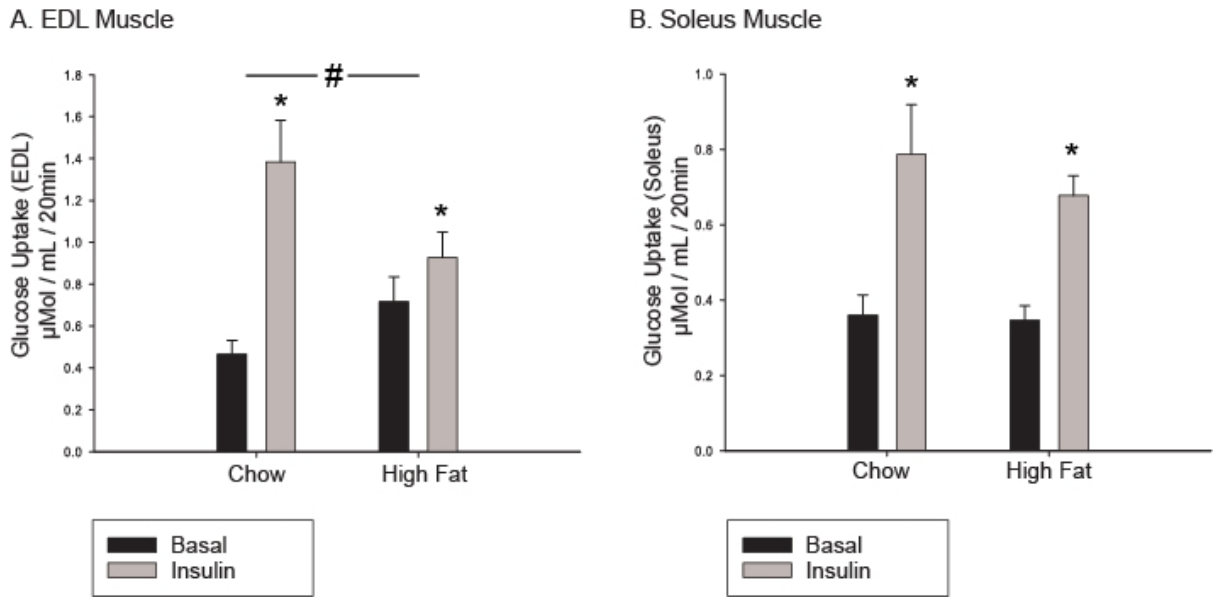
A. EDL Muscle
B. Soleus Muscle
Glucose Uptake (EDL)
µMol / mL / 20min
Glucose Uptake (Soleus)
µMol / mL / 20min
#
*
Chow
High Fat
Basal
Insulin

Figure 4.3. HF diet affects glucose transport in skeletal muscle. Glucose transport was measured to further characterize the effect of diet on peripheral insulin sensitivity. 2-deoxyglucose uptake was determined in EDL **(A)** and soleus **(B)** muscles incubated in the absence (black bars) or presence (gray bars) of 2mU/mL insulin. Insulin significantly increased glucose uptake in both the EDL and soleus muscles of all rats. In the EDL muscle, insulin stimulated glucose transport in HF rats was less than controls, indicating insulin resistance. Values are means ± SE for 10-12 muscles per group. *$p<0.05$ Basal vs. Insulin, #$p<0.05$ interaction effect between group and insulin.

FIGURE 4.4

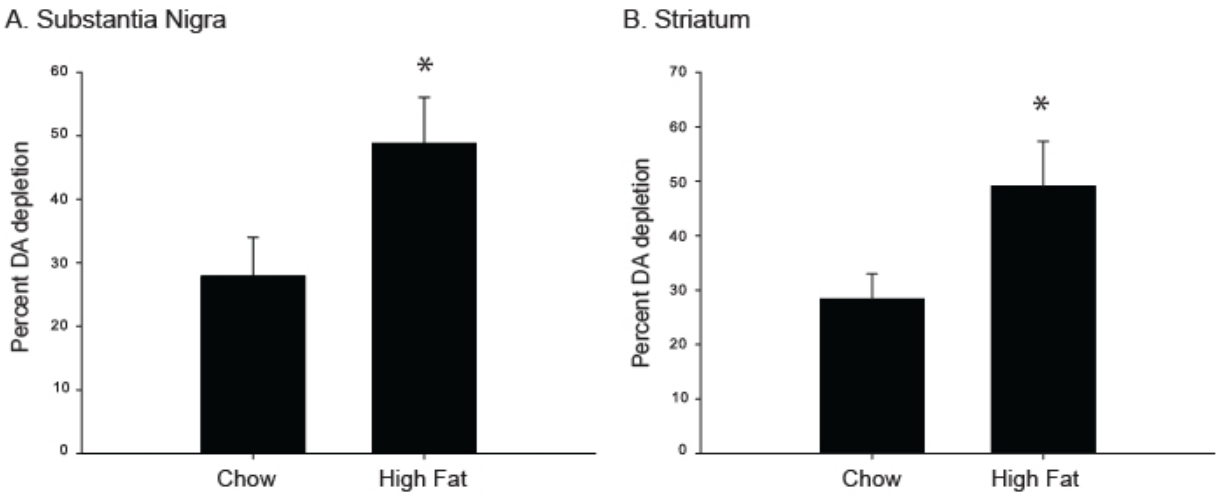
A. Substantia Nigra
Percent DA depletion
60
50
40
30
20
10
0
*
Chow
High Fat
B. Striatum
Percent DA depletion
70
60
50
40
30
20
10
0
*
Chow
High Fat

Figure 4.4 Effects of HF diet and 6-OHDA on tissue DA content. DA content in the right (lesioned) striatum was divided by DA levels in left (nonlesioned) striatum to obtain a percent depletion for each rat. Percent depletion was calculated in two different tissues: the SN **(A)**, and striatum **(B)**. HF-fed animals exhibited significantly greater DA depletion than controls in both tissues. Values are means ± SE for 8-10 samples per group. *$p<0.05$ Chow vs. HF.

FIGURE 4.5

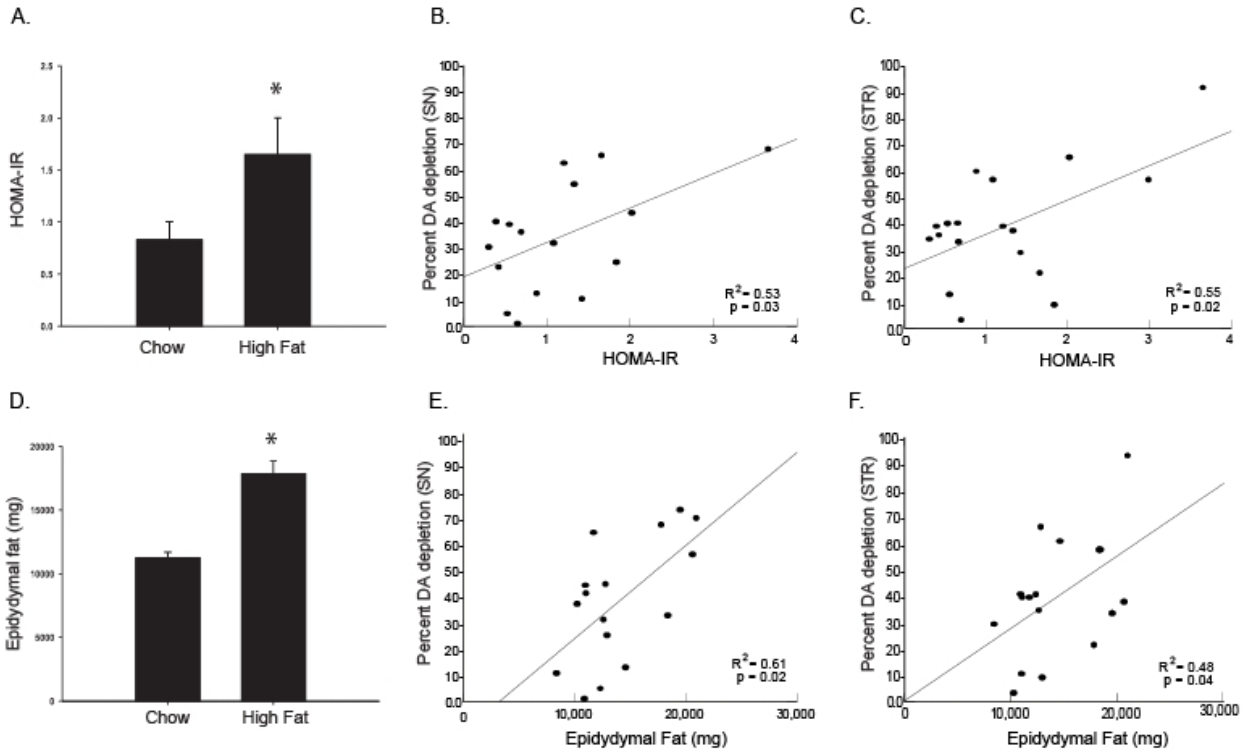
A.
HOMA-IR
Chow
High Fat
*
B.
Percent DA depletion (SN)
HOMA-IR
R² = 0.53
p = 0.03
C.
Percent DA depletion (STR)
HOMA-IR
R² = 0.55
p = 0.02
D.
Epididymal fat (mg)
Chow
High Fat
*
E.
Percent DA depletion (SN)
Epididymal Fat (mg)
R² = 0.61
p = 0.02
F.
Percent DA depletion (STR)
Epididymal Fat (mg)
R² = 0.48
p = 0.04

Figure 4.5. Systemic effects of HF feeding correlate with DA depletion. HF-fed rats exhibited a higher HOMA-IR value compared to chow fed rats **(A)**, indicating impaired insulin sensitivity. In all animals, there was a significant positive correlation between HOMA-IR and DA depletion levels in SN **(B)** and striatum **(C)**. The HF diet group also exhibited higher epididymal fat weight as expected **(D)**. Like HOMA-IR, epididymal fat also correlated significantly with DA depletion in both tissues **(E, F)**. Values are means ± SE 8-10 rats per group. *$p<0.05$ Chow vs. HF.

FIGURE 4.6

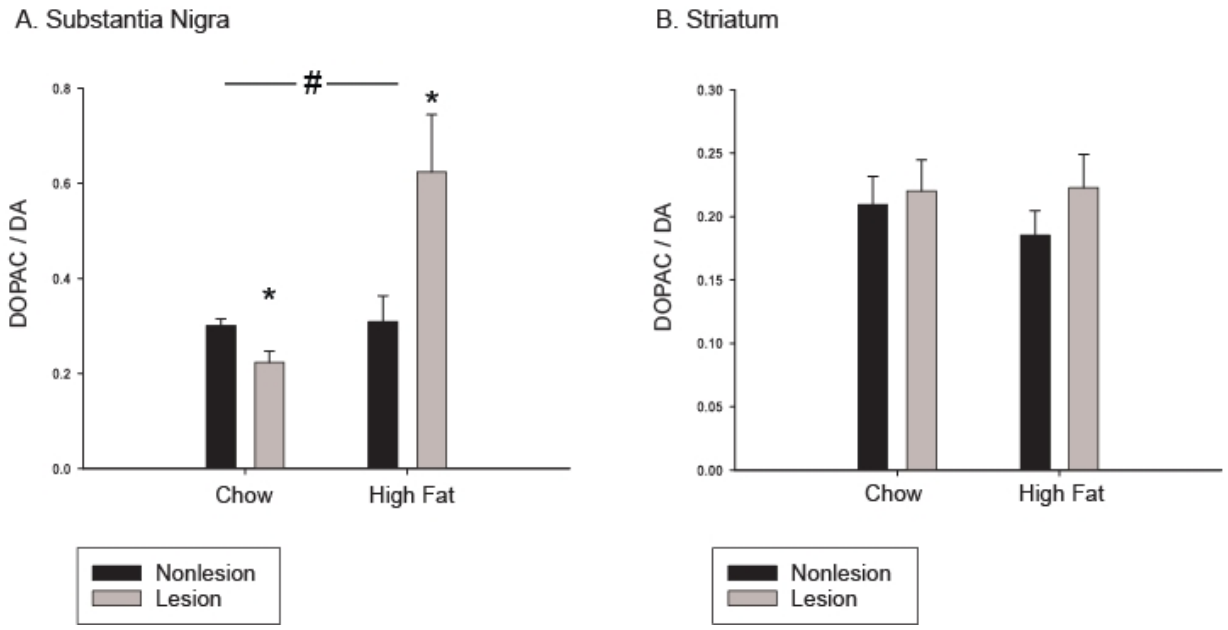
A. Substantia Nigra
B. Striatum
DOPAC / DA
0.8
0.6
0.4
0.2
0.0
0.30
0.25
0.20
0.15
0.10
0.05
0.00
#
*
*
Chow
High Fat
Nonlesion
Lesion

Figure 4.6. Effects of HF diet and 6-OHDA on DOPAC/DA ratio. The ratio of DOPAC divided by DA was calculated as an estimate of DA turnover in the SN **(A)** and the striatum **(B)**. In the SN, DA turnover was significantly increased in the lesioned hemisphere of HF-fed animals, but was decreased in the lesioned hemisphere of chow-fed animals. No difference between groups was observed in the striatum. Values are means ± SE for 8-10 samples per group. *$p<0.05$ chow vs. HF, #$p<0.05$ interaction effect between group and hemisphere.

FIGURE 4.7

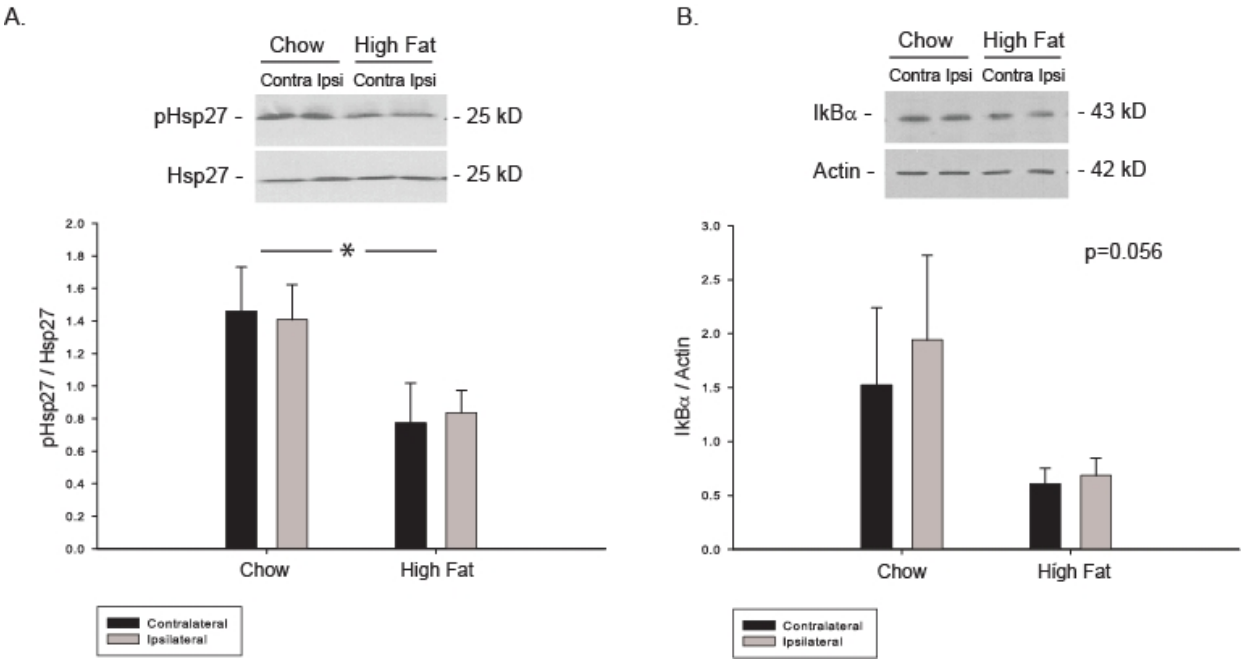
A.
Chow
High Fat
Contra Ipsi Contra Ipsi
pHsp27 -
- 25 kD
Hsp27 -
- 25 kD
pHsp27 / Hsp27
Chow
High Fat
Contralateral
Ipsilateral
B.
Chow
High Fat
Contra Ipsi Contra Ipsi
IkBα -
- 43 kD
Actin -
- 42 kD
p=0.056
IkBα / Actin
Chow
High Fat
Contralateral
Ipsilateral

Figure 4.7. HF feeding decreases heat shock protein activation and IkBα protein levels. Activation of Hsp25 (A) and IkBα expression (B) were analyzed in the SN. There was significantly less activation of Hsp25 in HF-fed animals compared to the chow group. The HF group also exhibited a strong trend ($p=0.056$) for a decrease in IkBα protein levels compared to chow rats. No difference between hemispheres was observed for either protein measure. Values are means ± SE for 5-7 samples per group. *$p<0.05$ Chow vs. HF.

Table 4.1

Characteristics of Chow- and HF-fed rats

	Chow	High Fat
Glucose (mg/dL)	115 ± 2.4	127 ± 1.8
Insulin (ng/mL)	0.675 ± 0.204	1.26 ± 0.420
Total Cholesterol (mg/dL)	93.3 ± 4.77	90.0 ± 4.13
LDL-C (mg/dL)	36.8 ± 2.17	30.2 ± 2.3
Distance Traveled (m)	44.28 ±3.6	45.27 ± 4.0
Ipsilateral Gastrocnemius wt (mg)	1955 ± 54.2	2005 ± 72.8
Contralateral Gastrocnemius wt (mg)	2045 ± 51.9	2017 ± 63.9

Table 4.2

Mean (+/- S.E.M.) striatal DA and DOPAC values for experimental groups (ng/g)

		Chow		High Fat	
Region	Metabolite	Nonlesion	Lesion	Nonlesion	Lesion
Striatum	DA	8485 ± 2683	6026 ± 1905	11329 ± 3776	5918 ± 1972
	DOPAC	1557 ± 492	1141 ± 360	1952 ± 650	1105 ± 368
Substantia Nigra	DA	629 ± 198	404 ± 127	647 ± 228	322 ± 113
	DOPAC	198 ± 62	88 ± 28	210 ± 74	163 ± 57

CHAPTER 5

DISCUSSION AND FUTURE DIRECTIONS

DISCUSSION AND FUTURE DIRECTIONS

Clinical studies suggest a potential casual link between T2D and PD. The aim of this study was to use animal models to investigate specific mechanisms that could mediate this link. Our goals were threefold: 1) to determine the effect of HF feeding on DA function in the basal ganglia, 2) to study the effect of DA depletion in insulin signaling in the basal ganglia and periphery, and 3) to investigate whether diet could exacerbate 6-OHDA mediated DA depletion.

5.1. Aim 1: HF diet model

To investigate T2D as a risk factor for PD, we used a HF diet model to induce insulin resistance. The ability of a HF diet to impair peripheral glucose metabolism has been well-characterized by our laboratory and others. As expected, we observed fasting hyperglycemia, hyperinsulinemia, and impaired glucose tolerance following a 12 week HF diet. Most interestingly, HF feeding resulted in striking effects on DA function in the basal ganglia. *In vivo* electrochemical studies revealed a significant decrease in striatal DA release and uptake; in fact, the observed alterations in DA function resembled those reported in aging studies (Hebert and Gerhardt, 1998). HPLC revealed that DA turnover was also significantly decreased. Although no overt DA depletion was observed, a decrease in DA turnover is in line with the observed electrochemical changes and may precede actual neuron loss. A drop in DA turnover could presumably indicate an increase in the length of time DA is present in the synapse and increase its propensity to undergo auto-oxidation. It could also decrease DA recycling and availability for re-packaging.

One of the most interesting findings from this aim was the alteration in iron mechanics. MRI analysis in live animals showed a marked T2 hypointensity in the SN. This indicates increased SN iron content, which is intriguing because protein analysis in that region showed significant alterations in expression of proteins involved in iron transport. One

weakness of our study is that we did not directly measure iron transport. This would be difficult to do *in vivo,* but future studies could measure the effect of insulin on membrane-associated transferrin receptors in cultured neurons in a similar manner as has been done in adipocytes (Davis et al., 1986). Because insulin signaling appears to be important to iron transport, it is also important to temporally characterize the point at which insulin resistance occurs in the brain. Although our study and previous studies in our laboratory have shown that peripheral insulin resistance is evident following a 12 week HF diet, these animals actually exhibit increased AKT phosphorylation in the SN (Figure 2.5). Because these animals are hyperinsulinemic, this would be expected in the absence of brain insulin resistance. We can speculate that by the time the brain does become insulin resistant, iron deposition and neuronal damage may already be in progress. Although no DA depletion resulted from the 12-week HF diet, impaired DA function and increased iron deposition could together make DA neurons even more vulnerable to damage and precede neuronal loss.

5.1.a.Future direction: Mitochondrial function and HF feeding

Data from this project indicate functional differences in nigrostriatal neurons between diet groups. As mentioned, one striking finding was that K^+-evoked DA release was significantly blunted following HF diet-induced insulin resistance. The reasons behind this effect are unclear: we observed iron dysregulation in the SN, but other possibilities have not been ruled out. One possibility is energy deficiency due to mitochondrial dysfunction. DA packaging into vesicles is accomplished by VMAT2 (Eiden et al., 2004). Because vesicular packaging occurs against electrochemical and concentration gradients, it requires energy expenditure. Mitochondrial damage can impair the ability of mitochondria to produce ATP efficiently. Impaired mitochondrial ATP production is part of the mitochondrial theory of aging (Navarro and Boveris, 2007), which is interesting because the effect of HF feeding on

DA release (Figure 2.2) was strikingly similar to the effect of aging on DA release (Hebert and Gerhardt, 1998). It is possible that these energy deficits could affect DA packaging via VMAT2. This may explain why alterations in DA function are observed in the absence of decreased DA content. Impaired vesicular partitioning would likely result in increased cytosolic DA, which has been shown to increase oxidative stress levels and lead to neurodegeneration (Caudle et al., 2007).

To test this hypothesis, striatal tissue will be harvested from rats following HF feeding. Fresh striatum samples from subsequent sections will be pooled from both hemispheres of each rat to obtain maximum tissue mass. Mitochondria will be density gradient purified from fresh tissue and oxygen consumption will be measured to determine mitochondrial capacity. SN tissue will be frozen and analyzed for expression of VMAT2 and proteins involved in mitochondrial function (i.e. cytochrome c, citrate synthase, Cox-1 and Cox-4, PGC1α, etc.) using western blot. These measures have been made in skeletal muscle following a HF diet (Gupte et al., 2009), but not in nigrostriatal neurons. Because these measures will be available from individual animals, mitochondrial measures can be correlated with electrochemical measures obtained *in vivo* to determine the contribution of mitochondria to differences in DA function.

5.1.b.Future direction: HF feeding and alpha synuclein

We also measured monomeric alpha-synuclein expression in the SN of HF fed animals. Intriguingly, we observed that HF feeding alone actually decreased endogenous levels of monomeric alpha-synuclein (Figure 5.1A). In addition, there was a strong positive correlation ($p<0.0001$, $R=0.77$) between monomeric alpha-synuclein expression and expression of the protein IkBα in our 12 wk HF-diet model (Figure 5.1B). This is interesting because IkBα is decreased in the face of oxidative stress due to increased expression of the upstream stress kinase IkKβ. Thus, an increase in IkBα would indicate less oxidative stress,

and a positive correlation between monomeric alpha-synuclein and IkBα indicates increased monomeric alpha synuclein expression in neurons with less oxidative stress. This is consistent with reports that alpha-synuclein plays a role as an antioxidant (Zhu et al., 2006). Processes that deplete monomeric alpha-synuclein, such as oligomerization or aggregation, could contribute to oxidation of lipid membranes in neurons (Zhu et al., 2006). Thus, it is possible that either increased (overexpressed) alpha-synuclein that results in aggregation or decreased monomeric alpha-synuclein could be detrimental to neuronal function.

FIGURE 5.1

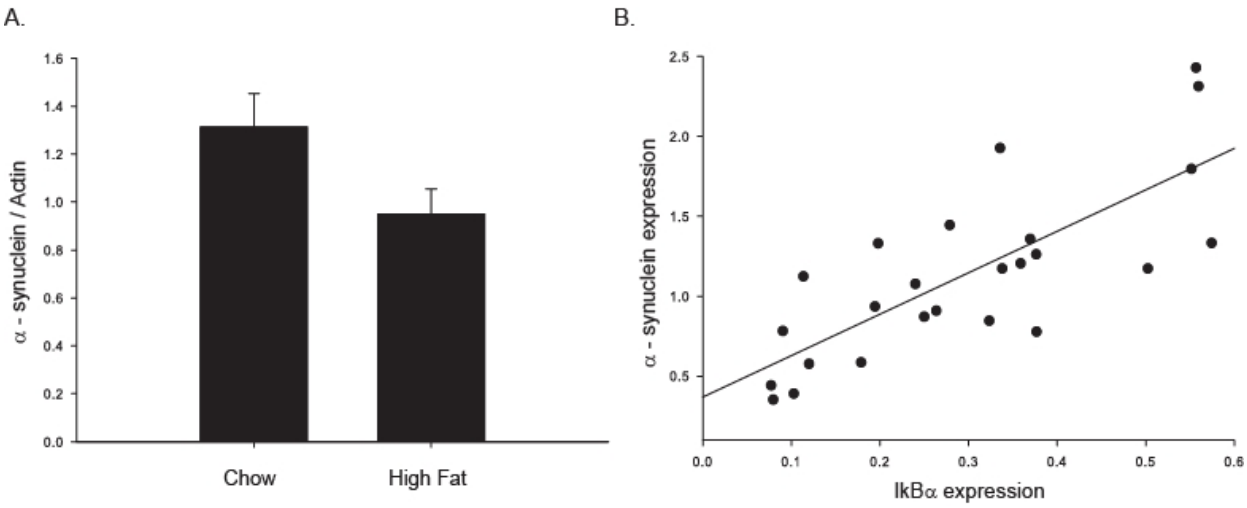

Figure 5.1. HF feeding decreases monomeric alpha-synuclein expression. A 12 week HF diet decreased expression of monomeric (14kd) alpha-synuclein protein. Alpha synuclein expression was positively correlated ($p<0.0001$, $R=0.77$) with expression of IkBα, supporting previous studies that indicate endogenous alpha-synuclein as having an antioxidant function.

5.2. Aim 2: 6-OHDA model

It is unclear whether the link between PD and T2D is bidirectional, so we designed experiments to test glucose tolerance in a well characterized preclinical PD model, the 6-OHDA lesion model. First, we tested whether insulin signaling was affected in the brain. Although it is recognized that the majority of glucose uptake into neurons is insulin-independent, insulin signaling proteins are abundant in many brain regions and the role of insulin signaling in the brain is still debated. In young animals, we observed a DA depletion-dependent, bilateral inhibition of insulin signaling in the striatum following a 6-OHDA administration. This is not surprising, because oxidative stress is known to impair insulin signaling, and the accepted mechanism for 6-OHDA mediated toxicity is oxidative damage.

Because the brain and periphery communicate via autonomic systems, and since catecholamine depletion occurs in the hypothalamus in PD patients, it is also possible that glucose disposal and insulin signaling could also be affected in the periphery. However, we did not observe any effect on glucose tolerance or peripheral insulin signaling in young rats. A follow up study using middle-aged animals also showed that striatal insulin signaling was affected, but again, glucose tolerance and peripheral insulin signaling was unchanged. It should be noted that, in the follow-up study, insulin levels were affected during the IPGTT.

It is possible that increased insulin early in the course of the glucose tolerance test may serve as a compensatory mechanism to help maintain normal glucose levels in lesioned animals. The increase in blood glucose levels at the end of the glucose tolerance test corresponded to a decrease in serum insulin, which supports this possibility. However, we did not see any changes in insulin-stimulated signaling in either fast or slow muscle, and rats were not hyperglycemic. Thus, we conclude that the unilateral 6-OHDA lesion model is not an optimal animal PD model to assess glucose tolerance.

5.1.a.Future direction: Bilateral 6-OHDA model

As mentioned, we measured small changes in serum insulin levels following a glucose tolerance test in animals treated unilaterally with 6-OHDA. Because the pancreas receives bilateral inputs from the brain, it is possible that we would see a greater effect with bilateral 6-OHDA administration. This model has been characterized (Salamone et al., 1993), and we have performed bilateral lesions in our laboratory (Figure 5.2). Peripheral glucose tolerance has not been assessed in this model. However, an important weakness of this more severe lesion model is that these animals experience drastic decreases in food intake and increased weight loss. These alterations alone may interfere with our investigation of glucose tolerance, as it takes many weeks for these animals to resume normal behavior. To minimize these effects, we could use a milder infusion (6 µg / side) into the striatum to obtain a lower degree of bilateral depletion. The length of recovery could also be increased from 6 weeks post-lesion.

FIGURE 5.2

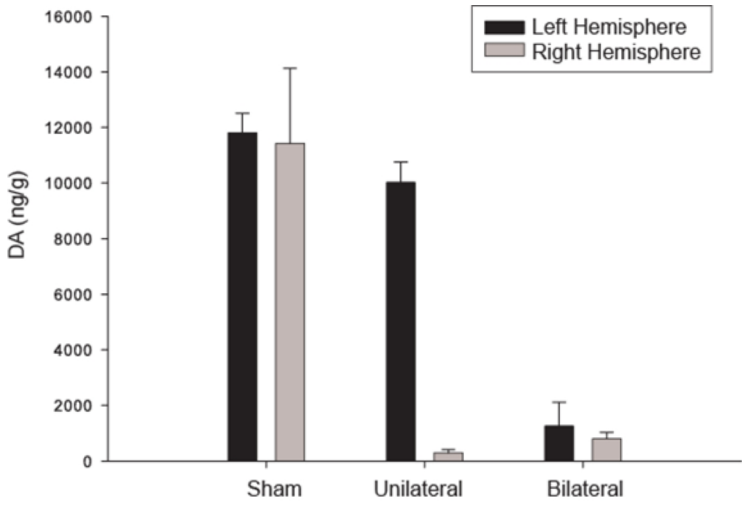

Figure 5.2. Comparison of DA content in unilateral and bilateral lesion models. Animals to be lesioned unilaterally were administered 9µg of 6-OHDA into the medial

forebrain bundle on the right hemisphere. Animals to be lesioned bilaterally were administered 12µg of 6-OHDA into the dorsal striatum in both hemispheres. DA content was quantified using HPLC. Values are means ± SE for 2-7 samples per group.

5.3. Aim 3: Discussion and future directions: HF + 6-OHDA

Finally, we aimed to investigate whether a HF diet could exacerbate DA depletion produced by the toxin 6-OHDA. This is of clinical relevance because several environmental toxins have been shown to either elicit or exacerbate DA depletion (Brooks et al., 1999, McEver, 1991, McGrew et al., 2000, Thrash et al., 2007, Walters et al., 1999). As expected, we observed that a low dose of 6-OHDA resulted in partial DA depletion in rats fed normal chow. However, the same dose of 6-OHDA elicited significantly greater DA depletion in animals consuming a HF diet. It has been shown that HF feeding increases measures of oxidative stress in several brain regions, including the SN. Because 6-OHDA is proposed to elicit toxicity through an oxidative mechanism (Blum et al., 2001), it is likely that 6-OHDA mediated damage is potentiated by the already high levels of oxidative stress in HF-fed animals.

Interestingly, DA depletion correlated significantly with HOMA-IR, an assessment of insulin sensitivity. This supports a role for insulin resistance in exacerbating DA depletion following toxin exposure. However, it remains to be determined whether it is actually insulin resistance itself or oxidative stress caused by insulin resistance that affects depletion levels. Insulin signaling does affect (increase) membrane associated DAT (Carvelli et al., 2002, Garcia et al., 2005), and we did not characterize brain insulin signaling in the combined HF+6-OHDA model. This is important to note because it is known that 6-OHDA uptake can occur via DAT (Blum et al., 2001). However, in this experiment, it is unlikely that high insulin, *per se*, directly caused increased 6-OHDA uptake for two reasons. First, the lesion was

performed at the beginning of the experiment. This was before increased glucose and insulin levels were apparent in the HF-fed group. Thus, high insulin at the time of the lesion should not have affected DAT membrane expression. Moreover, although we did not measure DAT membrane association, we did measure DAT protein levels by Western blot, and they were not significantly different between groups. Second, we have actually demonstrated that insulin signaling is inhibited by 6-OHDA six weeks following toxin administration (aim 2), meaning that even though high serum insulin levels were observed at tissue harvest, there is likely insulin resistance in the brain, as we have shown in previous studies using 6-OHDA and the 6-week timeframe. Furthermore, we have directly measured markers indicating increased oxidative stress (decreased reduced glutathione, increased oxidized:reduced glutathione ratio; aim 1) in serum of rats fed a HF diet for 12 weeks. Oxidative stress was likely increased in the periphery, and we saw a strong trend for a marker of increased oxidative stress (decreased Ikbα protein) in the SN. In sum, we observed higher DA depletion in HF-fed, insulin resistant rats in response to the same dose of 6-OHDA. The exact mechanism by which this increased vulnerability is mediated remains to be determined. However, it is likely that increased oxidative stress, a consequence of the observed insulin resistance, plays a role.

5.3.a. Future direction: HF diet and alpha-synuclein AAV vector model

One weakness of our experiments involves the exclusive use of 6-OHDA to model PD. While this widely-accepted animal model results in DA neuron degeneration, DA depletion, and motor deficits, it does not result in Lewy body pathology. Genetic mouse models expressing mutant alpha-synuclein or overexpressing wild-type alpha-synuclein can be used to study the effects of alpha-synuclein aggregation and Lewy body formation. Such genetic models are not available in the rat. However, recently it has been shown that SN

infusion of alpha-synuclein viral vector increases nigral alpha-synuclein expression and results in DA depletion.

Due to its presence in Lewy bodies, alpha-synuclein has been implicated in PD. In addition, iron and other metals have shown to induce alpha-synuclein aggregation (Uversky et al., 2001; Golts et al., 2002) and fibrillation (Uversky et al., 2002) which is interesting since our results implicate high SN iron following a HF diet. One development in recent years is targeted overexpression of alpha-synuclein using stereotaxic adeno-associated viral (AAV) vector delivery (Kirik and Bjorklund, 2003, Ulusoy et al., 2010). We have recently integrated the alpha-synuclein vector infusion model in our laboratory, demonstrating SN DA depletion and overexpression of alpha-synuclein four months after alpha-synuclein vector infusion (Figure 5.3). To expand on our findings regarding increased vulnerability of HF fed animals to 6-OHDA, we could examine the combined effect of HF feeding and alpha-synuclein expressing AAV vector infusion. Administration of alpha-synuclein expressing AAV vector reproduces some of the same phenotypes seen in PD, including cytoplasmic inclusions positive for alpha-synuclein (Kirik et al., 2003). We believe that this will complement our studies using 6-OHDA.

FIGURE 5.3

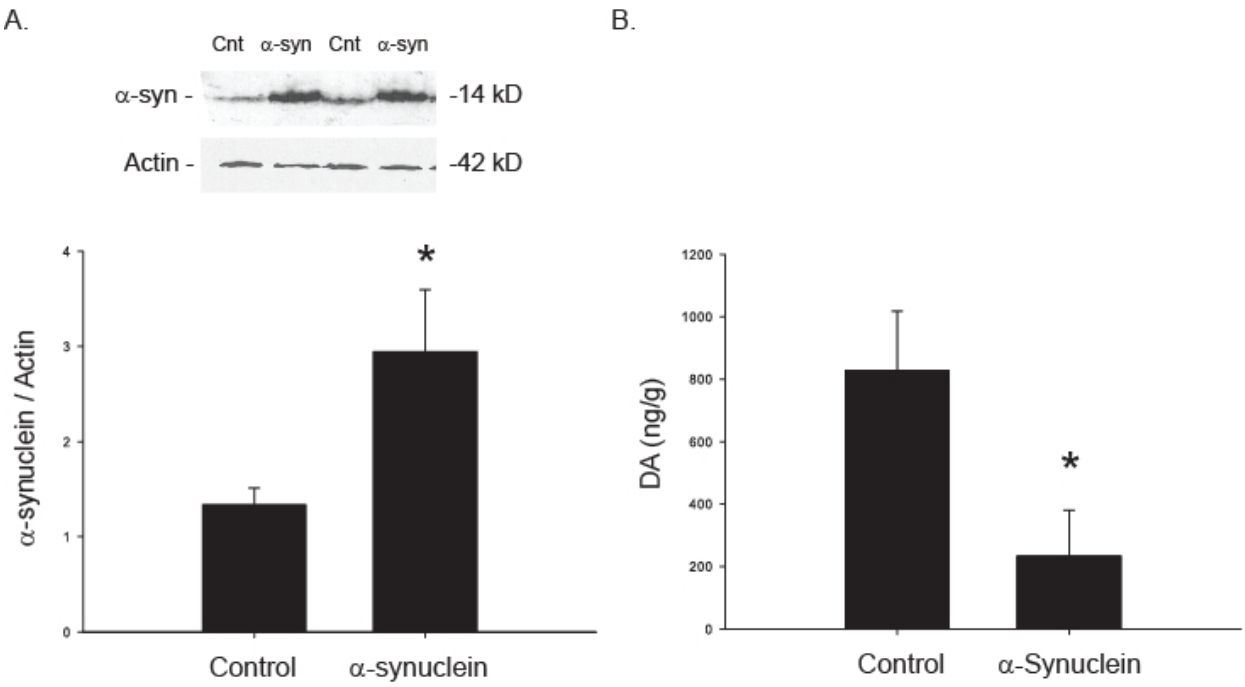

Figure 5.3. Nigral infusion of an α-synuclein vector results in DA depletion. Animals were infused unilatearlly with AAV vector expressing alpha-synuclein and allowed to survive for four months following infusion. Alpha-synuclein expression and DA content was analyzed in the non-infused (control) and vector-infused (α-synuclein) hemispheres. We have shown that α-synuclein vector infusion results in **(A)** increased alpha-synuclein expression and **(B)** decreased DA content in the SN. Values are means ± SE for 3 rats per group. *p<0.05 control vs. α-synuclein.

5.4. Additional interventions

During the course of this study, the potential for therapeutic interventions became apparent. The observed increase in nigral iron content and altered iron-responsive protein expression in our HF diet model suggest that normalizing SN iron levels may improve DA function. An intervention such as iron chelation would also allow us to investigate whether it is specifically iron that is contributing to impaired DA function. In addition, our laboratory has shown of heat shock proteins improve insulin resistance following a HF diet. We are

investigating a drug that can upregulate heat shock protein expression in the brain and periphery as another potential intervention. Upregulation of heat shock proteins will allow us to improve glucose metabolism during HF feeding and further investigate the mechanism behind impaired brain DA function.

5.4.a. Iron chelation

Our studies suggest that insulin may play a role in iron accumulation in the SN and potentially affect neuronal function. It has been known for some time that iron accumulation in the SN occurs in PD patients, and it has been shown that iron chelation can protect against DA neuron degradation (Andersen, 2004, Zhu et al., 2010). However, controlling iron-mediated DA neurodegeneration is not as straightforward as it seems. In fact, it has been shown clinically that some PD patients actually have decreased serum iron concentration when compared to controls (Logroscino et al., 1997) even though brain iron concentration is higher. Furthermore, although dietary iron chelation is neuroprotective against toxins such as MPTP, decreasing iron levels too much can actually decrease DA content, as iron is necessary for DA synthesis (Levenson et al., 2004).

It is likely iron transport, not systemic iron levels, that is important in PD pathogenesis. Impairment of iron transport into the nigra is protective against both MPTP and 6-OHDA (Hirsch, 2009), To build on this idea, we will investigate the effect of administering the iron chelator deferiprone (Ferriprox®). Deferiprone can cross the blood-brain barrier and is approved for use in treatment of neurodegeneration with brain iron accumulation and thalassemia (Forni et al., 2008). Deferiprone is unique because it works by redistributing iron to other cellular compartments or regions rather than promoting iron excretion (Kakhlon et al., 2010). As mentioned, this is important because iron plays important physiological roles within the cell.

5.4.b. Heat shock proteins as a therapeutic intervention

Molecular chaperones have long been recognized for their ability to mitigate cellular stress and maintain homeostasis. Recently, our laboratory has shown that induction of chaperone proteins by heat treatment improves insulin resistance following a HF diet (Gupte et al., 2009). Two chaperones central to the heat shock response are heat shock protein 90 (Hsp90) and heat shock protein 70 (Hsp70). Overexpression of Hsp70 in non-neuronal cell lines protects against cellular stress such as oxidative damage and apoptotic stimuli, and it has also been shown that Hsp70 prevents apoptosis in neuronal cells (Zheng and Yenari, 2006). Investigation of Hsp70 as a therapeutic agent in PD is important because a role for Hsp70 in the pathogenesis of PD has been implicated clinically. The protein ST13, a cofactor which interacts with and stabilizes Hsp70, was found to be one of 22 genes differentially expressed in PD patients (Scherzer et al., 2007). In sympathetic neurons, Hsp70 inhibits apoptosis upon NGF withdrawl by decreasing c-*Jun* activation (Bienemann et al., 2008). Because of its protective effects on neurons and ability to improve peripheral glycemia, upregulation of Hsp70 could provide a novel intervention in the pathways that may link PD and T2D.

Several studies have investigated the use of an Hsp90 inhibitor to increase Hsp70 expression. Normally, the heat shock response is restrained by a stable complex between Hsp90 and another protein, heat shock factor-1 (HSF1). However, this complex is destabilized in the presence of cellular stress, resulting in oligomerization, phosphorylation, and nuclear translocation of HSF1 (Ansar et al., 2007). Once in the nucleus, HSF1 induces heat shock protein expression. Pharmacological inhibition mimics this destabilization of the Hsp90/HSF1 complex (Ansar et al., 2007). One such Hsp90 inhibitor, Geldanamycin (GA), has been well-characterized for its ability to increase Hsp70 protein content, resulting in

protection against against both alpha-synuclein and ROS. (Shen, 2005)(Shen, 2005)This is likely mediated by a striatal increase in both Hsp70 and HSF1 (Shen et al., 2005). Flower et. al. showed that overexpression of the yeast heat shock protein SSA3 decreases ROS, and moreover, that GA also protected against ROS (Flower et al., 2005, Flower, 2005). However, a pitfall of Geldanamycin is its toxicity.

We have recently investigated the ability of a nontoxic Hsp90 inhibitor, KU-32, to upregulate Hsp expression in rat brain and skeletal muscle. Intraperitoneal administration of KU-32 upregulates Hsp expression in a dose dependent manner (Figure 5.3). Because Hsp70 upregulation can protect against insulin resistance, it is possible that it KU-32 administration could normalize the alterations in DA function that we observed following HF feeding.

Figure 5.4

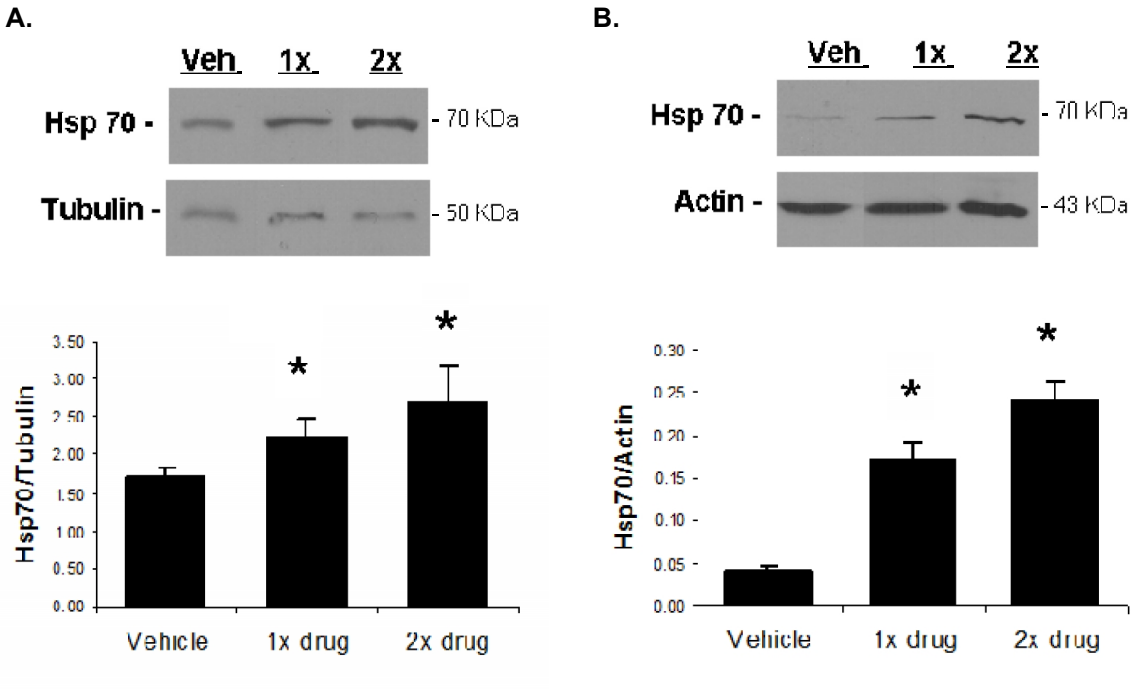

Figure 5.4. Induction of Hsp70 expression by KU-32 injection in skeletal muscle and striatum. (A) In soleus muscle, Hsp70 expression was increased 24% with 1 injection of KU-32, which was increased to a 37% increase with 2 injections of drug when compared to vehicle (saline) injected controls. In striatal tissue **(B)**, there was a 76% increase in Hsp70 expression with 1 injection of KU-32 and an 83% increase when 2 injections were administered vs. vehicle injected controls. Values are means of ± SE for 4-8 samples. *p<0.05 vehicle vs. drug administration.

General Summary

This project characterized the effect of insulin resistance on DA function in the basal ganglia, the effect of nigrostriatal DA depletion on peripheral metabolism, and the combined effect of HF feeding and toxin mediated DA depletion. Our preclinical studies present evidence that high fat diet-induced insulin resistance does affect the nigrostriatal pathway. Marked changes in DA release and uptake, as well as iron deposition, were observed. In addition, high fat diet-induced insulin resistance also increases the vulnerability of nigrostriatal neurons to toxin exposure. However, unilateral nigrostriatal dopamine depletion does not appear to discernibly affect glucose tolerance or peripheral insulin signaling. Our preclinical studies support a link between insulin resistance and nigrostriatal function, but suggest that this link is mainly one-directional, with insulin resistance preceding changes in nigrostriatal function. We feel that this work has significantly increased our understanding of how insulin resistance can affect the brain, and that the proposed future directions will contribute to our mechanistic understanding of insulin resistance and nigrostriatal function.

REFERENCES

1. Abbott, R. D., Ross, G. W., White, L. R., Nelson, J. S., Masaki, K. H., Tanner, C. M., Curb, J. D., Blanchette, P. L., Popper, J. S., and Petrovitch, H., 2002. Midlife adiposity and the future risk of Parkinson's disease. Neurology. 59, 1051-1057.
2. Adeghate, E., Schattner, P., and Dunn, E., 2006. An update on the etiology and epidemiology of diabetes mellitus. Ann N Y Acad Sci. 1084, 1-29.
3. Adler, G. S., 2008. Diabetes in the Medicare aged population, 2004. Health Care Financ Rev. 29, 69-79.
4. Agid, Y., Javoy, F., Glowinski, J., Bouvet, D., and Sotelo, C., 1973. Injection of 6-hydroxydopamine into the substantia nigra of the rat. II. Diffusion and specificity. Brain Res. 58, 291-301.
5. Aguirre, V., Uchida, T., Yenush, L., Davis, R., and White, M. F., 2000. The c-Jun NH(2)-terminal kinase promotes insulin resistance during association with insulin receptor substrate-1 and phosphorylation of Ser(307). J Biol Chem. 275, 9047-9054.
6. Aguirre, V., Werner, E. D., Giraud, J., Lee, Y. H., Shoelson, S. E., and White, M. F., 2002. Phosphorylation of Ser307 in insulin receptor substrate-1 blocks interactions with the insulin receptor and inhibits insulin action. J Biol Chem. 277, 1531-1537.
7. Ahren, B., 2000. Autonomic regulation of islet hormone secretion--implications for health and disease. Diabetologia. 43, 393-410.
8. Ahren, B., and Holst, J. J., 2001. The cephalic insulin response to meal ingestion in humans is dependent on both cholinergic and noncholinergic mechanisms and is important for postprandial glycemia. Diabetes. 50, 1030-1038.
9. Alessi, D. R., Andjelkovic, M., Caudwell, B., Cron, P., Morrice, N., Cohen, P., and Hemmings, B. A., 1996. Mechanism of activation of protein kinase B by insulin and IGF-1. Embo J. 15, 6541-6551.
10. Alim, M. A., Hossain, M. S., Arima, K., Takeda, K., Izumiyama, Y., Nakamura, M., Kaji, H., Shinoda, T., Hisanaga, S., and Ueda, K., 2002. Tubulin seeds alpha-synuclein fibril formation. J Biol Chem. 277, 2112-2117.
11. Altar, C. A., Marien, M. R., and Marshall, J. F., 1987. Time course of adaptations in dopamine biosynthesis, metabolism, and release following nigrostriatal lesions: implications for behavioral recovery from brain injury. J Neurochem. 48, 390-399.
12. Andersen, J. K., 2004. Iron dysregulation and Parkinson's disease. J Alzheimers Dis. 6, S47-52.
13. Anderson, C., Checkoway, H., Franklin, G. M., Beresford, S., Smith-Weller, T., and Swanson, P. D., 1999. Dietary factors in Parkinson's disease: the role of food groups and specific foods. Mov Disord. 14, 21-27.
14. Anderson, G. J., and Vulpe, C. D., 2009. Mammalian iron transport. Cell Mol Life Sci. 66, 3241-3261.
15. Andrew, R., Watson, D. G., Best, S. A., Midgley, J. M., Wenlong, H., and Petty, R. K., 1993. The determination of hydroxydopamines and other trace amines in the urine of parkinsonian patients and normal controls. Neurochem Res. 18, 1175-1177.
16. Andrews, Z. B., Erion, D., Beiler, R., Liu, Z. W., Abizaid, A., Zigman, J., Elsworth, J. D., Savitt, J. M., DiMarchi, R., Tschoep, M., Roth, R. H., Gao, X. B., and Horvath, T. L., 2009. Ghrelin promotes and protects nigrostriatal dopamine function via a UCP2-dependent mitochondrial mechanism. J Neurosci. 29, 14057-14065.

17. Andreyev, A. Y., Kushnareva, Y. E., and Starkov, A. A., 2005. Mitochondrial metabolism of reactive oxygen species. Biochemistry (Mosc). 70, 200-214.
18. Ansar, S., Burlison, J. A., Hadden, M. K., Yu, X. M., Desino, K. E., Bean, J., Neckers, L., Audus, K. L., Michaelis, M. L., and Blagg, B. S., 2007. A non-toxic Hsp90 inhibitor protects neurons from Abeta-induced toxicity. Bioorg Med Chem Lett. 17, 1984-1990.
19. Arvanitakis, Z., Wilson, R. S., Bienias, J. L., and Bennett, D. A., 2007. Diabetes and parkinsonian signs in older persons. Alzheimer Dis Assoc Disord. 21, 144-149.
20. Augustin, R., 2010. The protein family of glucose transport facilitators: It's not only about glucose after all. IUBMB Life. 62, 315-333.
21. Aydemir, F., Jenkitkasemwong, S., Gulec, S., and Knutson, M. D., 2009. Iron loading increases ferroportin heterogeneous nuclear RNA and mRNA levels in murine J774 macrophages. J Nutr. 139, 434-438.
22. Banks, W. A., 2004. The source of cerebral insulin. Eur J Pharmacol. 490, 5-12.
23. Barbeau, A., Giguere, R., and Hardy, J., 1961. [Clinical experience with tolbutamide in Parkinson's disease.]. Union Med Can. 90, 147-151.
24. Barbeau, A., and Pourcher, E., 1982. New data on the genetics of Parkinson's disease. Can J Neurol Sci. 9, 53-60.
25. Baum, L., Hansen, L., Masliah, E., and Saitoh, T., 1996. Glycogen synthase kinase 3 alteration in Alzheimer disease is related to neurofibrillary tangle formation. Mol Chem Neuropathol. 29, 253-261.
26. Beal, M. F., 2003. Mitochondria, oxidative damage, and inflammation in Parkinson's disease. Ann N Y Acad Sci. 991, 120-131.
27. Beaulieu, J. M., Gainetdinov, R. R., and Caron, M. G., 2007. The Akt-GSK-3 signaling cascade in the actions of dopamine. Trends Pharmacol Sci. 28, 166-172.
28. Becker, C., Brobert, G. P., Johansson, S., Jick, S. S., and Meier, C. R., 2008. Diabetes in patients with idiopathic Parkinson's disease. Diabetes Care. 31, 1808-1812.
29. Betchen, S. A., and Kaplitt, M., 2003. Future and current surgical therapies in Parkinson's disease. Curr Opin Neurol. 16, 487-493.
30. Bezard, E., Dovero, S., Prunier, C., Ravenscroft, P., Chalon, S., Guilloteau, D., Crossman, A. R., Bioulac, B., Brotchie, J. M., and Gross, C. E., 2001. Relationship between the appearance of symptoms and the level of nigrostriatal degeneration in a progressive 1-methyl-4-phenyl-1,2,3,6-tetrahydropyridine-lesioned macaque model of Parkinson's disease. J Neurosci. 21, 6853-6861.
31. Bharath, S., Hsu, M., Kaur, D., Rajagopalan, S., and Andersen, J. K., 2002. Glutathione, iron and Parkinson's disease. Biochem Pharmacol. 64, 1037-1048.
32. Bienemann, A. S., Lee, Y. B., Howarth, J., and Uney, J. B., 2008. Hsp70 suppresses apoptosis in sympathetic neurones by preventing the activation of c-Jun. J Neurochem. 104, 271-278.
33. Bjornholm, M., and Zierath, J. R., 2005. Insulin signal transduction in human skeletal muscle: identifying the defects in Type II diabetes. Biochem Soc Trans. 33, 354-357.
34. Bloch-Damti, A., and Bashan, N., 2005. Proposed mechanisms for the induction of insulin resistance by oxidative stress. Antioxid Redox Signal. 7, 1553-1567.
35. Bloch-Damti, A., Potashnik, R., Gual, P., Le Marchand-Brustel, Y., Tanti, J. F., Rudich, A., and Bashan, N., 2006. Differential effects of IRS1 phosphorylated on Ser307 or Ser632 in the induction of insulin resistance by oxidative stress. Diabetologia. 49, 2463-2473.

36. Blum, D., Torch, S., Lambeng, N., Nissou, M., Benabid, A. L., Sadoul, R., and Verna, J. M., 2001. Molecular pathways involved in the neurotoxicity of 6-OHDA, dopamine and MPTP: contribution to the apoptotic theory in Parkinson's disease. Prog Neurobiol. 65, 135-172.
37. Boden, G., 2008. Obesity and free fatty acids. Endocrinol Metab Clin North Am. 37, 635-646, viii-ix.
38. Borah, A., and Mohanakumar, K. P., L-DOPA-induced 6-hydroxydopamine production in the striata of rodents is sensitive to the degree of denervation. Neurochem Int. 56, 357-362.
39. Boushel, R., Gnaiger, E., Schjerling, P., Skovbro, M., Kraunsoe, R., and Dela, F., 2007. Patients with type 2 diabetes have normal mitochondrial function in skeletal muscle. Diabetologia. 50, 790-796.
40. Boyd, A. E., 3rd, Lebovitz, H. E., and Feldman, J. M., 1971. Endocrine function and glucose metabolism in patients with Parkinson's disease and their alternation by L-Dopa. J Clin Endocrinol Metab. 33, 829-837.
41. Brass, S. D., Chen, N. K., Mulkern, R. V., and Bakshi, R., 2006. Magnetic resonance imaging of iron deposition in neurological disorders. Top Magn Reson Imaging. 17, 31-40.
42. Brooks, A. I., Chadwick, C. A., Gelbard, H. A., Cory-Slechta, D. A., and Federoff, H. J., 1999. Paraquat elicited neurobehavioral syndrome caused by dopaminergic neuron loss. Brain Res. 823, 1-10.
43. Bruce-Keller, A. J., Keller, J. N., and Morrison, C. D., 2009. Obesity and vulnerability of the CNS. Biochim Biophys Acta. 1792, 395-400.
44. Bunn, R. C., Jensen, M. A., and Reed, B. C., 1999. Protein interactions with the glucose transporter binding protein GLUT1CBP that provide a link between GLUT1 and the cytoskeleton. Mol Biol Cell. 10, 819-832.
45. Burdo, J. R., Martin, J., Menzies, S. L., Dolan, K. G., Romano, M. A., Fletcher, R. J., Garrick, M. D., Garrick, L. M., and Connor, J. R., 1999. Cellular distribution of iron in the brain of the Belgrade rat. Neuroscience. 93, 1189-1196.
46. Cacho, J., Sevillano, J., de Castro, J., Herrera, E., and Ramos, M. P., 2008. Validation of simple indexes to assess insulin sensitivity during pregnancy in Wistar and Sprague-Dawley rats. Am J Physiol Endocrinol Metab. 295, E1269-1276.
47. Cadet, J. L., Kujirai, K., and Przedborski, S., 1991. Bilateral modulation of [3H]neurotensin binding by unilateral intrastriatal 6-hydroxydopamine injections: evidence from a receptor autoradiographic study. Brain Res. 564, 37-44.
48. Calabresi, P., Di Filippo, M., Ghiglieri, V., Tambasco, N., and Picconi, B., 2010. Levodopa-induced dyskinesias in patients with Parkinson's disease: filling the bench-to-bedside gap. Lancet Neurol. 9, 1106-1117.
49. Cano, P., Cardinali, D. P., Rios-Lugo, M. J., Fernandez-Mateos, M. P., Reyes Toso, C. F., and Esquifino, A. I., 2009. Effect of a high-fat diet on 24-hour pattern of circulating adipocytokines in rats. Obesity (Silver Spring). 17, 1866-1871.
50. Carvelli, L., Moron, J. A., Kahlig, K. M., Ferrer, J. V., Sen, N., Lechleiter, J. D., Leeb-Lundberg, L. M., Merrill, G., Lafer, E. M., Ballou, L. M., Shippenberg, T. S., Javitch, J. A., Lin, R. Z., and Galli, A., 2002. PI 3-kinase regulation of dopamine uptake. J Neurochem. 81, 859-869.
51. Cass, W. A., Zahniser, N. R., Flach, K. A., and Gerhardt, G. A., 1993. Clearance of exogenous dopamine in rat dorsal striatum and nucleus accumbens: role of metabolism and effects of locally applied uptake inhibitors. J Neurochem. 61, 2269-2278.

52. Caudle, W. M., Richardson, J. R., Wang, M. Z., Taylor, T. N., Guillot, T. S., McCormack, A. L., Colebrooke, R. E., Di Monte, D. A., Emson, P. C., and Miller, G. W., 2007. Reduced vesicular storage of dopamine causes progressive nigrostriatal neurodegeneration. J Neurosci. 27, 8138-8148.
53. Cepeda, C., Colwell, C. S., Itri, J. N., Chandler, S. H., and Levine, M. S., 1998. Dopaminergic modulation of NMDA-induced whole cell currents in neostriatal neurons in slices: contribution of calcium conductances. J Neurophysiol. 79, 82-94.
54. Chen, G., Bower, K. A., Ma, C., Fang, S., Thiele, C. J., and Luo, J., 2004. Glycogen synthase kinase 3beta (GSK3beta) mediates 6-hydroxydopamine-induced neuronal death. Faseb J. 18, 1162-1164.
55. Chess, D. J., Khairallah, R. J., O'Shea, K. M., Xu, W., and Stanley, W. C., 2009. A high-fat diet increases adiposity but maintains mitochondrial oxidative enzymes without affecting development of heart failure with pressure overload. Am J Physiol Heart Circ Physiol. 297, H1585-1593.
56. Choi, J. Y., Jang, E. H., Park, C. S., and Kang, J. H., 2005. Enhanced susceptibility to 1-methyl-4-phenyl-1,2,3,6-tetrahydropyridine neurotoxicity in high-fat diet-induced obesity. Free Radic Biol Med. 38, 806-816.
57. Cooksey, R. C., Jones, D., Gabrielsen, S., Huang, J., Simcox, J. A., Luo, B., Soesanto, Y., Rienhoff, H., Abel, E. D., and McClain, D. A., 2010. Dietary iron restriction or iron chelation protects from diabetes and loss of beta-cell function in the obese (ob/ob lep-/-) mouse. Am J Physiol Endocrinol Metab. 298, E1236-1243.
58. Cooper, A. A., Gitler, A. D., Cashikar, A., Haynes, C. M., Hill, K. J., Bhullar, B., Liu, K., Xu, K., Strathearn, K. E., Liu, F., Cao, S., Caldwell, K. A., Caldwell, G. A., Marsischky, G., Kolodner, R. D., Labaer, J., Rochet, J. C., Bonini, N. M., and Lindquist, S., 2006. Alpha-synuclein blocks ER-Golgi traffic and Rab1 rescues neuron loss in Parkinson's models. Science. 313, 324-328.
59. Coyle, J. T., and Puttfarcken, P., 1993. Oxidative stress, glutamate, and neurodegenerative disorders. Science. 262, 689-695.
60. D'Amelio, M., Ragonese, P., Callari, G., Di Benedetto, N., Palmeri, B., Terruso, V., Salemi, G., Famoso, G., Aridon, P., and Savettieri, G., 2009. Diabetes preceding Parkinson's disease onset. A case-control study. Parkinsonism Relat Disord. 15, 660-664.
61. Daniels, W. M., Jaffer, A., Russell, V. A., and Taljaard, J. J., 1993. Alpha 2- and beta-adrenergic stimulation of corticosterone secretion in rats. Neurochem Res. 18, 159-164.
62. Davis, J. F., Tracy, A. L., Schurdak, J. D., Tschop, M. H., Lipton, J. W., Clegg, D. J., and Benoit, S. C., 2008. Exposure to elevated levels of dietary fat attenuates psychostimulant reward and mesolimbic dopamine turnover in the rat. Behav Neurosci. 122, 1257-1263.
63. Davis, R. J., Corvera, S., and Czech, M. P., 1986. Insulin stimulates cellular iron uptake and causes the redistribution of intracellular transferrin receptors to the plasma membrane. J Biol Chem. 261, 8708-8711.
64. de la Monte, S. M., 2009. Insulin resistance and Alzheimer's disease. BMB Rep. 42, 475-481.
65. DeFronzo, R. A., Gunnarsson, R., Bjorkman, O., Olsson, M., and Wahren, J., 1985. Effects of insulin on peripheral and splanchnic glucose metabolism in noninsulin-dependent (type II) diabetes mellitus. J Clin Invest. 76, 149-155.
66. Delhanty, P. J., van der Eerden, B. C., van der Velde, M., Gauna, C., Pols, H. A., Jahr, H., Chiba, H., van der Lely, A. J., and van Leeuwen, J. P., 2006. Ghrelin and unacylated ghrelin stimulate human osteoblast growth via mitogen-activated protein kinase

(MAPK)/phosphoinositide 3-kinase (PI3K) pathways in the absence of GHS-R1a. J Endocrinol. 188, 37-47.
67. Dexter, D. T., Wells, F. R., Agid, F., Agid, Y., Lees, A. J., Jenner, P., and Marsden, C. D., 1987. Increased nigral iron content in postmortem parkinsonian brain. Lancet. 2, 1219-1220.
68. Dong, X., Park, S., Lin, X., Copps, K., Yi, X., and White, M. F., 2006. Irs1 and Irs2 signaling is essential for hepatic glucose homeostasis and systemic growth. J Clin Invest. 116, 101-114.
69. Downs, C. A., Jones, L. R., and Heckathorn, S. A., 1999. Evidence for a novel set of small heat-shock proteins that associates with the mitochondria of murine PC12 cells and protects NADH:ubiquinone oxidoreductase from heat and oxidative stress. Arch Biochem Biophys. 365, 344-350.
70. Driver, J. A., Smith, A., Buring, J. E., Gaziano, M., Kurth, T., and Logroscino, G., 2008. Prospective Cohort Study of Type 2 Diabetes and the Risk of Parkinson's Disease. Diabetes Care.
71. Eberhardt, M. S., Engelgau, M., and Cadwell, B, 2004. Prevalence of overweight and obesity among adults with diagnosed diabetes--United States, 1988-1994 and 1999-2002. MMWR Morb Mortal Wkly Rep. 53, 1066-1068.
72. Eiden, L. E., Schafer, M. K., Weihe, E., and Schutz, B., 2004. The vesicular amine transporter family (SLC18): amine/proton antiporters required for vesicular accumulation and regulated exocytotic secretion of monoamines and acetylcholine. Pflugers Arch. 447, 636-640.
73. El Messari, S., Leloup, C., Quignon, M., Brisorgueil, M. J., Penicaud, L., and Arluison, M., 1998. Immunocytochemical localization of the insulin-responsive glucose transporter 4 (Glut4) in the rat central nervous system. J Comp Neurol. 399, 492-512.
74. Enna, S. J., Reisman, S. A., and Stanford, J. A., 2006. CGP 56999A, a GABA(B) receptor antagonist, enhances expression of brain-derived neurotrophic factor and attenuates dopamine depletion in the rat corpus striatum following a 6-hydroxydopamine lesion of the nigrostriatal pathway. Neurosci Lett. 406, 102-106.
75. Escobedo, J., Pucci, A. M., and Koh, T. J., 2004. HSP25 protects skeletal muscle cells against oxidative stress. Free Radic Biol Med. 37, 1455-1462.
76. Evans, J. L., Goldfine, I. D., Maddux, B. A., and Grodsky, G. M., 2003. Are oxidative stress-activated signaling pathways mediators of insulin resistance and beta-cell dysfunction? Diabetes. 52, 1-8.
77. Fachinetto, R., Burger, M. E., Wagner, C., Wondracek, D. C., Brito, V. B., Nogueira, C. W., Ferreira, J., and Rocha, J. B., 2005. High fat diet increases the incidence of orofacial dyskinesia and oxidative stress in specific brain regions of rats. Pharmacol Biochem Behav. 81, 585-592.
78. Farrell, P. A., Beard, J. L., and Druckenmiller, M., 1988. Increased insulin sensitivity in iron-deficient rats. J Nutr. 118, 1104-1109.
79. Fernandez-Real, J. M., Lopez-Bermejo, A., and Ricart, W., 2002. Cross-talk between iron metabolism and diabetes. Diabetes. 51, 2348-2354.
80. Figlewicz, D. P., Evans, S. B., Murphy, J., Hoen, M., and Baskin, D. G., 2003. Expression of receptors for insulin and leptin in the ventral tegmental area/substantia nigra (VTA/SN) of the rat. Brain Res. 964, 107-115.
81. Fink, R. I., Kolterman, O. G., Griffin, J., and Olefsky, J. M., 1983. Mechanisms of insulin resistance in aging. J Clin Invest. 71, 1523-1535.

82. Flower, T. R., Chesnokova, L. S., Froelich, C. A., Dixon, C., and Witt, S. N., 2005. Heat shock prevents alpha-synuclein-induced apoptosis in a yeast model of Parkinson's disease. J Mol Biol. 351, 1081-1100.
83. Flower, T. R., Chesnokova, L.S., Froelich, C.A., Dixon, C., and S.N. Witt, 2005. Heat shock prevents alpha-synuclein induced apoptosis in a yest model of Parkinson's Disease. J. Mol. Biol. 351, 1081-1100.
84. Folli, F., Bonfanti, L., Renard, E., Kahn, C. R., and Merighi, A., 1994. Insulin receptor substrate-1 (IRS-1) distribution in the rat central nervous system. J Neurosci. 14, 6412-6422.
85. Forni, G. L., Balocco, M., Cremonesi, L., Abbruzzese, G., Parodi, R. C., and Marchese, R., 2008. Regression of symptoms after selective iron chelation therapy in a case of neurodegeneration with brain iron accumulation. Mov Disord. 23, 904-907.
86. Friedlich, A. L., Tanzi, R. E., and Rogers, J. T., 2007. The 5'-untranslated region of Parkinson's disease alpha-synuclein messengerRNA contains a predicted iron responsive element. Mol Psychiatry. 12, 222-223.
87. Fulton, S., Pissios, P., Manchon, R. P., Stiles, L., Frank, L., Pothos, E. N., Maratos-Flier, E., and Flier, J. S., 2006. Leptin regulation of the mesoaccumbens dopamine pathway. Neuron. 51, 811-822.
88. Gallego, M., Setien, R., Izquierdo, M. J., Casis, O., and Casis, E., 2003. Diabetes-induced biochemical changes in central and peripheral catecholaminergic systems. Physiol Res. 52, 735-741.
89. Garcia-Segura, L. M., Diz-Chaves, Y., Perez-Martin, M., and Darnaudery, M., 2007. Estradiol, insulin-like growth factor-I and brain aging. Psychoneuroendocrinology. 32 Suppl 1, S57-61.
90. Garcia, B. G., Wei, Y., Moron, J. A., Lin, R. Z., Javitch, J. A., and Galli, A., 2005. Akt is essential for insulin modulation of amphetamine-induced human dopamine transporter cell-surface redistribution. Mol Pharmacol. 68, 102-109.
91. Geiger, B. M., Haburcak, M., Avena, N. M., Moyer, M. C., Hoebel, B. G., and Pothos, E. N., 2009. Deficits of mesolimbic dopamine neurotransmission in rat dietary obesity. Neuroscience. 159, 1193-1199.
92. Geiger, P. C., Hancock, C., Wright, D. C., Han, D. H., and Holloszy, J. O., 2007. IL-6 increases muscle insulin sensitivity only at superphysiological levels. Am J Physiol Endocrinol Metab. 292, E1842-1846.
93. Gloire, G., Legrand-Poels, S., and Piette, J., 2006. NF-kappaB activation by reactive oxygen species: fifteen years later. Biochem Pharmacol. 72, 1493-1505.
94. Golts, N., Snyder, H., Frasier, M., Theisler, C., Choi, P., and Wolozin, B., 2002. Magnesium inhibits spontaneous and iron-induced aggregation of alpha-synuclein. J Biol Chem. 277, 16116-16123.
95. Gonzalez, E., and McGraw, T. E., 2006. Insulin signaling diverges into Akt-dependent and -independent signals to regulate the recruitment/docking and the fusion of GLUT4 vesicles to the plasma membrane. Mol Biol Cell. 17, 4484-4493.
96. Gorell, J. M., Ordidge, R. J., Brown, G. G., Deniau, J. C., Buderer, N. M., and Helpern, J. A., 1995. Increased iron-related MRI contrast in the substantia nigra in Parkinson's disease. Neurology. 45, 1138-1143.
97. Graham, J. M., Paley, M. N., Grunewald, R. A., Hoggard, N., and Griffiths, P. D., 2000. Brain iron deposition in Parkinson's disease imaged using the PRIME magnetic resonance sequence. Brain. 123 Pt 12, 2423-2431.

98. Gupte, A. A., Bomhoff, G. L., and Geiger, P. C., 2008. Age-related differences in skeletal muscle insulin signaling: the role of stress kinases and heat shock proteins. J Appl Physiol. 105, 839-848.
99. Gupte, A. A., Bomhoff, G. L., Morris, J. K., Gorres, B. K., and Geiger, P. C., 2009. Lipoic acid increases heat shock protein expression and inhibits stress kinase activation to improve insulin signaling in skeletal muscle from high-fat-fed rats. J Appl Physiol. 106, 1425-1434.
100. Gupte, A. A., Bomhoff, G. L., Swerdlow, R. H., and Geiger, P. C., 2009. Heat treatment improves glucose tolerance and prevents skeletal muscle insulin resistance in rats fed a high-fat diet. Diabetes. 58, 567-578.
101. Hacker, H., and Karin, M., 2006. Regulation and function of IKK and IKK-related kinases. Sci STKE. 2006, re13.
102. Hall, W. D., 1990. An Overview of the Autonomic Nervous System.
103. Harley, A., Cooper, J. M., and Schapira, A. H., 1993. Iron induced oxidative stress and mitochondrial dysfunction: relevance to Parkinson's disease. Brain Res. 627, 349-353.
104. Hatcher, J. M., Richardson, J. R., Guillot, T. S., McCormack, A. L., Di Monte, D. A., Jones, D. P., Pennell, K. D., and Miller, G. W., 2007. Dieldrin exposure induces oxidative damage in the mouse nigrostriatal dopamine system. Exp Neurol. 204, 619-630.
105. Hebert, M. A., and Gerhardt, G. A., 1998. Normal and drug-induced locomotor behavior in aging: comparison to evoked DA release and tissue content in fischer 344 rats. Brain Res. 797, 42-54.
106. Henriksen, E. J., Kinnick, T. R., Teachey, M. K., O'Keefe, M. P., Ring, D., Johnson, K. W., and Harrison, S. D., 2003. Modulation of muscle insulin resistance by selective inhibition of GSK-3 in Zucker diabetic fatty rats. Am J Physiol Endocrinol Metab. 284, E892-900.
107. Hey-Mogensen, M., Hojlund, K., Vind, B. F., Wang, L., Dela, F., Beck-Nielsen, H., Fernstrom, M., and Sahlin, K., 2010. Effect of physical training on mitochondrial respiration and reactive oxygen species release in skeletal muscle in patients with obesity and type 2 diabetes. Diabetologia. 53, 1976-1985.
108. Hindle, J. V., 2010. Ageing, neurodegeneration and Parkinson's disease. Age Ageing. 39, 156-161.
109. Hirsch, E. C., 2009. Iron transport in Parkinson's disease. Parkinsonism Relat Disord. 15 Suppl 3, S209-211.
110. Hoffman, A. F., and Gerhardt, G. A., 1998. In vivo electrochemical studies of dopamine clearance in the rat substantia nigra: effects of locally applied uptake inhibitors and unilateral 6-hydroxydopamine lesions. J Neurochem. 70, 179-189.
111. Hotamisligil, G. S., 2005. Role of endoplasmic reticulum stress and c-Jun NH2-terminal kinase pathways in inflammation and origin of obesity and diabetes. Diabetes. 54 Suppl 2, S73-78.
112. Hu, G., Jousilahti, P., Bidel, S., Antikainen, R., and Tuomilehto, J., 2007. Type 2 diabetes and the risk of Parkinson's disease. Diabetes Care. 30, 842-847.
113. Hu, G., Jousilahti, P., Nissinen, A., Antikainen, R., Kivipelto, M., and Tuomilehto, J., 2006. Body mass index and the risk of Parkinson disease. Neurology. 67, 1955-1959.
114. Hudson, J. L., van Horne, C. G., Stromberg, I., Brock, S., Clayton, J., Masserano, J., Hoffer, B. J., and Gerhardt, G. A., 1993. Correlation of apomorphine- and amphetamine-induced turning with nigrostriatal dopamine content in unilateral 6-hydroxydopamine lesioned rats. Brain Res. 626, 167-174.
115. Jaffer, A., Daniels, W. M., Russell, V. A., and Taljaard, J. J., 1991. The effect of medial forebrain bundle lesion on thyrotropin secretion in the rat. Neurochem Res. 16, 577-581.

116. Jaffer, A., Daniels, W. M., Russell, V. A., and Taljaard, J. J., 1992. Effects of alpha 2- and beta-adrenoceptor agonists on growth hormone secretion following lesion of the noradrenergic system of the rat. Neurochem Res. 17, 1255-1260.
117. Jellinger, K., Linert, L., Kienzl, E., Herlinger, E., and Youdim, M. B., 1995. Chemical evidence for 6-hydroxydopamine to be an endogenous toxic factor in the pathogenesis of Parkinson's disease. J Neural Transm Suppl. 46, 297-314.
118. Jellinger, K., Paulus, W., Grundke-Iqbal, I., Riederer, P., and Youdim, M. B., 1990. Brain iron and ferritin in Parkinson's and Alzheimer's diseases. J Neural Transm Park Dis Dement Sect. 2, 327-340.
119. Jenner, P., 2003. Oxidative stress in Parkinson's disease. Ann Neurol. 53 Suppl 3, S26-36; discussion S36-28.
120. Johnson, C. C., Gorell, J. M., Rybicki, B. A., Sanders, K., and Peterson, E. L., 1999. Adult nutrient intake as a risk factor for Parkinson's disease. Int J Epidemiol. 28, 1102-1109.
121. Kakhlon, O., Breuer, W., Munnich, A., and Cabantchik, Z. I., 2010. Iron redistribution as a therapeutic strategy for treating diseases of localized iron accumulation. Can J Physiol Pharmacol. 88, 187-196.
122. Kanwar, M., Chan, P. S., Kern, T. S., and Kowluru, R. A., 2007. Oxidative damage in the retinal mitochondria of diabetic mice: possible protection by superoxide dismutase. Invest Ophthalmol Vis Sci. 48, 3805-3811.
123. Kaur, D., Lee, D., Ragapolan, S., and Andersen, J. K., 2009. Glutathione depletion in immortalized midbrain-derived dopaminergic neurons results in increases in the labile iron pool: implications for Parkinson's disease. Free Radic Biol Med. 46, 593-598.
124. Kelley, D. E., He, J., Menshikova, E. V., and Ritov, V. B., 2002. Dysfunction of mitochondria in human skeletal muscle in type 2 diabetes. Diabetes. 51, 2944-2950.
125. Khan, A. H., and Pessin, J. E., 2002. Insulin regulation of glucose uptake: a complex interplay of intracellular signalling pathways. Diabetologia. 45, 1475-1483.
126. Kim, B., van Golen, C. M., and Feldman, E. L., 2005. Insulin-like growth factor I induces preferential degradation of insulin receptor substrate-2 through the phosphatidylinositol 3-kinase pathway in human neuroblastoma cells. Endocrinology. 146, 5350-5357.
127. Kirik, D., Annett, L. E., Burger, C., Muzyczka, N., Mandel, R. J., and Bjorklund, A., 2003. Nigrostriatal alpha-synucleinopathy induced by viral vector-mediated overexpression of human alpha-synuclein: a new primate model of Parkinson's disease. Proc Natl Acad Sci U S A. 100, 2884-2889.
128. Kirik, D., and Bjorklund, A., 2003. Modeling CNS neurodegeneration by overexpression of disease-causing proteins using viral vectors. Trends Neurosci. 26, 386-392.
129. Klintworth, H., Newhouse, K., Li, T., Choi, W. S., Faigle, R., and Xia, Z., 2007. Activation of c-Jun N-terminal protein kinase is a common mechanism underlying paraquat- and rotenone-induced dopaminergic cell apoptosis. Toxicol Sci. 97, 149-162.
130. Klip, A., and Paquet, M. R., 1990. Glucose transport and glucose transporters in muscle and their metabolic regulation. Diabetes Care. 13, 228-243.
131. Ko, K. W., Avramoglu, R. K., McLeod, R. S., Vukmirica, J., and Yao, Z., 2001. The insulin-stimulated cell surface presentation of low density lipoprotein receptor-related protein in 3T3-L1 adipocytes is sensitive to phosphatidylinositide 3-kinase inhibition. Biochemistry. 40, 752-759.
132. Kotecha, S. A., Oak, J. N., Jackson, M. F., Perez, Y., Orser, B. A., Van Tol, H. H., and MacDonald, J. F., 2002. A D2 class dopamine receptor transactivates a receptor tyrosine kinase to inhibit NMDA receptor transmission. Neuron. 35, 1111-1122.

133. Krueger, B. K., 1990. Kinetics and block of dopamine uptake in synaptosomes from rat caudate nucleus. J Neurochem. 55, 260-267.
134. Langston, J. W., and Forno, L. S., 1978. The hypothalamus in Parkinson disease. Ann Neurol. 3, 129-133.
135. Larsen, S., Stride, N., Hey-Mogensen, M., Hansen, C. N., Andersen, J. L., Madsbad, S., Worm, D., Helge, J. W., and Dela, F., 2011. Increased mitochondrial substrate sensitivity in skeletal muscle of patients with type 2 diabetes. Diabetologia.
136. LaVaute, T., Smith, S., Cooperman, S., Iwai, K., Land, W., Meyron-Holtz, E., Drake, S. K., Miller, G., Abu-Asab, M., Tsokos, M., Switzer, R., 3rd, Grinberg, A., Love, P., Tresser, N., and Rouault, T. A., 2001. Targeted deletion of the gene encoding iron regulatory protein-2 causes misregulation of iron metabolism and neurodegenerative disease in mice. Nat Genet. 27, 209-214.
137. Lawler, C. P., Gilmore, J. H., Watts, V. J., Walker, Q. D., Southerland, S. B., Cook, L. L., Mathis, C. A., and Mailman, R. B., 1995. Interhemispheric modulation of dopamine receptor interactions in unilateral 6-OHDA rodent model. Synapse. 21, 299-311.
138. Lee, J., and Kim, M. S., 2007. The role of GSK3 in glucose homeostasis and the development of insulin resistance. Diabetes Res Clin Pract. 77 Suppl 1, S49-57.
139. Leroy, K., and Brion, J. P., 1999. Developmental expression and localization of glycogen synthase kinase-3beta in rat brain. J Chem Neuroanat. 16, 279-293.
140. Levenson, C. W., Cutler, R. G., Ladenheim, B., Cadet, J. L., Hare, J., and Mattson, M. P., 2004. Role of dietary iron restriction in a mouse model of Parkinson's disease. Exp Neurol. 190, 506-514.
141. Liberman, Z., Plotkin, B., Tennenbaum, T., and Eldar-Finkelman, H., 2008. Coordinated phosphorylation of insulin receptor substrate-1 by glycogen synthase kinase-3 and protein kinase C betaII in the diabetic fat tissue. Am J Physiol Endocrinol Metab. 294, E1169-1177.
142. Lin, X., Taguchi, A., Park, S., Kushner, J. A., Li, F., Li, Y., and White, M. F., 2004. Dysregulation of insulin receptor substrate 2 in beta cells and brain causes obesity and diabetes. J Clin Invest. 114, 908-916.
143. Linert, W., Herlinger, E., Jameson, R. F., Kienzl, E., Jellinger, K., and Youdim, M. B., 1996. Dopamine, 6-hydroxydopamine, iron, and dioxygen--their mutual interactions and possible implication in the development of Parkinson's disease. Biochim Biophys Acta. 1316, 160-168.
144. Lipman, I. J., Boykin, M. E., and Flora, R. E., 1974. Glucose intolerance in Parkinson's disease. J Chronic Dis. 27, 573-579.
145. Liu, G., Zhang, C., Yin, J., Li, X., Cheng, F., Li, Y., Yang, H., Ueda, K., Chan, P., and Yu, S., 2009. alpha-Synuclein is differentially expressed in mitochondria from different rat brain regions and dose-dependently down-regulates complex I activity. Neurosci Lett. 454, 187-192.
146. Logroscino, G., Marder, K., Cote, L., Tang, M. X., Shea, S., and Mayeux, R., 1996. Dietary lipids and antioxidants in Parkinson's disease: a population-based, case-control study. Ann Neurol. 39, 89-94.
147. Logroscino, G., Marder, K., Graziano, J., Freyer, G., Slavkovich, V., LoIacono, N., Cote, L., and Mayeux, R., 1997. Altered systemic iron metabolism in Parkinson's disease. Neurology. 49, 714-717.
148. Lopes, K. O., Sparks, D. L., and Streit, W. J., 2008. Microglial dystrophy in the aged and Alzheimer's disease brain is associated with ferritin immunoreactivity. Glia. 56, 1048-1060.

149. Lozoff, B., Beard, J., Connor, J., Barbara, F., Georgieff, M., and Schallert, T., 2006. Long-lasting neural and behavioral effects of iron deficiency in infancy. Nutr Rev. 64, S34-43; discussion S72-91.
150. Macdonald, P. A., and Monchi, O., 2011. Differential effects of dopaminergic therapies on dorsal and ventral striatum in Parkinson's disease: implications for cognitive function. Parkinsons Dis. 2011, 572743.
151. Maher, F., Vannucci, S. J., and Simpson, I. A., 1994. Glucose transporter proteins in brain. Faseb J. 8, 1003-1011.
152. Manning, B. D., and Cantley, L. C., 2007. AKT/PKB signaling: navigating downstream. Cell. 129, 1261-1274.
153. Martin, H. L., and Teismann, P., 2009. Glutathione--a review on its role and significance in Parkinson's disease. Faseb J. 23, 3263-3272.
154. Mastroberardino, P. G., Hoffman, E. K., Horowitz, M. P., Betarbet, R., Taylor, G., Cheng, D., Na, H. M., Gutekunst, C. A., Gearing, M., Trojanowski, J. Q., Anderson, M., Chu, C. T., Peng, J., and Greenamyre, J. T., 2009. A novel transferrin/TfR2-mediated mitochondrial iron transport system is disrupted in Parkinson's disease. Neurobiol Dis. 34, 417-431.
155. Matsuzawa-Nagata, N., Takamura, T., Ando, H., Nakamura, S., Kurita, S., Misu, H., Ota, T., Yokoyama, M., Honda, M., Miyamoto, K. I., and Kaneko, S., 2008. Increased oxidative stress precedes the onset of high-fat diet-induced insulin resistance and obesity. Metabolism. 57, 1071-1077.
156. McCarthy, M. I., 2010. Genomics, type 2 diabetes, and obesity. N Engl J Med. 363, 2339-2350.
157. McEver, R. P., 1991. Leukocyte interactions mediated by selectins. Thromb Haemost. 66, 80-87.
158. McGrew, D. M., Irwin, I., and Langston, J. W., 2000. Ethylenebisdithiocarbamate enhances MPTP-induced striatal dopamine depletion in mice. Neurotoxicology. 21, 309-312.
159. McLean, P. J., Kawamata, H., Ribich, S., and Hyman, B. T., 2000. Membrane association and protein conformation of alpha-synuclein in intact neurons. Effect of Parkinson's disease-linked mutations. J Biol Chem. 275, 8812-8816.
160. Migrenne, S. C.-G., Celine; Kang, Ling; Wang, Ruokun; Rouch, Claude; Lefevre, Anne-Laure; Ktorza, Alain; Routh, Vanessa; Levin, Barry; and Magnan, Christophe, 2006. Fatty Acid Signaling in the Hypothalamus and Neural Control of Insulin Secretion. Diabetes. 55, S139-S144.
161. Mogensen, M., Sahlin, K., Fernstrom, M., Glintborg, D., Vind, B. F., Beck-Nielsen, H., and Hojlund, K., 2007. Mitochondrial respiration is decreased in skeletal muscle of patients with type 2 diabetes. Diabetes. 56, 1592-1599.
162. Moon, M., Kim, H. G., Hwang, L., Seo, J. H., Kim, S., Hwang, S., Kim, S., Lee, D., Chung, H., Oh, M. S., Lee, K. T., and Park, S., 2009. Neuroprotective effect of ghrelin in the 1-methyl-4-phenyl-1,2,3,6-tetrahydropyridine mouse model of Parkinson's disease by blocking microglial activation. Neurotox Res. 15, 332-347.
163. Moos, T., Oates, P. S., and Morgan, E. H., 1998. Expression of the neuronal transferrin receptor is age dependent and susceptible to iron deficiency. J Comp Neurol. 398, 420-430.
164. Moreira, P. I., Santos, M. S., Seica, R., and Oliveira, C. R., 2007. Brain mitochondrial dysfunction as a link between Alzheimer's disease and diabetes. J Neurol Sci. 257, 206-214.

165. Moroo, I., Yamada, T., Makino, H., Tooyama, I., McGeer, P. L., McGeer, E. G., and Hirayama, K., 1994. Loss of insulin receptor immunoreactivity from the substantia nigra pars compacta neurons in Parkinson's disease. Acta Neuropathol. 87, 343-348.
166. Morris, J. K., Bomhoff, G. L., Stanford, J. A., and Geiger, P. C., 2010. Neurodegeneration in an animal model of Parkinson's disease is exacerbated by a high fat diet. Am J Physiol Regul Integr Comp Physiol. 299(4):R1082-90.
167. Morris, J. K., Zhang, H., Gupte, A. A., Bomhoff, G. L., Stanford, J. A., and Geiger, P. C., 2008. Measures of striatal insulin resistance in a 6-hydroxydopamine model of Parkinson's disease. Brain Res. 1240, 185-195.
168. Morrison, C. D., Pistell, P. J., Ingram, D. K., Johnson, W. D., Liu, Y., Fernandez-Kim, S. O., White, C. L., Purpera, M. N., Uranga, R. M., Bruce-Keller, A. J., and Keller, J. N., 2010. High fat diet increases hippocampal oxidative stress and cognitive impairment in aged mice: implications for decreased Nrf2 signaling. J Neurochem. 114, 1581-1589.
169. Morrison, C. D., Pistell, P. J., Ingram, D. K., Johnson, W. D., Liu, Y., Fernandez-Kim, S. O., White, C. L., Purpera, M. N., Uranga, R. M., Bruce-Keller, A. J., and Keller, J. N., 2010. High Fat Diet Increases Hippocampal Oxidative Stress and Cognitive Impairment in Aged Mice: Implications for decreased Nrf2 signaling. J Neurochem.
170. Morton, G. J., 2007. Hypothalamic leptin regulation of energy homeostasis and glucose metabolism. J Physiol. 583, 437-443.
171. Morton, J. P., Maclaren, D. P., Cable, N. T., Campbell, I. T., Evans, L., Bongers, T., Griffiths, R. D., Kayani, A. C., McArdle, A., and Drust, B., 2007. Elevated core and muscle temperature to levels comparable to exercise do not increase heat shock protein content of skeletal muscle of physically active men. Acta Physiol (Oxf). 190, 319-327.
172. Navarro, A., and Boveris, A., 2007. The mitochondrial energy transduction system and the aging process. Am J Physiol Cell Physiol. 292, C670-686.
173. Nicklas, W. J., Youngster, S. K., Kindt, M. V., and Heikkila, R. E., 1987. MPTP, MPP+ and mitochondrial function. Life Sci. 40, 721-729.
174. Nikolaus, S., Larisch, R., Beu, M., Forutan, F., Vosberg, H., and Muller-Gartner, H. W., 2003. Bilateral increase in striatal dopamine D2 receptor density in the 6-hydroxydopamine-lesioned rat: a serial in vivo investigation with small animal PET. Eur J Nucl Med Mol Imaging. 30, 390-395.
175. Olefsky, J. M., 2001. Prospects for research in diabetes mellitus. Jama. 285, 628-632.
176. Onyango, I. G., 2008. Mitochondrial dysfunction and oxidative stress in Parkinson's disease. Neurochem Res. 33, 589-597.
177. Ostrerova, N., Petrucelli, L., Farrer, M., Mehta, N., Choi, P., Hardy, J., and Wolozin, B., 1999. alpha-Synuclein shares physical and functional homology with 14-3-3 proteins. J Neurosci. 19, 5782-5791.
178. Ott, A., Stolk, R. P., Hofman, A., van Harskamp, F., Grobbee, D. E., and Breteler, M. M., 1996. Association of diabetes mellitus and dementia: the Rotterdam Study. Diabetologia. 39, 1392-1397.
179. Palmiter, R. D., 2007. Is dopamine a physiologically relevant mediator of feeding behavior? Trends Neurosci. 30, 375-381.
180. Pandey, N., Schmidt, R. E., and Galvin, J. E., 2006. The alpha-synuclein mutation E46K promotes aggregation in cultured cells. Exp Neurol. 197, 515-520.
181. Papapetropoulos, S., Ellul, J., Argyriou, A. A., Talelli, P., Chroni, E., and Papapetropoulos, T., 2004. The effect of vascular disease on late onset Parkinson's disease. Eur J Neurol. 11, 231-235.

182. **Pardini, A. W., Nguyen, H. T., Figlewicz, D. P., Baskin, D. G., Williams, D. L., Kim, F., and Schwartz, M. W., 2006. Distribution of insulin receptor substrate-2 in brain areas involved in energy homeostasis. Brain Res. 1112, 169-178.**

183. **Park, K. J., Gaynor, R. B., and Kwak, Y. T., 2003. Heat shock protein 27 association with the I kappa B kinase complex regulates tumor necrosis factor alpha-induced NF-kappa B activation. J Biol Chem. 278, 35272-35278.**

184. **Parker, W. D., Jr., Boyson, S. J., and Parks, J. K., 1989. Abnormalities of the electron transport chain in idiopathic Parkinson's disease. Ann Neurol. 26, 719-723.**

185. **Parsons, S. M., 2000. Transport mechanisms in acetylcholine and monoamine storage. Faseb J. 14, 2423-2434.**

186. **Paz, K., Hemi, R., LeRoith, D., Karasik, A., Elhanany, E., Kanety, H., and Zick, Y., 1997. A molecular basis for insulin resistance. Elevated serine/threonine phosphorylation of IRS-1 and IRS-2 inhibits their binding to the juxtamembrane region of the insulin receptor and impairs their ability to undergo insulin-induced tyrosine phosphorylation. J Biol Chem. 272, 29911-29918.**

187. **Pederson, T. M., Kramer, D. L., and Rondinone, C. M., 2001. Serine/threonine phosphorylation of IRS-1 triggers its degradation: possible regulation by tyrosine phosphorylation. Diabetes. 50, 24-31.**

188. **Peng, J., and Andersen, J. K., 2003. The role of c-Jun N-terminal kinase (JNK) in Parkinson's disease. IUBMB Life. 55, 267-271.**

189. **Pezzella, A., d'Ischia, M., Napolitano, A., Misuraca, G., and Prota, G., 1997. Iron-mediated generation of the neurotoxin 6-hydroxydopamine quinone by reaction of fatty acid hydroperoxides with dopamine: a possible contributory mechanism for neuronal degeneration in Parkinson's disease. J Med Chem. 40, 2211-2216.**

190. **Plaas, M., Karis, A., Innos, J., Rebane, E., Baekelandt, V., Vaarmann, A., Luuk, H., Vasar, E., and Koks, S., 2008. Alpha-synuclein A30P point-mutation generates age-dependent nigrostriatal deficiency in mice. J Physiol Pharmacol. 59, 205-216.**

191. **Polymeropoulos, M. H., Lavedan, C., Leroy, E., Ide, S. E., Dehejia, A., Dutra, A., Pike, B., Root, H., Rubenstein, J., Boyer, R., Stenroos, E. S., Chandrasekharappa, S., Athanassiadou, A., Papapetropoulos, T., Johnson, W. G., Lazzarini, A. M., Duvoisin, R. C., Di Iorio, G., Golbe, L. I., and Nussbaum, R. L., 1997. Mutation in the alpha-synuclein gene identified in families with Parkinson's disease. Science. 276, 2045-2047.**

192. **Porte, D., Jr., Baskin, D. G., and Schwartz, M. W., 2005. Insulin signaling in the central nervous system: a critical role in metabolic homeostasis and disease from C. elegans to humans. Diabetes. 54, 1264-1276.**

193. **Pressley, J. C., Louis, E. D., Tang, M. X., Cote, L., Cohen, P. D., Glied, S., and Mayeux, R., 2003. The impact of comorbid disease and injuries on resource use and expenditures in parkinsonism. Neurology. 60, 87-93.**

194. **Priyadarshi, A., Khuder, S. A., Schaub, E. A., and Priyadarshi, S. S., 2001. Environmental risk factors and Parkinson's disease: a metaanalysis. Environ Res. 86, 122-127.**

195. **Priyadarshi, A., Khuder, S. A., Schaub, E. A., and Shrivastava, S., 2000. A meta-analysis of Parkinson's disease and exposure to pesticides. Neurotoxicology. 21, 435-440.**

196. **Rabol, R., Larsen, S., Hojberg, P. M., Almdal, T., Boushel, R., Haugaard, S. B., Andersen, J. L., Madsbad, S., and Dela, F., 2010. Regional anatomic differences in skeletal muscle mitochondrial respiration in type 2 diabetes and obesity. J Clin Endocrinol Metab. 95, 857-863.**

197. Rajpathak, S. N., Crandall, J. P., Wylie-Rosett, J., Kabat, G. C., Rohan, T. E., and Hu, F. B., 2009. The role of iron in type 2 diabetes in humans. Biochim Biophys Acta. 1790, 671-681.

198. Rawal, N., Parish, C., Castelo-Branco, G., and Arenas, E., 2007. Inhibition of JNK increases survival of transplanted dopamine neurons in Parkinsonian rats. Cell Death Differ. 14, 381-383.

199. Reagan, L. P., 2005. Neuronal insulin signal transduction mechanisms in diabetes phenotypes. Neurobiol Aging. 26 Suppl 1, 56-59.

200. Reimann, W., Bartoszyk, G. D., Kollhofer, U., Schneider, F., and Schoenherr, U., 1993. Effects of ageing and long-term operant conditioning on behavior and presynaptic cholinergic and dopaminergic neuronal mechanisms in rats. Arch Int Pharmacodyn Ther. 325, 5-20.

201. Rhodes, S. L., and Ritz, B., 2008. Genetics of iron regulation and the possible role of iron in Parkinson's disease. Neurobiol Dis. 32, 183-195.

202. Richardson, D. R., Lane, D. J., Becker, E. M., Huang, M. L., Whitnall, M., Rahmanto, Y. S., Sheftel, A. D., and Ponka, P., 2010. Mitochondrial iron trafficking and the integration of iron metabolism between the mitochondrion and cytosol. Proc Natl Acad Sci U S A. 107, 10775-10782.

203. Riederer, P., Sofic, E., Rausch, W. D., Schmidt, B., Reynolds, G. P., Jellinger, K., and Youdim, M. B., 1989. Transition metals, ferritin, glutathione, and ascorbic acid in parkinsonian brains. J Neurochem. 52, 515-520.

204. Ries, V., Silva, R. M., Oo, T. F., Cheng, H. C., Rzhetskaya, M., Kholodilov, N., Flavell, R. A., Kuan, C. Y., Rakic, P., and Burke, R. E., 2008. JNK2 and JNK3 combined are essential for apoptosis in dopamine neurons of the substantia nigra, but are not required for axon degeneration. J Neurochem. 107, 1578-1588.

205. Ristow, M., 2004. Neurodegenerative disorders associated with diabetes mellitus. J Mol Med. 82, 510-529.

206. Ritov, V. B., Menshikova, E. V., Azuma, K., Wood, R., Toledo, F. G., Goodpaster, B. H., Ruderman, N. B., and Kelley, D. E., 2010. Deficiency of electron transport chain in human skeletal muscle mitochondria in type 2 diabetes mellitus and obesity. Am J Physiol Endocrinol Metab. 298, E49-58.

207. Robertson, R. P., 2006. Oxidative stress and impaired insulin secretion in type 2 diabetes. Curr Opin Pharmacol. 6, 615-619.

208. Ronnemaa, E., Zethelius, B., Sundelof, J., Sundstrom, J., Degerman-Gunnarsson, M., Berne, C., Lannfelt, L., and Kilander, L., 2008. Impaired insulin secretion increases the risk of Alzheimer disease. Neurology. 71, 1065-1071.

209. Rubi, B., Ljubicic, S., Pournourmohammadi, S., Carobbio, S., Armanet, M., Bartley, C., and Maechler, P., 2005. Dopamine D2-like receptors are expressed in pancreatic beta cells and mediate inhibition of insulin secretion. J Biol Chem. 280, 36824-36832.

210. Rui, L., Aguirre, V., Kim, J. K., Shulman, G. I., Lee, A., Corbould, A., Dunaif, A., and White, M. F., 2001. Insulin/IGF-1 and TNF-alpha stimulate phosphorylation of IRS-1 at inhibitory Ser307 via distinct pathways. J Clin Invest. 107, 181-189.

211. Rui, L., Fisher, T. L., Thomas, J., and White, M. F., 2001. Regulation of insulin/insulin-like growth factor-1 signaling by proteasome-mediated degradation of insulin receptor substrate-2. J Biol Chem. 276, 40362-40367.

212. Rui, L., Yuan, M., Frantz, D., Shoelson, S., and White, M. F., 2002. SOCS-1 and SOCS-3 block insulin signaling by ubiquitin-mediated degradation of IRS1 and IRS2. J Biol Chem. 277, 42394-42398.

213. Salamone, J. D., Mahan, K., and Rogers, S., 1993. Ventrolateral striatal dopamine depletions impair feeding and food handling in rats. Pharmacol Biochem Behav. 44, 605-610.
214. Saltiel, A. R., and Kahn, C. R., 2001. Insulin signaling and the regulation of glucose and lipid metabolism. Nature. 414, 799-806.
215. Sanchez-Iglesias, S., Rey, P., Mendez-Alvarez, E., Labandeira-Garcia, J. L., and Soto-Otero, R., 2007. Time-course of brain oxidative damage caused by intrastriatal administration of 6-hydroxydopamine in a rat model of Parkinson's disease. Neurochem Res. 32, 99-105.
216. Sandyk, R., 1989. Hypothalamic compensatory mechanisms in Parkinson's disease. Int J Neurosci. 44, 135-142.
217. Sandyk, R., 1993. The relationship between diabetes mellitus and Parkinson's disease. Int J Neurosci. 69, 125-130.
218. Sandyk, R., and Iacono, R. P., 1987. The hypothalamus in Parkinson's disease. Int J Neurosci. 33, 257-259.
219. Savica, R., Rocca, W. A., and Ahlskog, J. E., 2010. When does Parkinson disease start? Arch Neurol. 67, 798-801.
220. Savitt, J. M., Dawson, V. L., and Dawson, T. M., 2006. Diagnosis and treatment of Parkinson disease: molecules to medicine. J Clin Invest. 116, 1744-1754.
221. Sawka-Verhelle, D., Baron, V., Mothe, I., Filloux, C., White, M. F., and Van Obberghen, E., 1997. Tyr624 and Tyr628 in insulin receptor substrate-2 mediate its association with the insulin receptor. J Biol Chem. 272, 16414-16420.
222. Schapira, A. H., Cooper, J. M., Dexter, D., Jenner, P., Clark, J. B., and Marsden, C. D., 1989. Mitochondrial complex I deficiency in Parkinson's disease. Lancet. 1, 1269.
223. Schapira, A. H., Emre, M., Jenner, P., and Poewe, W., 2009. Levodopa in the treatment of Parkinson's disease. Eur J Neurol. 16, 982-989.
224. Schenck, J. F., and Zimmerman, E. A., 2004. High-field magnetic resonance imaging of brain iron: birth of a biomarker? NMR Biomed. 17, 433-445.
225. Schernhammer, E., Hansen, J., Rugbjerg, K., Wermuth, L., and Ritz, B., 2011. Diabetes and the Risk of Developing Parkinson's Disease in Denmark. Diabetes Care.
226. Scherzer, C. R., Eklund, A. C., Morse, L. J., Liao, Z., Locascio, J. J., Fefer, D., Schwarzschild, M. A., Schlossmacher, M. G., Hauser, M. A., Vance, J. M., Sudarsky, L. R., Standaert, D. G., Growdon, J. H., Jensen, R. V., and Gullans, S. R., 2007. Molecular markers of early Parkinson's disease based on gene expression in blood. Proc Natl Acad Sci U S A. 104, 955-960.
227. Schober, A., 2004. Classic toxin-induced animal models of Parkinson's disease: 6-OHDA and MPTP. Cell Tissue Res. 318, 215-224.
228. Seidell, J. C., 2000. Obesity, insulin resistance and diabetes--a worldwide epidemic. Br J Nutr. 83 Suppl 1, S5-8.
229. Sengstock, G. J., Olanow, C. W., Dunn, A. J., and Arendash, G. W., 1992. Iron induces degeneration of nigrostriatal neurons. Brain Res Bull. 28, 645-649.
230. Seo, A. Y., Xu, J., Servais, S., Hofer, T., Marzetti, E., Wohlgemuth, S. E., Knutson, M. D., Chung, H. Y., and Leeuwenburgh, C., 2008. Mitochondrial iron accumulation with age and functional consequences. Aging Cell. 7, 706-716.
231. Shannak, K., Rajput, A., Rozdilsky, B., Kish, S., Gilbert, J., and Hornykiewicz, O., 1994. Noradrenaline, dopamine and serotonin levels and metabolism in the human hypothalamus: observations in Parkinson's disease and normal subjects. Brain Res. 639, 33-41.

232. Sharfi, H., and Eldar-Finkelman, H., 2008. Sequential phosphorylation of insulin receptor substrate-2 by glycogen synthase kinase-3 and c-Jun NH2-terminal kinase plays a role in hepatic insulin signaling. Am J Physiol Endocrinol Metab. 294, E307-315.
233. Shen, H. Y., He, J. C., Wang, Y., Huang, Q. Y., and Chen, J. F., 2005. Geldanamycin induces heat shock protein 70 and protects against MPTP-induced dopaminergic neurotoxicity in mice. J Biol Chem. 280, 39962-39969.
234. Shen, H. Y., He, J.-C., Wang, Y., Huang, Q.-Y., and J.-F. Chen, 2005. Geldanamycin induces Hsp70 and protects against MPTP-induced dopaminergic neurotoxicity in mice. J. Biol. Chem. 280, 39962-39969.
235. Shimomura, Y., Shimizu, H., Takahashi, M., Sato, N., Uehara, Y., Suwa, K., Kobayashi, I., Tadokoro, S., and Kobayashi, S., 1988. Changes in ambulatory activity and dopamine turnover in streptozotocin-induced diabetic rats. Endocrinology. 123, 2621-2625.
236. Simon, K. C., Chen, H., Schwarzschild, M., and Ascherio, A., 2007. Hypertension, hypercholesterolemia, diabetes, and risk of Parkinson disease. Neurology. 69, 1688-1695.
237. Sims-Robinson, C., Kim, B., Rosko, A., and Feldman, E. L., 2010. How does diabetes accelerate Alzheimer disease pathology? Nat Rev Neurol. 6, 551-559.
238. Sirtori, C. R., Bolme, P., and Azarnoff, D. L., 1972. Metabolic responses to acute and chronic L-dopa administration in patients with parkinsonism. N Engl J Med. 287, 729-733.
239. Skitek, E. B., Fowler, S. C., and Tessel, R. E., 1999. Effects of unilateral striatal dopamine depletion on tongue force and rhythm during licking in rats. Behav Neurosci. 113, 567-573.
240. Smiley, D., and Umpierrez, G., 2007. Metformin/rosiglitazone combination pill (Avandamet) for the treatment of patients with Type 2 diabetes. Expert Opin Pharmacother. 8, 1353-1364.
241. Smith, J. L., Ju, J. S., Saha, B. M., Racette, B. A., and Fisher, J. S., 2004. Levodopa with carbidopa diminishes glycogen concentration, glycogen synthase activity, and insulin-stimulated glucose transport in rat skeletal muscle. J Appl Physiol. 97, 2339-2346.
242. Snyder, A. M., and Connor, J. R., 2009. Iron, the substantia nigra and related neurological disorders. Biochim Biophys Acta. 1790, 606-614.
243. Sofic, E., Riederer, P., Heinsen, H., Beckmann, H., Reynolds, G. P., Hebenstreit, G., and Youdim, M. B., 1988. Increased iron (III) and total iron content in post mortem substantia nigra of parkinsonian brain. J Neural Transm. 74, 199-205.
244. South, T., and Huang, X. F., 2008. High-fat diet exposure increases dopamine D2 receptor and decreases dopamine transporter receptor binding density in the nucleus accumbens and caudate putamen of mice. Neurochem Res. 33, 598-605.
245. Spina, M. B., and Cohen, G., 1989. Dopamine turnover and glutathione oxidation: implications for Parkinson disease. Proc Natl Acad Sci U S A. 86, 1398-1400.
246. Stanford, J. A., Currier, T. D., and Gerhardt, G. A., 2002. Acute locomotor effects of fluoxetine, sertraline, and nomifensine in young versus aged Fischer 344 rats. Pharmacol Biochem Behav. 71, 325-332.
247. Stanford, J. A., Currier, T. D., Purdom, M. S., and Gerhardt, G. A., 2001. Nomifensine reveals age-related changes in K(+)-evoked striatal DA overflow in F344 rats. Neurobiol Aging. 22, 495-502.
248. Stanford, J. A., and Gerhardt, G. A., 2004. Aged F344 rats exhibit altered electrophysiological activity in locomotor-unrelated but not locomotor-related striatal neurons. Neurobiol Aging. 25, 509-515.
249. Storch, A., Ludolph, A. C., and Schwarz, J., 2004. Dopamine transporter: involvement in selective dopaminergic neurotoxicity and degeneration. J Neural Transm. 111, 1267-1286.

250. Stumvoll, M., Mitrakou, A., Pimenta, W., Jenssen, T., Yki-Jarvinen, H., Van Haeften, T., Renn, W., and Gerich, J., 2000. Use of the oral glucose tolerance test to assess insulin release and insulin sensitivity. Diabetes Care. 23, 295-301.

251. Sulzer, D., 2007. Multiple hit hypotheses for dopamine neuron loss in Parkinson's disease. Trends Neurosci. 30, 244-250.

252. Supiano, M. A., Hogikyan, R. V., Morrow, L. A., Ortiz-Alonso, F. J., Herman, W. H., Galecki, A. T., and Halter, J. B., 1993. Aging and insulin sensitivity: role of blood pressure and sympathetic nervous system activity. J Gerontol. 48, M237-243.

253. Swaminathan, S., Fonseca, V. A., Alam, M. G., and Shah, S. V., 2007. The role of iron in diabetes and its complications. Diabetes Care. 30, 1926-1933.

254. Sykiotis, G. P., and Papavassiliou, A. G., 2001. Serine phosphorylation of insulin receptor substrate-1: a novel target for the reversal of insulin resistance. Mol Endocrinol. 15, 1864-1869.

255. Szkudelski, T., 2001. The mechanism of alloxan and streptozotocin action in B cells of the rat pancreas. Physiol Res. 50, 537-546.

256. Taguchi, A., Wartschow, L. M., and White, M. F., 2007. Brain IRS2 signaling coordinates life span and nutrient homeostasis. Science. 317, 369-372.

257. Takahashi, M., Yamada, T., Tooyama, I., Moroo, I., Kimura, H., Yamamoto, T., and Okada, H., 1996. Insulin receptor mRNA in the substantia nigra in Parkinson's disease. Neurosci Lett. 204, 201-204.

258. Tang, T. S., and Bezprozvanny, I., 2004. Dopamine receptor-mediated Ca(2+) signaling in striatal medium spiny neurons. J Biol Chem. 279, 42082-42094.

259. Tanner, L. I., and Lienhard, G. E., 1989. Localization of transferrin receptors and insulin-like growth factor II receptors in vesicles from 3T3-L1 adipocytes that contain intracellular glucose transporters. J Cell Biol. 108, 1537-1545.

260. Teff, K. L., 2007. Visceral Nerves: Vagal and Sympathetic Innervation. JPEN J Parenter Enteral Nutr. 32, 569-571.

261. Thiruchelvam, M., Brockel, B. J., Richfield, E. K., Baggs, R. B., and Cory-Slechta, D. A., 2000. Potentiated and preferential effects of combined paraquat and maneb on nigrostriatal dopamine systems: environmental risk factors for Parkinson's disease? Brain Res. 873, 225-234.

262. Thomas, B., and Beal, M. F., 2007. Parkinson's disease. Hum Mol Genet. 16 Spec No. 2, R183-194.

263. Thrash, B., Uthayathas, S., Karuppagounder, S. S., Suppiramaniam, V., and Dhanasekaran, M., 2007. Paraquat and maneb induced neurotoxicity. Proc West Pharmacol Soc. 50, 31-42.

264. Tolwani, R. J., Jakowec, M. W., Petzinger, G. M., Green, S., and Waggie, K., 1999. Experimental models of Parkinson's disease: insights from many models. Lab Anim Sci. 49, 363-371.

265. Ulusoy, A., Decressac, M., Kirik, D., and Bjorklund, A., 2010. Viral vector-mediated overexpression of alpha-synuclein as a progressive model of Parkinson's disease. Prog Brain Res. 184, 89-111.

266. Ungerstedt, U., 1968. 6-Hydroxy-dopamine induced degeneration of central monoamine neurons. Eur J Pharmacol. 5, 107-110.

267. Uranga, R. M., Bruce-Keller, A. J., Morrison, C. D., Fernandez-Kim, S. O., Ebenezer, P. J., Zhang, L., Dasuri, K., and Keller, J. N., 2010. Intersection between metabolic dysfunction, high fat diet consumption, and brain aging. J Neurochem. 114, 344-361.

268. Uversky, V. N., Li, J., Bower, K., and Fink, A. L., 2002. Synergistic effects of pesticides and metals on the fibrillation of alpha-synuclein: implications for Parkinson's disease. Neurotoxicology. 23, 527-536.
269. Uversky, V. N., Li, J., and Fink, A. L., 2001. Metal-triggered structural transformations, aggregation, and fibrillation of human alpha-synuclein. A possible molecular NK between Parkinson's disease and heavy metal exposure. J Biol Chem. 276, 44284-44296.
270. Uyama, N., Geerts, A., and Reynaert, H., 2004. Neural connections between the hypothalamus and the liver. Anat Rec A Discov Mol Cell Evol Biol. 280, 808-820.
271. Vali, L., Hahn, O., Kupcsulik, P., Drahos, A., Sarvary, E., Szentmihalyi, K., Pallai, Z., Kurucz, T., Sipos, P., and Blazovics, A., 2008. Oxidative stress with altered element content and decreased ATP level of erythrocytes in hepatocellular carcinoma and colorectal liver metastases. Eur J Gastroenterol Hepatol. 20, 393-398.
272. van der Heide, L. P., Ramakers, G. M., and Smidt, M. P., 2006. Insulin signaling in the central nervous system: learning to survive. Prog Neurobiol. 79, 205-221.
273. Vanitallie, T. B., 2008. Parkinson disease: primacy of age as a risk factor for mitochondrial dysfunction. Metabolism. 57 Suppl 2, S50-55.
274. Wallace, T. M., Levy, J. C., and Matthews, D. R., 2004. Use and abuse of HOMA modeling. Diabetes Care. 27, 1487-1495.
275. Wallis, L. I., Paley, M. N., Graham, J. M., Grunewald, R. A., Wignall, E. L., Joy, H. M., and Griffiths, P. D., 2008. MRI assessment of basal ganglia iron deposition in Parkinson's disease. J Magn Reson Imaging. 28, 1061-1067.
276. Walters, T. L., Irwin, I., Delfani, K., Langston, J. W., and Janson, A. M., 1999. Diethyldithiocarbamate causes nigral cell loss and dopamine depletion with nontoxic doses of MPTP. Exp Neurol. 156, 62-70.
277. Wang, Q., Somwar, R., Bilan, P. J., Liu, Z., Jin, J., Woodgett, J. R., and Klip, A., 1999. Protein kinase B/Akt participates in GLUT4 translocation by insulin in L6 myoblasts. Mol Cell Biol. 19, 4008-4018.
278. Wang, W., Knovich, M. A., Coffman, L. G., Torti, F. M., and Torti, S. V., 2010. Serum ferritin: Past, present and future. Biochim Biophys Acta. 1800, 760-769.
279. Wang, X., Zheng, W., Xie, J. W., Wang, T., Wang, S. L., Teng, W. P., and Wang, Z. Y., 2010. Insulin deficiency exacerbates cerebral amyloidosis and behavioral deficits in an Alzheimer transgenic mouse model. Mol Neurodegener. 5, 46.
280. Waxman, E. A., and Giasson, B. I., 2009. Molecular mechanisms of alpha-synuclein neurodegeneration. Biochim Biophys Acta. 1792, 616-624.
281. Welsh, G. I., Hers, I., Berwick, D. C., Dell, G., Wherlock, M., Birkin, R., Leney, S., and Tavare, J. M., 2005. Role of protein kinase B in insulin-regulated glucose uptake. Biochem Soc Trans. 33, 346-349.
282. Werner, E. D., Lee, J., Hansen, L., Yuan, M., and Shoelson, S. E., 2004. Insulin resistance due to phosphorylation of insulin receptor substrate-1 at serine 302. J Biol Chem. 279, 35298-35305.
283. West, A. R., and Galloway, M. P., 1998. Nitric oxide and potassium chloride-facilitated striatal dopamine efflux in vivo: role of calcium-dependent release mechanisms. Neurochem Int. 33, 493-501.
284. White, M. F., 1998. The IRS-signalling system: a network of docking proteins that mediate insulin action. Mol Cell Biochem. 182, 3-11.
285. White, M. F., 2002. IRS proteins and the common path to diabetes. Am J Physiol Endocrinol Metab. 283, E413-422.

286. **Wild, S., Roglic, G., Green, A., Sicree, R., and King, H., 2004. Global prevalence of diabetes: estimates for the year 2000 and projections for 2030. Diabetes Care. 27, 1047-1053.**

287. **Wilhelm, K. R., Yanamandra, K., Gruden, M. A., Zamotin, V., Malisauskas, M., Casaite, V., Darinskas, A., Forsgren, L., and Morozova-Roche, L. A., 2007. Immune reactivity towards insulin, its amyloid and protein S100B in blood sera of Parkinson's disease patients. Eur J Neurol. 14, 327-334.**

288. **Xu, Q., Park, Y., Huang, X., Hollenbeck, A., Blair, A., Schatzkin, A., and Chen, H., 2011. Diabetes and risk of Parkinson's disease. Diabetes Care. 34, 910-915.**

289. **Yan, Z., Hsieh-Wilson, L., Feng, J., Tomizawa, K., Allen, P. B., Fienberg, A. A., Nairn, A. C., and Greengard, P., 1999. Protein phosphatase 1 modulation of neostriatal AMPA channels: regulation by DARPP-32 and spinophilin. Nat Neurosci. 2, 13-17.**

290. **Yang, F., Wang, X., Haile, D. J., Piantadosi, C. A., and Ghio, A. J., 2002. Iron increases expression of iron-export protein MTP1 in lung cells. Am J Physiol Lung Cell Mol Physiol. 283, L932-939.**

291. **Yokoyama, H., Kuroiwa, H., Yano, R., and Araki, T., 2008. Targeting reactive oxygen species, reactive nitrogen species and inflammation in MPTP neurotoxicity and Parkinson's disease. Neurol Sci. 29, 293-301.**

292. **York, D. A., Teng, L., and Park-York, M., 2010. Effects of dietary fat and enterostatin on dopamine and 5-hydroxytrytamine release from rat striatal slices. Brain Res. 1349, 48-55.**

293. **Younes-Mhenni, S., Frih-Ayed, M., Kerkeni, A., Bost, M., and Chazot, G., 2007. Peripheral blood markers of oxidative stress in Parkinson's disease. Eur Neurol. 58, 78-83.**

294. **Young, D. A., Uhl, J. J., Cartee, G. D., and Holloszy, J. O., 1986. Activation of glucose transport in muscle by prolonged exposure to insulin. Effects of glucose and insulin concentrations. J Biol Chem. 261, 16049-16053.**

295. **Yuan, H., Sarre, S., Ebinger, G., and Michotte, Y., 2005. Histological, behavioural and neurochemical evaluation of medial forebrain bundle and striatal 6-OHDA lesions as rat models of Parkinson's disease. J Neurosci Methods. 144, 35-45.**

296. **Yuan, M., Konstantopoulos, N., Lee, J., Hansen, L., Li, Z. W., Karin, M., and Shoelson, S. E., 2001. Reversal of obesity- and diet-induced insulin resistance with salicylates or targeted disruption of Ikkbeta. Science. 293, 1673-1677.**

297. **Zhande, R., Mitchell, J. J., Wu, J., and Sun, X. J., 2002. Molecular mechanism of insulin-induced degradation of insulin receptor substrate 1. Mol Cell Biol. 22, 1016-1026.**

298. **Zhang, X., Dong, F., Ren, J., Driscoll, M. J., and Culver, B., 2005. High dietary fat induces NADPH oxidase-associated oxidative stress and inflammation in rat cerebral cortex. Exp Neurol. 191, 318-325.**

299. **Zheng, Z., and Yenari, M. A., 2006. The application of HSP70 as a target for gene therapy. Front Biosci. 11, 699-707.**

300. **Zhu, M., Qin, Z. J., Hu, D., Munishkina, L. A., and Fink, A. L., 2006. Alpha-synuclein can function as an antioxidant preventing oxidation of unsaturated lipid in vesicles. Biochemistry. 45, 8135-8142.**

301. **Zhu, W., Li, X., Xie, W., Luo, F., Kaur, D., Andersen, J. K., Jankovic, J., and Le, W., 2010. Genetic iron chelation protects against proteasome inhibition-induced dopamine neuron degeneration. Neurobiol Dis. 37, 307-313.**

302. **Zick, Y., 2005. Ser/Thr phosphorylation of IRS proteins: a molecular basis for insulin resistance. Sci STKE. 2005, pe4.**

303. Zigmond, M. J., Abercrombie, E. D., Berger, T. W., Grace, A. A., and Stricker, E. M., 1990. Compensations after lesions of central dopaminergic neurons: some clinical and basic implications. Trends Neurosci. 13, 290-296.